Zeitschrift: IABSE reports = Rapports AIPC = IVBH Berichte
Band: 51 (1986)

Rubrik: Session C: Planning and design

SESSION C

Planning and Design

Leere Seite
Blank page
Page vide

Optimisation of Measures for Quality Assurance

Optimisation des mesures prises pour l'assurance de la qualité

Optimale Verteilung von Qualitätssicherungsmassnahmen

Rüdiger RACKWITZ
Dr.-Ing.
TU Munich
Munich, FR Germany

Rüdiger Rackwitz, born 1941, has been head of a research group in structural reliability at the Technical University of Munich for more than ten years.

SUMMARY

Planning for quality also involves quantitative optimisation provided that the overall reliability problem has been modelled appropriately. Importance and sensitivity measures are defined in the context of first-order reliability methods which can be used for optimisation of quality assurance measures.

RÉSUMÉ

La planification de la qualité est aussi une question d'optimisation quantitative lorsque le problème général de la fiabilité a pu être modélisé de façon appropriée. Des mesures d'importance et de sensibilité sont définies dans le cadre de la méthode de fiabilité du premier ordre. Celles-ci peuvent être utilisées avec avantage pour optimiser les mesures prises pour l'assurance de la qualité.

ZUSAMMENFASSUNG

Qualitätsplanung ist auch zahlenmässige Optimierung, wenn das allgemeine Zuverlässigkeitsproblem in geeigneter Weise modelliert werden konnte. Importanz- und Empfindlichkeitsmasse werden im Rahmen der Zuverlässigkeitsmethode 1. Ordnung definiert. Diese können mit Vorteil für die Optimierung von Qualitätssicherungsmassnahmen eingesetzt werden.

1. INTRODUCTION

"Quality" of a technical facility in the broad sense can be taken as is its property to fulfill its intended purpose reliably during the anticipated time of use. Quality must be produced. In particular, the facility must be designed, constructed and, possibly, maintained such that it withstands all foreseen internal and external actions. But both the capacities and the demands usually are highly uncertain and, thus, performance and safety requirements can only be met with a certain probability. Quality could exist without being assured. But, usually, efforts are being undertaken to specifically provide quality and this activity is called "quality assurance" herein. Clearly, the success of an activity needs to be verified. Thus, we shall include those passive actions into our notion of quality assurance although these are only of limited interest in our context. Here, any quality assurance action is understood to serve either for the control or, and preferably, for the reduction of prior uncertainties. On the other hand, the resources in money, man-power or time, individually or jointly, are always limited. Since, as a rule, increasing investments into the various means to achieve quality have a favourable effect on reliability a prominent engineering task is to specify the types of appropriate quality assurance measures and to allocate their intensity in the most efficient way.

Obviously, quality assurance activities should start in the very first phases of a project as they guide the amount of pre-investigations on the specific environmental parameters and potential building materials, the general lay-out of the system, and later, the scope of design calculations and, possibly, development tests, the constructions procedures and their control, and type and extent of the final qualification procedures; to name a few of those quality assurance measures. And it should also be clear that, under given performance and/or reliability constraints, each project has its own optimal distribution of quality assurance efforts.

Those uncertainties may be classified into several categories:

- classical (random) variations in the physical quantities such as material properties, structural geometry, internal and environmental actions on the structure.
- parameter and model uncertainties
- human errors
- professional ignorance

Almost nothing can be done about the last type of uncertainty. For the other types of uncertainties, however, reasonable quantitative models of varying realism and sophistication exist. The first type of uncertainty is the subject of modelling in classical structural reliability. Sufficient knowledge has been accumulated in the past years so that there is no need for further discussion, herein. The second type of uncertainties, which frequently dominates those of the first kind, can usually be removed by valid experiments, at least in principle. One of the primary aims of quality assurance, no doubt, is just to diminuish these uncertainties to a reasonable level. Human errors are the subject of a number of contributions at

this conference, both with respect to the aspects of modelling and to the design of efficient prevention resp. detection systems. Formally, there is no specific difference in the treatment of human errors as uncertain events compared with the two other types of uncertainties. Supporting data are either available or are to be collected or even assessed subjectively during quality assurance for all of these types of uncertainties.

In the following some technical tools will be given both for the reliability analysis of complex systems and the optimal allocation of quality assurance actions. It will be demonstrated that a crucial ingredient of quantitative planning of quality assurance is the existence of importance and sensitivity measures for the parameters in quality assurance. At present, no commonly agreed definitions appear to exist. Therefore, suitable measures will be derived and discussed to some degree. Furthermore, these measures must be computable in the sense that a quantitative assessment of quality assurance can be carried out during practical work. Again, some proposals for suitable methods will be given. Finally, a few remarks on optimisation are made in order to outline the general methodology to be followed when planning quality assurance measures.

2. SYSTEM MODELLING AND RELIABILITY ANALYSIS

A convenient way to describe the logical structure of a system is by means of event trees for componential failures [2]. In general, a number of event trees have to be analysed each of those associated with an initiating event defining also the leading event of the hazard scenario under consideration. Then, the failure probability of a time-invariant problem can be given as [2]

$$P_f = P\left(\bigcup_i \left(\bigcup_j \bigcap_k F_{ijk}\right)\right) \qquad (1)$$

where i runs over the index set of the hazard scenarios, j over the index set of all branch tips in the event tree to failure in the corresponding scenario i and k over the index set of all componential failure events along the j-th branch in scenario i. F_{ijk} denotes the failure event which always can be given in the form

$$F_{ijk} = (\underline{X} \in V_{ijk}) = (h_{ijk}(\underline{X};\underline{p}) \leq 0) \qquad (2)$$

with $\underline{X}$ the vector of uncertain variables and $\underline{p}$ a vector of deterministic parameters to be defined later. Let further a probability distribution transformation $\underline{X} = \underline{T}(\underline{U})$ exist where $\underline{U}$ is an independent standard normal vector [3]. Then, a first-order approximation (bound) for the failure probability is

$$P_f \leq \sum_i \sum_j P\left(\bigcap_k h_{ijk}(\underline{X};\underline{p}) \leq 0\right)$$

$$= \sum_i \sum_j P\left(\bigcap_k g_{ijk}(\underline{U};p) \leq 0\right)$$

$$\approx \sum_i \sum_j P\left(\bigcap_k \left(\underline{\alpha}_{ijk}(\underline{p})\underline{U} + \beta_{ijk}(\underline{p}) \leq 0\right)\right)$$

$$= \sum_i \sum_j \phi_k(\underline{\beta}_{ij}; \underline{\underline{R}}_{ij}) \qquad (3)$$

with $\underline{\beta}_{ij} = (\beta_{ij1}, \ldots, \beta_{ijk})^T$ and $\underline{\underline{R}}_{ij} = (\underline{\alpha}_{ijr}^T \underline{\alpha}_{ijs};\ r,s=1,\ldots k)$. Herein, the vectors $\underline{\alpha}_{ijk}$ are the negative gradients (normalized by $\|\underline{\alpha}_{ijk}\|$) of $g_{ijk}(\underline{u};\underline{p}) = 0$ at the so-called individual β-points $\underline{u}^*_{ijk}$ defined as [2,4]

$$\beta_{ijk} = \|\underline{u}^*_{ijk}\| = \min(\|\underline{u}\|) \quad \text{for } (\underline{u}: g_{ijk}(\underline{u}) \leq 0) \qquad (4)$$

Theory and numerical procedures of this first-order reliability method (FORM) are now well developed and are not further discussed. The method can be simplified to a certain extent as well as refined towards an asymptotically exact second-order reliability method [4]. Usually, the first-order results are totally satisfying from a practical point of view and it can be shown that a first-order approach is even sufficient for the derivations of sensitivity and importance measures to come [5]. As mentioned, an easy calculation of these quantities is essential for the optimal distribution of quality assurance efforts in practice.

3. SENSITIVITY AND IMPORTANCE MEASURES

We are now going to define several relevant additional quantities. It is useful to introduce first the so-called equivalent safety index [6,7].

$$\beta_E = -\phi^{-1}\left[P\left(\underline{U} \in V\right)\right] \qquad (5)$$

Consider the elementary case $V = (\underline{\alpha}^T\underline{U} + \beta \leq 0)$. Let the coordinate origin be translated by a small quantity $\underline{\epsilon}$ or $\underline{U}$ be changed into $\underline{U} + \underline{\epsilon}$. Then,

$$\beta_E = -\phi^{-1}[P(\underline{U} + \underline{\epsilon}) \in V]$$

$$= -\phi^{-1}[P(\underline{\alpha}^T(\underline{U} + \underline{\epsilon}) + \beta \leq 0]$$

$$= -\phi^{-1}[\phi(-\beta - \underline{\alpha}^T\epsilon)]$$

$$= \beta + \underline{\alpha}^T\underline{\epsilon} \qquad (6)$$

and

$$\left.\frac{\partial \beta_E}{\partial \epsilon_i}\right|_{\underline{\epsilon} \to \underline{0}} = \alpha_i \qquad (7)$$

Alternatively, one derives

$$\left.\frac{\partial P_f(\underline{\epsilon})}{\partial \epsilon_i}\right|_{\underline{\epsilon}\to\underline{0}} = \left.\frac{\partial\, \phi(-\beta_E(\underline{\epsilon})}{\partial \epsilon_i}\right|_{\underline{\epsilon}\to\underline{0}} = -\,\varphi(\beta_E)\,\alpha_i \tag{8}$$

Obviously, α_i is a measure of sensitivity of β_E against (small) changes in the variable U_i. Moreover, let $\underline{U}$ now be replaced by an independent normal vector with mean $\underline{m}$ and covariance matrix $\underline{\underline{\Sigma}} = (\text{diag}\ \sigma_i^2)$. It is easily shown that

$$V(\underline{m},\underline{\underline{\Sigma}}) = (\sum_{i=1}^{n} \alpha_i(\sigma_i V_i + m_i) + \beta \le 0)$$

$$= (Z \le -\frac{\beta + \sum_{i=1}^{n} \alpha_i m_i}{(\sum_{i=1}^{n} (\alpha_i\sigma_i)^2)^{1/2}})$$

$$= (Z \le -\beta_E(\underline{m},\underline{\underline{\Sigma}})) \tag{9}$$

and, therefore,

$$\alpha_{m,i} = \frac{\partial \beta_E(\underline{m}\to\underline{0},\underline{\underline{\Sigma}}\to\underline{\underline{I}})}{\partial m_i} = \alpha_i \tag{10}$$

$$\alpha_{\sigma,i} = \frac{\partial \beta_E(\underline{m}\to\underline{0},\underline{\underline{\Sigma}}\to\underline{\underline{I}})}{\partial \sigma_i} = -\,\beta\alpha_i^2 \tag{11}$$

Hence, eq. (10) which formally coincides with eq. (7) is a sensitivity measure of β_E against (small) changes in the mean of a variable whereas eq. (11) can be interpreted as a measure of the stochastic importance of a variable.

These measures can, of course, also be defined for non-linear failure surfaces by using their β-point linearisation and they carry over to sets of unions of failure events. For the cut set it is

$$\beta_E(\underline{m},\ \underline{\underline{\Sigma}}) = -\phi^{-1}[P(\bigcap_{k=1}^{K} (Z_k \le -\frac{\beta_k + \sum_{i=1}^{n} \alpha_{ki} m_i}{(\sum_{i=1}^{n} (\alpha_{ki}\sigma_i)^2)^{1/2}})] \tag{12}$$

One obtains

$$\tilde{\alpha}_{E,i} = \frac{\partial \beta_E(\underline{m}\to\underline{0},\ \underline{\underline{\Sigma}}\to\underline{\underline{I}})}{\partial m_i}$$

$$= - \frac{1}{\varphi(\beta_E)} \frac{\partial}{\partial m_i} P\left(\bigcap_{k=1}^{K} \{Z_k \leq - \beta_k - \underline{\alpha}_k^T \underline{m}\}\right)$$

$$= - \frac{1}{\varphi(\beta_E)} \sum_{k=1}^{K} \alpha_{ki} \frac{\partial}{\partial \beta_k} P\left(\bigcap_{k=1}^{K} \{Z_k \leq - \beta_k\}\right) \qquad (13)$$

with

$$\tilde{\gamma}_K = \frac{\partial}{\partial \beta_k} P\left(\bigcap_{k=1}^{K} \{Z_k \leq -\beta_k\}\right) = \frac{\partial}{\partial \beta_k} \int_{-\infty}^{-\beta_k} P\left(\bigcap_{\substack{j=1 \\ j \neq k}}^{K} \{Z_j \leq -\beta_j | Z_k = u\}\right) \varphi(u) du$$

$$= \varphi(\beta_k) \; P\left(\bigcap_{\substack{j=1 \\ j \neq k}}^{K} \{Z_j \leq -\beta_j | Z_k = -\beta_k\}\right)$$

$$= \Phi_{K-1}(\underline{\beta}_k; \underline{\underline{R}}_k) \qquad (14)$$

For example, let k=1 and the Rosenblatt-transformation of the vector $\underline{Z}$ be given by [2,3]:

$$Z_j = \sum_{r=1}^{j} \delta_{jr} V_r \quad (\delta_{11}=1) \qquad (15)$$

Then, $\underline{\beta}_k = - \underline{\beta} + \underline{\delta}_k \beta_k$ and $\underline{\underline{R}}_k = \{\underline{\delta}_r^T \underline{\delta}_s ; r,s \neq k\}$ in eq. (14). Normalization yields:

$$\underline{\alpha}_{m,i} = \frac{1}{\| \underline{\tilde{\alpha}}_m \|} \sum_{k=1}^{K} \alpha_{ki} \varphi(\beta_k) \Phi_{K-1}(\underline{\beta}_k; \underline{\underline{R}}_k) \qquad (16)$$

Similarly,

$$\underline{\alpha}_{\sigma,i} = \frac{1}{\| \underline{\tilde{\alpha}}_\sigma \|} = \sum_{k=1}^{K} (-\beta_k \alpha_{ki}^2) \varphi(\beta_k) \Phi_{K-1}(\underline{\beta}_k; \underline{\underline{R}}_k) \qquad (17)$$

Note that $\tilde{\gamma}_k$ or the normalized version $\gamma_k = \tilde{\gamma}_k / \| \underline{\tilde{\gamma}} \|$ can be interpreted as importance measures for the components. A large value of γ_k indicates that this component is significant for system reliability and quality assurance activities should be directed towards improvement of its individual reliability. Alternatively, one may add additional (redundant) components. Further, it is added that the corresponding measures for (minimal) cut set representations in the form $V = \bigcup \bigcap V_{ij}$ are easily derived if one makes use of $P(\bigcup A_i) \leq \sum_i P(A_i)$. Finally, one might wish to introduce sensitivity measures for the deterministic parameter vector $\underline{p}$. This is most easily done by treating it as a vector of

uncertain variables with vanishing standard deviation. In any case and if the logical structure of the system is retained, a change of the location parameters of the uncertain variables resp. those constants in the direction of $-\underline{\alpha}_m$ will improve reliability at the fastest possible rate. If the system originally had the equivalent safety index $\beta_{E,0}$ but $\beta_{E,1} = \beta_{E,0} + \Delta$ is required we need to modify $\underline{p}_0$ to $p_1 = p_0 - \Delta\underline{\alpha}_E$. Clearly, this might not result in an optimal solution in general.

4. OPTIMISATION

It is not possible and not necessary to elaborate in detail on various suitable optimisation techniques. These are standard especially if derivatives of the objective function and/or the constraints are available. To show that those can be computed rather easily with FORM was the primary purpose of the foregoing section. Here, we additionally assume that quality assurance cost can be given as $C(\underline{p})$ and that the gradient

$$\tilde{\underline{c}} = \text{grad}(C(p_0)) \tag{18}$$

exists. For convenience, the normalized gradient $\underline{c} = \tilde{\underline{c}}/\|\tilde{\underline{c}}\|$ is also introduced. Then, two basic tasks have to be solved. The initial set-up for quality assurance, i.e. the parameter $\underline{p}_0$, does not fulfill the safety requirements but a new parameter $\underline{p}_1 = \underline{p}_0 + \underline{\Delta p} = \underline{p}_0 + \Delta\underline{d}$ is required. It can be shown that the optimal direction $\underline{d}$ (the direction in which the increase in reliability is maximal without substantially increasing cost) is:

$$\underline{d}^R = \underline{\alpha}_E - (\underline{\alpha}_E^T\underline{c})\underline{c} \tag{19}$$

On the other hand, if the reliability requirements are already met but the possibility of cost savings has to be investigated, the optimal direction (maximal cost savings at essentially constant reliability) is:

$$\underline{d}^C = -[\underline{c} - (\underline{c}^T\underline{\alpha}_E)\underline{\alpha}_E] \tag{20}$$

A globally optimal quality assurance setup is obtained if $\underline{d}^R$ and $\underline{d}^C$ approach zero which implies that $\underline{\alpha}_E = \underline{c}$. This situation will, however, rarely occur in practice.

5. NUMERICAL ILLUSTRATION

As an example the reliability of a simple life-line system is studied (see figure below). Two sources S1 and S2 supply two areas A1 and A2 by a network of life-lines. The arrows indicate the possible direction of flow. The system is exposed to some extreme

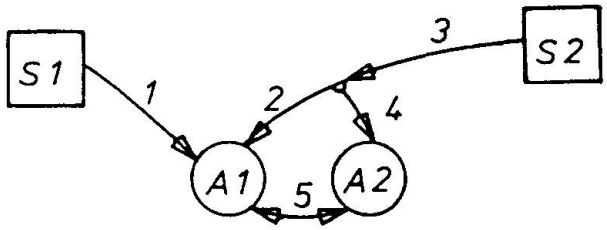

event, e.g. an earthquake. The system is said to fail if either of the areas are no longer supplied. The system failure event can be written down directly or by construction of a fault tree.

$$V = \{[V_1 \cap (V_2 \cup V_3) \cap (V_3 \cup V_4 \cup V_5)] \cup [V_1 \cap V_5) \cup (V_3 \cap V_4) \cup (V_2 \cap V_3 \cap V_5)]\}$$

The minimal cut set representation is:

$$V = \{(V_1 \cap V_3) \cup (V_3 \cap V_5) \cup (V_4 \cap V_5) \cup (V_1 \cap V_2 \cap V_4) \cup (V_1 \cap V_2 \cap V_5)\}$$

This simplistic system is now investigated on the lines presented in sections 2 and 3. We assume a very simple componential state function:

$$g(\underline{X}) = R_k - S \leq 0$$

The "resistances" R_k are assumed to be independently log-normally distributed with mean 6 and standard deviation 2 (in appropriate units). The "loads" S on all components are Rayleigh-distributed with mean 2/3 and independent of the R_k's. Applying the corresponding probability distribution yields

$$g_k(\underline{U}) = \exp[U_{k+1}\,\eta + \xi] - \{2\sigma[-\ln \phi(-U_i)]\}^{1/2} \leq 0$$

with $\eta = 0.3246$, $\xi = 1.7391$ and $\sigma = 0.5319$. The componential safety index is $\beta_k = 3.722$ ($P_{f,k} \approx 10^{-4}$) and the componential sensitivity factors are $\alpha_1 = -0.655$ and $\alpha_k = 0.755$. On a component level the location parameter of the resistances, therefore, is slightly more relevant than the location parameter of the load. The system reliability analysis yields an equivalent safety index of $\beta = 4.48$ ($P_f = 3.8 \cdot 10^{-6}$) indicating rather significant redundancy in the system.The analysis of the componential importance factors, which, by definition, range between 0 and 1 for coherent systems, are:

$$\underline{\gamma} = (0.329, 0.016, 0.625, 0.329, 0.625)$$

This illustrates that component 2 is not important for system reliability although it is not true that it could easily be removed

from the system without substantially changing overall reliability. Components 3 and 5 are most important. Already here, common sense appears to be inefficient in explaining the result.

The analysis of the location sensitivity factors according to eq.(16) gives:

$$\underline{\alpha} = (-0.855, 0.195, 0.007, 0.317, 0.170, 0.317)$$

The computed values are considered as quite a surprise by the author. First of all, the location parameter of the load now becomes most important in contrast to the componential consideration. Secondly, the location parameters of component 3 and 5 are most important followed by component 1 and then 4. Again, the median resistance of component 2 has little relevance. These results have been obtained by using so-called crude FORM but almost exact results can be produced with higher order methods which are not given here. Nevertheless, the general picture does not change with the application of more sophisticated reliability methods. That any possible effort should be directed towards a better quantification of the load in that system as opposed to the componential consideration certainly would not have been detected by a less systematic analysis. At most, intuition had suggested that component 5 ought to be made strong.

Given a reliability requirement, for example, $\beta = 4.76$ ($P_f = 10^{-6}$) and constant unit cost when increasing the resistance in the system components the location parameters of the R_k's should be increased proportional to the computed α-values until the required reliability is achieved. Obviously, because reliability is affected rather non-linearly by changes in those parameters, an exact solution requires iteration.

With eq. (19) and the assumption that the cost of the system components are proportional to the location parameters of the R_k's and to the length of the pipe it is easy to determine the appropriate direction $\underline{d}^R$ to modify the R_k's in a cost optimal manner. It is to be mentioned that in this case the direction $\underline{d}^R$ is almost identical to $\underline{\alpha}$ unless the lengths of the pipes differ dramatically.

6. CONCLUSIONS

Planning of efficient quality assurance measures is optimisation involving an appropriate modelling of the system and the computation of importance and sensitivity measures. Approximate methods suitable in practical applications are available. Such a formal reliability analysis quite frequently results in actions to improve the quality which are not expected from classical deterministic analysis. The author even presumes that a probabilistic sensitivity analysis makes more engineering sense than the substitution of classical safety provisions by their probabilistic counter part.

REFERENCES

[1] RACKWITZ R., Planning for Quality-Concept and Numerical Tools, Introductory Report of IABSE-Workshop on Quality Assurance within the Building Process, 08.06. - 10.06.1983, Rigi, Schweiz, pp. 49-64

[2] HOHENBICHLER M., RACKWITZ R., First-Order Concepts in System Reliability, Struct. Safety. 1, 3, 1983, pp. 177-188

[3] HOHENBICHLER M., RACKWITZ R., Non-Normal Dependent Vectors in Structural Reliability, Journ. of the Eng. Mech. Div., ASCE, Vol 107, No. 6, 1981, pp. 1227-1249

[4] HOHENBICHLER M., GOLLWITZER S., KRUSE W., RACKWITZ R., New Light on First- and Second-Order Reliability Methods, to be published

[5] HOHENBICHLER M., Mathematische Grundlagen der Zuverlaessigkeitsmethode erster Ordnung und einige Erweiterungen, Berichte zur Zuverlaessigkeitstheorie der Bauwerke, Technische Universitaet Muenchen, SFB 96, Heft 72, 1984

[6] DITLEVSEN O., Generalized Second Moment Reliability Index, Journ. of Struct. Mech., Vol. 7, 4, 1979, pp. 435-451

[7] GOLLWITZER S., RACKWITZ R., Equivalent Components in First-Order System Reliability, Rel. Eng., Vol. 5, 1983, pp. 99-115

Recent Advances in Structural Systems Reliability Theory

Développements de la théorie de la fiabilité des systèmes structuraux

Fortschritte in der Zuverlässigkeitstheorie für Systeme

Palle THOFT-CHRISTENSEN
Prof. of Applied Mathematics
University of Aalborg
Aalborg, Denmark

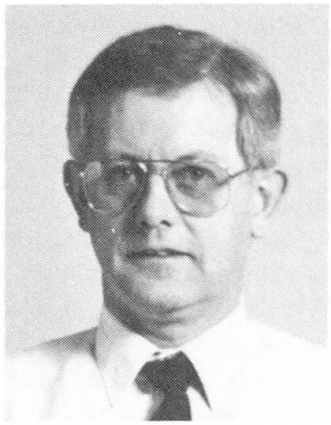

Palle Thoft-Christensen, born in 1936, M.Sc. in engineering in 1960 and Ph.D. in plasticity theory 1963. Research Associate at Brown University, USA, and the Technical University of Denmark. Since 1966 Professor of Applied Mathematics at the Engineering Academy of Denmark and the University of Aalborg. He works on structural reliability problems.

SUMMARY

The paper gives a brief review of recent advances in structural systems reliability with emphasis on the research performed at the University of Aalborg, Denmark. It is shown that stability and fatigue reliability analysis can be integrated into the β-unzipping method. Finally, optimal design with reliability constraints is described.

RÉSUMÉ

L'article rappelle brièvement les développements récents dans la théorie de la fiabilité des systèmes structuraux et mentionne les recherches effectuées à l'Université d'Aalborg, Danemark. Il montre comment les problèmes de stabilité et du comportement à la fatigue peuvent être analysés et introduits dans la théorie de la fiabilité. L'article conclut avec quelques remarques concernant le dimensionnement optimal des systèmes structuraux.

ZUSAMMENFASSUNG

Die an der Universität von Aalborg kürzlich erzielten Fortschritte in der Zuverlässigkeitstheorie für Systeme werden dargestellt. Es wird gezeigt, in welcher Weise auch Stabilitäts- und Ermüdungs-Probleme in eine Zuverlässigkeits-Analyse eingefügt werden können. Zuletzt werden Fragen der optimalen Bemessung von Systemen angeschnitten.

1. INTRODUCTION

In this paper recent advances in structural systems reliability are discussed from an application point of view. It is not attempted to give a concise and comprehensive presentation here, but rather a brief orientation on what can be performed to-day. The design procedure based on a set of partial coefficients is probably the most advanced procedure widely used at present. Clearly, it has many advantages compared with the traditional methods, especially if the partial factors are calibrated by a rational procedure. However, until recently partial coefficients have often been updated on the basis of experience, i.e. if during - say a 10 year period - only few failures are observed for a given type of structure then the corresponding partial coefficients are relaxed and vice versa. A much more satisfactory approach is determination of rational sets of partial coefficients by using modern structural reliability theory. Several different procedures have already been used by code committees. One approach is described in detail by Thoft-Christensen & Baker [1].

It is well known that most structural failures occur for unexpected reasons (gross errors) and therefore, they are not included in the usual structural reliability analysis. In structural reliability theory only recognised failure modes such as buckling, plastic collapse, fatigue failure, etc. and modes of unserviceability are included. Gross errors are usually major mistakes either in planning, design, analysis, construction, use or maintenance of the structure. In general, gross errors are not direct included in the estimate of the safety or reliability of a structure, but they are treated separately. As emphasized by Thoft-Christensen & Baker [1] the most natural way to treat gross errors is to improve the quality assurance.

Estimation of the probability of failure of single structural elements is now considered a rather trivial task although there is still a need for data concerning the probability distributions of material properties (e.g. yield stresses), load parameters (e.g. wind loads), and geometrical quantities (e.g. cross-sectional areas). When probability distributions for these so-called basic variables are known and the failure criterion for a given structural element is given then the probability of failure is

$$P_f = \int_{\omega_f} f_{\overline{X}}(\overline{x})\,d\overline{x} \tag{1}$$

where ω_f is the failure domain (the domain of unsafe states in the space of basic variables) and $f_{\overline{X}}$ is the joint distribution function for the set of basic variables $\overline{X} = (X_1, \ldots, X_n)$. Calculation of P_f on the basis of (1) will require estimation of an n-dimensional integral and such an estimate will in most cases be very time consuming. Further, $f_{\overline{X}}$ is only known in a few simple situations. Therefore, a more simplified measure of the reliability is needed. The so-called reliability index is now accepted by most researchers in this field as a satisfactory measure for the safety (or reliability) of a structural element. This reliability index is described in detail by Thoft-Christensen & Baker [1]. A brief definition of the reliability index can be given in the following way.

Let the relevant basic variables be $\overline{X} = (X_1, \ldots, X_n)$. By a suitable transformation $\overline{X}$ is transformed into a set of independent standard normal variables $\overline{Z} = (Z_1, \ldots, Z_n)$. Further, let the so-called failure function (limit state function) f divide the z-space into a failure region ($f(z) \leq 0$) and a safe region ($f(z) > 0$). The reliability index β is then defined as the smallest distance from the origin to the failure surface ($f(z) = 0$) in the standard normal z-system. It can then be shown that

$$P_f \approx \Phi(-\beta) \tag{2}$$

where Φ is the standard normal distribution function. $M = f(\overline{Z})$ is called the safety margin.

The reliability index β can be estimated for any failure mode of a structural element if the corresponding failure function is known. It is much more complicated to estimate the probability of failure for the complete (redundant) structure. However, in the last decade several heuristic techniques have been developed. Two methods - the β-unzipping method and the branch-and-bound method - are presented in detail in a new book by Thoft-Christensen & Murotsu [2]. In this paper only the β-unzipping method developed at the University of Aalborg will be presented.

It has of course for many years been recognised that a fully satisfactory estimate of the reliability of a structure must be based on a systems approach. For statically determinate (non-redundant) structures failure in any member will result in failure of the total system (structure). However, failure in a single element in a structural system will not always result in failure of the total system, because the remaining elements may be able to sustain the external load by redistribution of the internal load effects (statically indeterminate or redundant structures). Further, a structural system will in general have a large number of potential failure modes and the most important modes must be taken into account in an estimate of the reliability of a structure. Identification of the most important (significant) failure modes can be performed by the β-unzipping method.

2. DEFINITION OF FAILURE

It is convenient to divide the different types of failure definitions into three groups:

- failure of a failure element
- failure of a structural element
- failure of a structural system.

To illustrate these different groups of definitions consider the simple frame in figure 1 loaded by two concentrated loads P_1 and P_2. The *structural system* consists of three *structural elements* and each structural element has a number of failure modes called *failure elements.* For the sake of simplicity assume that a failure element is a potential yield hinge. Then the frame has 7 failure elements as indicated by × in figure 1. Let P_1 and P_2 be normally distributed N(55 kN, 5.5 kN) and N(45 kN, 4.5 kN) and let the bending moment capacity R_i of all failure elements be identical and normally distributed N(135 kNm, 13.5 kNm). Further, let R_1, R_2, R_6, and R_7 be fully correlated and likewise R_3, R_4, and R_5 fully correlated. It is then (see Thoft-Christensen & Murotsu [2]) straightforward to calculate the reliability indices β_i, i = 1, 2, . . . , 7 for all failure elements (see table 1).

Failure element, i	1	2	3	4	5	6	7
β_i	4.40	8.48	8.48	4.46	2.55	2.55	1.67

Table 1

A simple definition of failure would be failure in a single failure element. That is, the structure is considered to be in a state of failure when a single failure element fails. The probability of failure P_f is then calculated as the probability of having failure in failure element 1 and/or in failure element 2 . . . and/or in failure element 7, and it can be shown that a good estimate of P_f is

$$P_f \approx 1 - \Phi_7(\bar{\beta} \; ; \bar{\bar{\rho}}) = 0.0529 \tag{3}$$

where Φ_7 is the 7-dimensional standardized normal distribution function, $\bar{\beta} = (\beta_1, \ldots, \beta_7)$ and $\bar{\bar{\rho}}$ is the correlation matrix for the safety margins. This definition is called a failure modelling at level 1 and

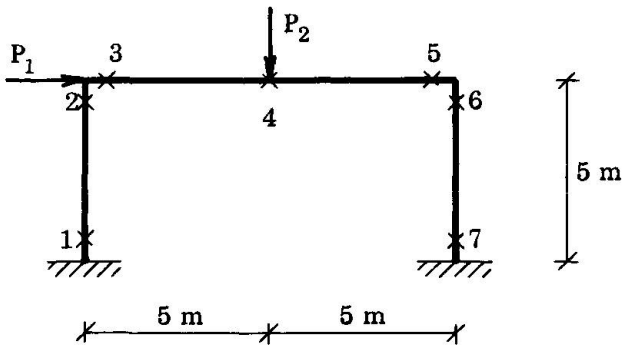

Figure 1. One-storey frame.

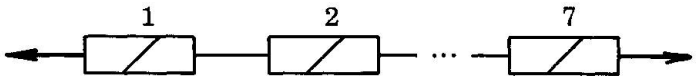

Figure 2. Failure modelling at level 1.

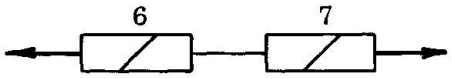

Figure 3. Failure modelling of the right-hand column.

can be illustrated as a series system where the elements are failure elements (see figure 2). A formal reliability index can then be defined as

$$\beta = -\Phi^{-1}(P_f) = 1.62 \tag{4}$$

Note that more failure elements could have been included in the estimate of P_f, e.g. instability failure of the two columns.

For some structures it is useful to consider the single structural elements separately and define failure of a structural element as failure of a single failure element in the structural element. Consider as an example the right-hand column of the frame in figure 1. This column has two failure elements, namely failure elements 6 and 7. Failure of the structure could be defined as failure of any of the three structural elements (one beam and two columns). For the specific column above the probability of failure is the probability of having failure in failure element 6 or/and in failure element 7. This can be modelled as shown in figure 3. The reliability indices for failure elements 6 and 7 are shown in table 1 and it can be shown that the correlation coefficient between the corresponding safety margins is 0.98. Therefore, the probability of failure of the structural element is

$$P_f \approx 1 - \Phi_2(1.67,\ 2.55\ ;\ 0.97) = 0.04746 \tag{5}$$

The corresponding reliability index is $\beta = 1.67$, which is equal to the reliability index for failure element 6 due to the fact that the correlation coefficient is close to 0.98 and β_6 is much smaller than β_7.

For redundant structures failure in a single failure element or a single structural element will in general not be considered as failure of the complete structure. For some elasto-plastic structures it may be more relevant to define failure of the structure as formation of a mechanism. For other structures is could be more natural to define failure of the structure as failure in two failure elements (level 2 modelling). Independently of the definition chosen it is important to have at disposal a method by which the most significant failure elements, pairs of failure elements or mechanisms can be identified because the total number of failure elements, pairs of failure elements or mechanisms are usually too high to include all in the reliability analysis.

3. IDENTIFICATION OF SIGNIFICANT FAILURE MODES

Return to the simple frame in figure 1. Estimation of the probability of failure when failure of the frame is defined at level 1 is based on the series system shown in figure 2 and the calculation of P_f is given by (3). However, the number of failure elements in the series system can easily without loss of accuracy be reduced to a system with only three elements, namely nos. 5, 6, and 7, because these elements have much smaller β-values than those erased. The calculated probability of systems

failure will then be almost unaffected and the calculation procedure simplified. Failure elements 5, 6, and 7 are called significant (or critical) failure elements.

To obtain the significant pairs of failure elements at level 2 the structure is modified by assuming in turn failure in the significant failure elements and adding fictitious loads corresponding to the load-carrying capacities of the elements in failure. As an illustration modify the simple frame in figure 1 by assuming failure (formation of a yield hinge) in failure element 7 and add a set of fictitious bending moments if the element is ductile. If the failed element is brittle no ficitious bending moments are added. The modified structure is then analysed and new β-values are calculated for the remaining elements. In this case failure elements 6, 5, and 1 have the smallest β-values, namely 2.48, 2.64, and 3.39, respectively. By this procedure the significant pairs of failure elements, namely (7, 6), (7, 5), and (7, 1) are identified. By continuing this procedure (assuming failure in failure elements 5 and 6) one more significant pair is identified, namely (6, 7). It turns out that the corresponding reliability index for the frame (at level 2) is 2.45.

When failure is defined as formation of a mechanism the procedure mentioned above can be continued but it is much more efficient to base the identification of significant mechanisms on so-called fundamental mechanisms. This procedure is described in detail by Thoft-Christensen & Murotsu [2] and will not be treated here. It can be mentioned that this definition of systems failure results in a β-value equal to 4.19 for the frame in figure 1.

In a paper by Sørensen, Thoft-Christensen & Sigurdsson [3] a program package is described by which significant mechanisms in plane and space frame and lattice structures are identified automatically.

It is obvious that the method (β-unzipping method) presented above will give an upper bound for the systems reliability index β as some failure modes are omitted. However, it is the experience that the upper bounds obtained are very close to the correct value. Methods exist by which lower values can be obtained, but it seems to be much more difficult to obtain »good» lower bounds.

Combined failure conditions (e.g. between the bending moment and the axial force) for a failure element are a little complicated to include in the systems reliability analysis. However, when failure is defined as formation of a mechanism and when the β-unzipping method is used to identify significant mechanisms, the procedure is quite simple (see Thoft-Christensen, Sigurdsson & Sørensen [4].

4. FATIGUE RELIABILITY ANALYSIS

The β-unzipping method described is quite general in some sense. It can be used in connection with several systems failure definitions, and a large number of failure modes for structural elements and joints can be included by an appropriate choice of failure elements. However, the method has until now only been used for static loading. It is not yet clear how to modify the method so that dynamic effects of dynamically sensitive structures can be included.

For some structures one of the most important forms of failure is due to fatigue. This is e.g. the case for offshore structures of the jacket type on deep water where estimates of the fatigue life of the welded tubular joints are associated with great uncertainty. Two different approaches in fatigue life assessment, namely

- the S-N approach
- the fracture mechanics approach

can be used. The traditional applications of these approaches are non-probalistic since all parameters affecting the fatigue life are assumed deterministic. Conservative values for the relevant parameters are chosen to ensure a satisfactory safety factor. In the last decade probabilistic models for fatigue damage and assessment of fatigue reliability of structures have been developed (see e.g. Madsen, Skjong & Maghtaderi-Zadeh [5], Wirsching [6]).

Both approaches can easily be integrated with the systems reliability analysis at level 1 presented above by simply considering fatigue of a joint as a failure element. The corresponding reliability index is calculated on the basis of a safety margin which can be formulated in at least two equivalent forms when the S-N approach is used, namely

$$M_1 = D - D_0 \tag{6}$$

or

$$M_2 = L - L_0 \tag{7}$$

where D is the actual accumulated fatigue damage and D_0 the accepted accumulated fatigue damage in the required lifetime L_0 of the structure. L is the actual lifetime of the structure. When the fracture mechanics approach is used the following type of safety margin can be applied

$$M_3 = C_0 - C \tag{8}$$

where C_0 is the critical crack size and C the actual crack size in the required lifetime of the structure.

As an example consider fatigue reliability analysis of a tubular joint of an offshore structure (see Wirsching [6]). Such an analysis is not trivial due to the many sources of uncertainty involved. All the way from the statistical description of the wave loading to the calculation of the stress process considerable uncertainty must be taken into account. A number of parameters will affect e.g. the accumulated fatigue damage D used in the S-N approach. First of all, model uncertainty must be modelled by a random variable B. The load effect on D is modelled by two variables, namely the number of zero upcrossings ν of the assumed narrow-banded stress response process and the variance σ_S^2 of the stress range process. The S-N curve (S is the stress range and N the number of cycles to failure) characterizing the fatigue performance under constant amplitude loading is given by two empirical constants m and K. Correction for non-narrow banded response is introduced by a parameter η. The effect of the material thickness t is modelled by t and a power parameter M_1. Finally, D will of course depend on the required lifetime ℓ_0. Therefore,

$$D = f(\ell_0, \nu, \sigma_S, B, m, K, \eta, t, M_1) \tag{9}$$

where f is a function of 9 variables. B, K, and M_1 are modelled by random variables and the remaining parameters are assumed deterministic. If f is known and data for all parameters (including the random variable D_0) are given then the reliability index β for the fatigue reliability of the joint can be calculated.

From a systems point of view fatigue failure of a joint is considered a failure element and is therefore included in the series system used by level 1 modelling. The correlation between the safety margin used for the fatigue failure element and the bending moment failure elements need to be estimated e.g. by simply assuming independence. When systems failure is defined at level two it is more difficult to include fatigue failure elements because the reserve strength of e.g. a joint after fatigue has taken place must be estimated. For a tubular joint fatigue failure will often occur as a brittle failure between the brace and the chord. When this is the case the brace is simply completely removed and the structure modified in this way is then reanalysed.

5. STABILITY RELIABILITY ANALYSIS

Stability reliability analysis can be performed at two levels, namely analysis of the local stability of the single structural elements and global analysis of the complete structure. The critical load P_{cr} of a single structural element in compression is usually written as

$$P_{cr} = (\frac{\pi}{\ell_e})^2 EI \tag{10}$$

where E is the modulus of elasticity, I the moment of inertia, and ℓ_e the so-called effective length of the structural element. ℓ_e is readily determined as a function of the rotational restraints at the end of the bar. Within the limits of validity of (10) it is straightforward to integrate the stability reliability analysis with the β-unzipping method simply by considering the stability failure mode as a failure element with the safety margin

$$M = P_{cr} - AP \tag{11}$$

where A is a model uncertainty variable and P the axial load in compression in the structural element.

When a beam is subjected to a combination of axial load P and a bending moment B the stability reliability can in some cases be estimated on the basis of an interaction formula as the following:

$$\frac{P}{P_{cr}} + \frac{B_0}{B_{cr}}\left(\frac{1}{1-(P/P_E)}\right) = 1 \tag{12}$$

where P_{cr} is a function of the effective slenderness of the beam, B_0 is the maximum moment, B_{cr} the critical moment, and P_E the critical Euler load for elastic buckling in the plane of applied moments. P_{cr}, B_{cr}, P_E, and the interaction curve will in general be associated with some uncertainty. This can be taken into account, e.g. by introducing four model uncertainty variables X_1, X_2, X_3, and X_4 in the safety margin in the following way

$$M = X_1 - \frac{P}{X_2 P_{cr}} - \frac{B_0}{X_3 B_{cr}}\left(\frac{1}{1-(P/X_4 P_E)}\right) \tag{13}$$

The mean values and standard deviations of X_i, $i = 1, \ldots, 4$ must be estimated from experimental data.

Formulas like (10) and (12) are based on the assumption that the beams are perfectly straight. However, in practice this assumption is seldom satisfied. The reduction effect of imperfections in the load-carrying capacity of structural members with instability failure modes is a research area which has been subject to growing interest in the last decades (see e.g. Elishakoff [7]). It is a fact that imperfections ranging from residual stresses, from manufacturing to eccentricities in joints and loading are unavoidable in real structures, and they are very seldom predictable. Imperfections are best introduced in the stability analysis through a probabilistic approach where the imperfections are modelled as random variables (or stochastic processes).

Faber & Thoft-Christensen [8] have investigated the reliability of a plane lattice structure (see figure 4) with local imperfections. In the paper it is shown that the reduced critical load-carrying capacity P_i due to imperfections can be written $P_i = \lambda_i 2P_{CL}$, where P_{CL} is the local critical load of the individual simply supported columns. λ_i is the reduced critical load-carrying intensity given by

$$\lambda_i = \lambda_1\left(1 + \tfrac{1}{2}\, b(1-\lambda_i)^{-3}\right)^{-1} \tag{14}$$

where $\lambda_1 = P_{CG}/2P_{CL}$ (P_{CG} is the global critical load of the structure) and where $b = b_0/i_m$ (b_0 is the amplitude of the imperfections and i_m the radius of gyration of the horizontal members). The load intensity is λ (see figure 1).

The load intensity λ and the imperfection amplitude b are modelled by random variables Δ and B. Then λ_i will be the outcome of a random variable Δ_i and a natural safety margin is $M = \Delta_i - \Delta$. The reliability index β can then be calculated. The conclusion from this special example was that β is insensitive to variations in the imperfection uncertainty.

The global buckling capacity of a complete structure is in general very time-consuming to obtain. Research in this field is being performed at the University of Aalborg, but the results are not yet published. The approach can be briefly described in the following way. By non-linear analysis (proportionally increased loading) of the structure a number of points of the unknown limit curve are identified. The safety margin corresponding to the limit curve is then used in estimating the stability reliability of the structure.

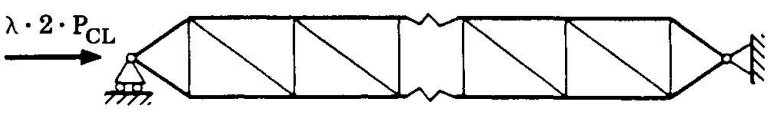

Figure 4. Plane lattice structure.

6. OPTIMAL DESIGN AND RELIABILITY

In the classical deterministic structural optimization for truss and frame structures all variables (dimensions, loads, strengths, etc.) are assumed to be deterministic and the design variables are usually the cross-sectional areas A_i, $i = 1, \ldots, k$, where k is the number of structural elements. The objective function is naturally the total cost of the structure. However, it is often assumed that the cost of the structure is proportional to the weight of the structure. In structures where only one material is used the weight is proportional to $W(\overline{A}) = \overline{\ell}^T \overline{A}$, where $\overline{A} = (A_1, \ldots, A_k)$ and $\ell = (\ell_1, \ldots, \ell_k)$ is the deterministic lengths of the structural elements. The constraints signify that the stresses and the displacements should everywhere be smaller than some prescribed design values.

In modern design theory based on a probabilistic point of view loads and strengths are modelled by random variables. The objective function is unchanged but the constraints are now replaced by only one constraint, namely $\beta_S(\overline{A}) - \beta_S^0 \geq 0$, where β_S is a measure of the systems reliability and β_S^0 the corresponding target value.

Optimal design with reliability constraints is an area where significant progress has taken place in the last few years (see e.g. Thoft-Christensen & Murotsu [2]). Research, where the β-unzipping method is used in estimating the systems reliability index β_S has been conducted at the University of Aalborg (see Thoft-Christensen & Sørensen [9] and Sørensen & Thoft-Christensen [10, 11]). A number of different effective optimization procedures are discussed in these papers and applied to a number of examples, e.g. jacket structures with tubular joints.

7. REFERENCES

1. THOFT-CHRISTENSEN, P. & M. J. BAKER: Structural Reliability Theory and Its Applications. Springer-Verlag, 1982.
2. THOFT-CHRISTENSEN, P. & Y. MUROTSU: Application of Structural Systems Reliability Theory. Springer-Verlag, 1986.
3. SØRENSEN, J. D., P. THOFT-CHRISTENSEN & G. SIGURDSSON: Development of Applicable Methods for Evaluating the Safety of Offshore Structures. Part 2. Structural Reliability Theory, Paper no. 11, The University of Aalborg 1985.
4. THOFT-CHRISTENSEN, P., G. SIGURDSSON & J. D. SØRENSEN: Development of Applicable Methods for Evaluating the Safety of Offshore Structures. Part 3. Structural Reliability Theory, Paper no. 17, The University of Aalborg, 1986.
5. MADSEN, H. O., R. SKJONG & M. MOGHTADERI-ZADEH: Experience on Probabilistic Fatigue Analysis of Offshore Structures. OMAE Conference, Tokyo, Japan, April 13 - 17, 1986.
6. WIRSCHING, P. H.: Fatigue Reliability for Offshore Structures. J. Struct. Eng., Vol. 110, No. 10, 1984, pp. 2340 - 2356.
7. ELISHAKOFF, I.: How to Introduce the Imperfection-Sensitivity Concept in Design. Collapse: The Buckling of Structures in Theory and Practice (eds. J. M. T. Thompson & G. W. Hunt), Cambridge University Press, 1983.
8. FABER, M. H. & P. THOFT-CHRISTENSEN: Reliability Analysis of a Plane Lattice Structure with Local Imperfections. Structural Reliability Theory, Paper no. 14. The Univ. of Aalborg, 1985.
9. THOFT-CHRISTENSEN, P. & J. D. SØRENSEN: Optimization and Reliability of Structural Systems. Structural Reliability Theory, paper no. 6. The University of Aalborg, 1984.
10. SØRENSEN, J. D. & P. THOFT-CHRISTENSEN: Structural Optimization with Reliability Constraints. Structural Reliability Theory, paper no. 13. The University of Aalborg, 1985.
11. SØRENSEN, J. D. & P. THOFT-CHRISTENSEN: Recent Advances in Optimal Design of Structures from a Reliability Point of View. 9th Advances in Reliability Technology Symposium, Bradford, England, April 1986.

Role of Probabilistic Analysis for Quality Assurance

Rôle des calculs probabilistes pour l'assurance de qualité

Die Rolle probabilistischer Berechnungen in der Qualitätssicherung

Dieter D. PFAFFINGER
Dr. sc. techn.
P + W Engineering
Zurich, Switzerland

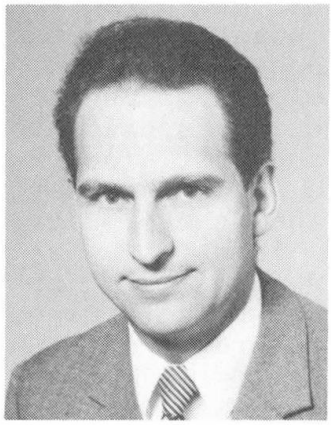

Dieter D. Pfaffinger studied Civil Engineering at the ETH Zurich where he also received his Ph.D. degree. He then went to Brown University, USA. Returning to Switzerland he worked for more than 10 years in private industry and has been a consultant in numerous structural projects. He is now a partner of P + W Engineering.

SUMMARY

In the present contribution, first a survey of probabilistic analysis methods is given. In two examples probabilistic and deterministic results are compared. The advantages and the limits of probabilistic analyses are discussed. in the conclusions the most important points which have to be considered in order to obtain meaningful probabilistic results are listed.

RÉSUMÉ

La contribution présente un aperçu des méthodes de calcul probabilistes. A l'aide de deux exemples, on compare les résultats des méthodes déterministe et probabiliste. On présente ensuite les avantages et les limites des calculs probabilistes. En conclusion, on relève les principales conditions à respecter pour l'obtention de résultats probabilistes sensés.

ZUSAMMENFASSUNG

Im vorliegenden Beitrag wird zunächst ein Überblick über probabilistische Berechnungsmethoden gegeben. An zwei Beispielen werden probabilistische und deterministische Ergebnisse verglichen. Die Möglichkeiten und Grenzen probabilistischer Berechnungen werden diskutiert. In den Schlussfolgerungen werden die wichtigsten Punkte zusammengestellt, welche für sinnvolle probabilistische Ergebnisse beachtet werden müssen.

1. INTRODUCTION

Many dynamic excitations such as wind forces, waves or strong earthquakes have inherent probabilistic properties. This random character concerns the occurrance as well as the dynamic characteristics of the loads such as frequency content, maximum excitation and length of duration. In order to judge the behaviour of a structure under such loads, their probabilistic nature should be taken into account.

On the side of the structure the resistances are also not sharply defined deterministic quantities but consist of mean values and variances. The variances, however, are usually much smaller than the variances of the loads. Therefore the resistances of the structure are frequently assumed to be deterministic. To assure the integrity of a structure also under extreme loads, failure mechanisms leading to collaps or partial collaps have to be investigated. If for instance the probability of occurrance of certain plastic hinges which lead to a failure mechanism is known from a probabilistic analysis, then the probabilities of corresponding failure mechanisms can be determined. From these the probability of collaps of the structure is obtained.

A probabilistic structural analysis usually involves more complex analysis methods or more time consuming calculations than conventional deterministic methods. Therefore the question of the significance as well as of the cost/benefit-ratio of such investigations has to be asked. In the following some of the characteristic properties of probabilistic analyses are worked out. From these insights their role for the quality assurance of a structure is discussed.

2. METHODS OF PROBABILISTIC ANALYSIS

The methods available for a probabilistic analysis are basically different for linear and for nonlinear structural behaviour. In the simplest case the structure is linear and the loads consist of stationary random processes with normal distributions. In the frequency domain the loads are then completely defined by their power spectral (p.s.d.f.) and cross spectral density functions (c.s.d.f.). For the discretized structural model, the input and output processes are related by the transfer function theorem. In the case of a displacement $q_i(t)$

$$S_{q_i}(\Omega) = \sum_{j=1}^{n} \sum_{k=1}^{n} H_{ij}(\Omega)\overline{H_{ik}(\Omega)}S_{jk}(\Omega) \qquad (1)$$

holds, where $S_{q_i}(\Omega)$ denotes the p.s.d.f. of $q_i(t)$, $H_{ij}(\Omega)$ and $H_{ik}(\Omega)$ are the complex frequency response functions between degrees of freedom i,j and i,k, respectively, and $S_{jk}(\Omega)$ are the p.s.d.f. and c.s.p.f. of the loads. Similar relationships hold for forces, stresses, accelerations etc. Integration of eq.(1) furnishes the variance σ^2. With the expected frequency

$$f = \frac{1}{2\pi} \left[\frac{\int_0^\infty \Omega^2 S_{q_i}(\Omega) d\Omega}{\int_0^\infty S_{q_i}(\Omega) d\Omega} \right]^{1/2} \qquad (2)$$

and the duration T of the process the probability distribution p(x) of the extreme values

$$x = |q_{extr.}| \qquad (3)$$

can be derived. For example in the case of uncorrelated extreme values

$$p(x) = \frac{2fT}{\sigma} \left(\frac{x}{\sigma}\right) \exp\left[-2fTe^{-\frac{1}{2}\left(\frac{x}{\sigma}\right)^2} - \frac{1}{2}\left(\frac{x}{\sigma}\right)^2\right] \qquad (4)$$

is obtained. Again similar expressions hold for the processes of forces, stresses a.s.o. By integrating p(x) the probability of exeedance of a value x is obtained. The inverse relationship furnishes the values of x associated with given confidence levels. The analysis can be performed either in modal coordinates by superposition of the modal contributions or by working with the original degrees of freedom (direct method). In most cases modal superposition is more efficient than direct integration. It should be mentioned that instead of working in the frequency domain the analysis can also be performed in the time domain using auto- and cross-correlation functions.

The resistances of the structure can be taken as deterministic or probabilistic quantities. In the latter case the joint probability density function of the inner forces and of the resistances is the product of both probability density functions:

$$p(r,f) = p_r(r) p_f(f) \qquad (5)$$

Here $p_r(r)$ denotes the distribution of the resistance and $p_f(f)$ is the distribution of the force. In this equation the force and the resistance are assumed to be statistically independent. Integration over the appropriate bounds furnishes failure probabilities of specific sections.

In the case of nonstationary excitations, all probabilistic quantities become time-dependent. In some cases, however, the loads can be represented as the product of a stationary process and a time-dependent shape function. If linearity of the structure is maintained, the transfer function approach can still be used in a modified form. Again modal superposition is usually computationally more efficient than direct integration. For a general nonstationary process, Monte Carlo simulations have to be made either in modal coordinates or by direct integration.

If the structural behaviour is nonlinear, the principle of superposition is no longer valid. Therefore the transfer function method and modal superposition cannot be applied. The only applicable method is Monte Carlo simulation using direct integration. In the simulations the structure is analysed many times using samples for

the excitations and the resistances. All parameters characterizing the loads and the structure can be changed for each calculation. The structural response quantities are then evaluated by statistics and thus expected maximum values and variances are obtained. In order to get reliable results especially for the extreme values, quite a number of analyses have to be made. Therefore the amount of effort and computing time for such simulations can be substantial.

3. COMPARATIVE EXAMPLES

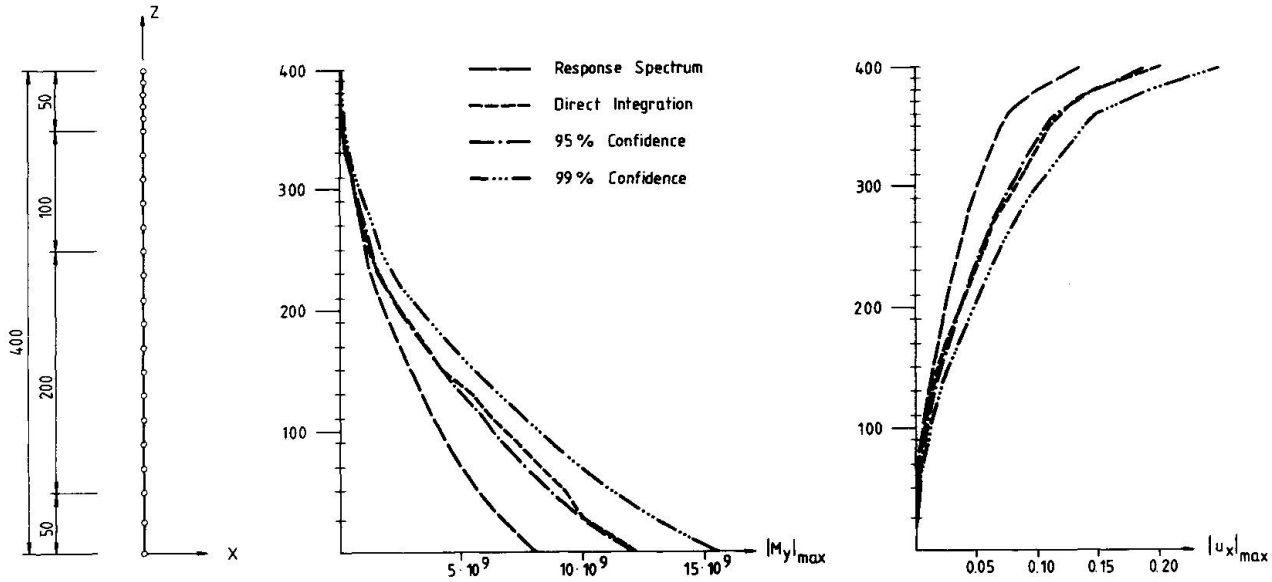

Fig. 1 Probabilistic Analysis of a Skyscraper

In order to get some insight into the results obtained from a probabilistic dynamic analysis as compared to conventional methods, two examples of seismic analysis are shown. Fig.1 shows the FE-model of a high-rise building which is uniformly excited in the x-direction at node 1. The structure has a structural damping coefficient of 0.10. From a probabilistic analysis by the transfer function method the 95 per cent and 99 per cent confidence ranges for the horizontal displacement $|u_x|$ and the bending moment $|M_y|$ were determined. The duration of the output processes was 5 sec. For 5 time functions determined from the p.s.d.f. also Monte Carlo simulations were made by direct time integration to obtain the extreme values. In addition an equivalent response spectrum was determined and a response spectrum analysis was performed. It is seen, that the extreme values from the Monte Carlo simulation are in the vicinity of the 95 per cent confidence range. If the number of samples is increased, these maximum values will further go up. The amount of computing time for the probabilistic analysis was much smaller than for the simulations and was comparable to the computing time for the response spectrum analysis. The results from the latter analysis are much smaller than the results from the simulations and from the probabilistic analysis. This is primarily due to the fact, that response spectra are obtained from average maximum values. In cases of high damping, however, the peak values

are considerably reduced. In addition, modal coupling is neglected in the response spectrum method but is important for higher damping ratios and/or close frequencies. In the probabilistic analysis, on the other hand, modal coupling is always taken into account. This example demonstrates that a probabilistic reanalysis of the structure provides an inexpensive way to check the results from other analyses.

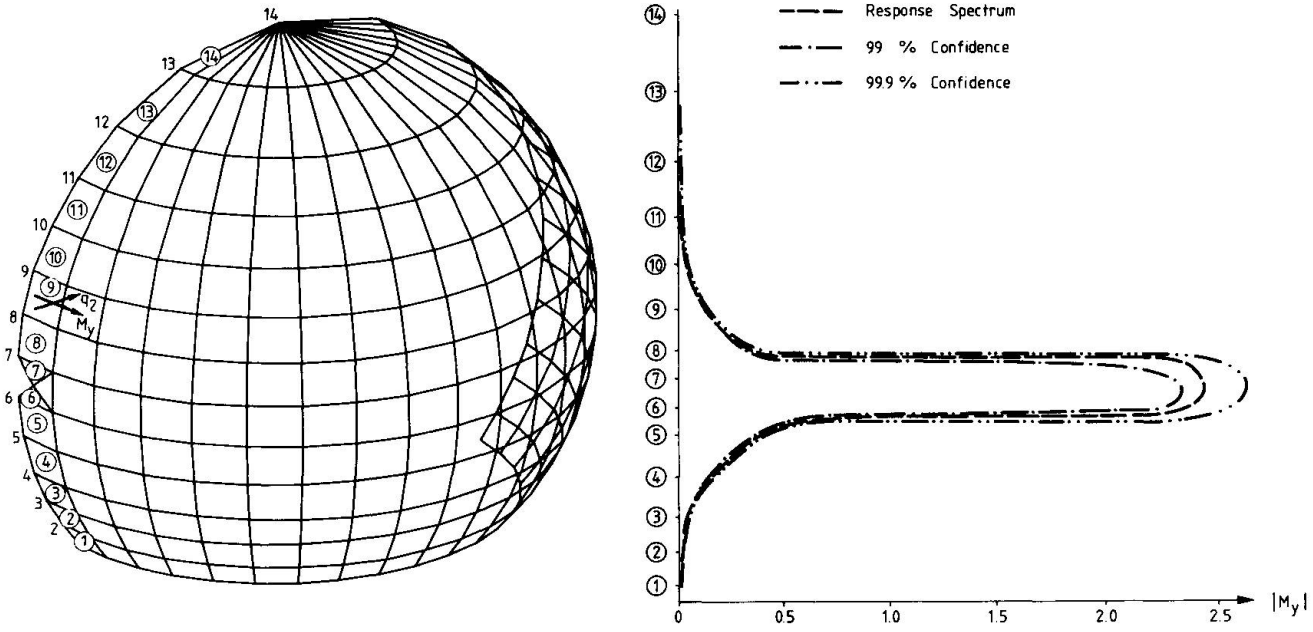

Fig. 2 Probabilistic Analysis of a Nuclear Containment

Fig.2 shows the model of a nuclear containment. The load again consists of uniform seismic excitation in x-direction. The structure has 2 per cent viscous damping. The results show the bending moment $|M_y|$ along a section as calculated by probabilistic analysis with a duration of 2.5 sec. and by response spectra. Here the response spectrum method furnishes results between the 99 per cent and 99.9 per cent confidence interval of the expected maximum values. The sharp increase of the bending moment in the vicinity of nodes 6 and 7 is due to a concentrated mass in that area. If the duration of the excitation increases, the probabilistic results are directly influenced. In the response spectrum analysis, however, the results will not change unless a new set of spectra is used. In this example modal coupling is not important.

In both examples the probability distribution of the forces can be combined with the distribution of the corresponding resistances leading to failure probabilities. Furthermore, also the occurrance of the excitation can be modelled by a probability distribution. Thus for instance the probability of failure during the lifetime of the structure can be determined.

4. ADVANTAGES AND RESTRICTIONS OF PROBABILISTIC ANALYSES

A probabilistic analysis permits the quantification of uncertainties on the side of the loads and of the structure. By introducing confidence levels as in the above examples, different risks are made comparable in a rational way. Probabilistic investigations also allow to take into account risks stemming from different sources and to identify their influence. Considering the computational effort, a probabilistic analysis of a linear structure under stationary excitation is comparable with the effort for a traditional response spectrum analysis and thus much cheaper than time integration. The results are, however, more realistic than response spectrum results because the duration of the excitation as well as modal coupling effects are taken into account.

There are, on the other hand, a number of restrictions to a probabilistic analysis. As all probabilistic formulations are based on random deviations, they will not take into account non-random effects such as design and construction errors. This is, however, also true for conventional calculations. The difficulties to obtain reliable analysis data for the structure and the excitations are usually greater for a probabilistic analysis than for conventional methods. If simulation techniques have to be used such as in the case of nonlinear structural behaviour, they are usually very expensive with respect of problem preparation, computation and evaluation of the results. Thus in order to reduce this effort there is a danger of using too few samples or an oversimplified structure.

5. CONCLUSIONS AND RECOMMENDATIONS

A probabilistic analysis can be a valuable source of information if the following points are kept in mind:

1. All results are only as good as the input data. Therefore great care has to be taken to derive a realistic characterisation of the loads and of the structural properties.

2. For linear structures the transfer function method is usually most efficient in modal coordinates.

3. As for conventional analyses, a probabilistic analysis should first of all always be performed for the linear case and stationary excitation.

4. The duration of the processes directly influences the results. It therefore has to be carefully estimated.

5. Monte Carlo simulations have be done with a sufficient number of samples. The demand of computing time and man hours should be estimated before the beginning of the task.

6. The results of a probabilistic analysis should be considered as one additional source of information on the behaviour of the structure. Together with the results from conventional analyses it provides an improved basis to judge the quality of the design of a structure.

REFERENCES

1. DAVENPORT A.G., Note on the Distribution of the Largest Value of a Random Function with Application to Gust Loading. Proceedings of the Institution of Civil Engineers, Vol.28, Paper No.6739, 1964, pp.187-196.

2. VANMARCKE E.H., On the Distribution of the First-Passage Time for Normal Stationary Random Processes. Journal of Applied Mechanics, Vol.42, March 1975, pp.215-220.

3. PFAFFINGER D., Comparative Seismic Analysis. Proceedings European NASTRAN User's Conference. Munich, 1976.

4. PFAFFINGER D., Die Methode der Antwortspektren aus der Sicht der probabilistischen Tragwerksdynamik. Bericht No.90, Institut für Baustatik und Konstruktion ETH Zürich. Birkhäuser Verlag, Basel, 1979.

5. SCHUELLER G.I., Einführung in die Sicherheit und Zuverlässigkeit von Tragwerken. Verlag von Wilhelm Ernst und Sohn. Berlin, 1981.

6. PFAFFINGER D., Calculation of Power Spectra from Response Spectra. Journal of Engineering Mechanics, American Society of Civil Engineers, Vol.109, No.1, February, 1983.

7. PFAFFINGER D., Zur probabilistischen Erdbebenberechnung von Tragwerken. Festschrift Prof. Dr. B. Thürlimann zum 60. Geburtstag. ETH Zürich, 1983.

8. Proceedings of the International Seminar on Probabilistic and Extreme Load Design of Nuclear Plant Facilities. San Francisco, 1977. American Society of Civil Engineers, New York, 1979.

Leere Seite
Blank page
Page vide

Probabilistic Methods in Dutch Offshore Geotechnics

Méthodes probabilistes en géotechnique offshore aux Pays-Bas

Geotechnische Anwendung der Zuverlässigkeitstheorie bei Niederländischen Meeresbauten

Louis DE QUELERIJ
Civil engineer
Rijkswaterstaat
The Hague, The Netherlands

Louis de Quelerij, born in 1952, obtained his civil engineering degree at the Delft Technical University, the Netherlands. For nine years he was involved in foundation problems of sea-defence systems (storm surge barrier, dams and dikes). Since 1985 he is head of the R & D section for Hydraulic Structures Engineering.

SUMMARY

This paper presents a review of the main geotechnical applications of probabilistic methods with respect to the quality control of the design, construction and maintenance of the storm surge barrier in the south western part of the Netherlands. Attention is paid respectively to the overall fault-tree of the barrier, reliability analysis of the stability of the pier foundation including the economic optimization, risk analysis of flow slides due to scour at the edges of the seabottom protection.

RÉSUMÉ

L'article traite d'applications des méthodes probabilistes pour le contrôle de la qualité du projet, de la construction et de l'entretien de la fondation du barrage anti-tempête dans le sud-ouest des Pays.-Bas. Il traite de l'arbre d'erreur pour le barrage, du calcul de la sécurité de la fondation des piliers, prenant en compte l'optimisation économique et l'analyse du risque d'érosion aux bords du tapis de protection posé sur le sol marin.

ZUSAMMENFASSUNG

Der Aufsatz stellt die wichtigsten Anwendungen der Zuverlässigkeitstheorie auf die Qualitätskontrolle des Entwurfs, der Erstellung und der Unterhaltung des Fundaments eines Sturmflutwehrs in den Südwest-Niederlanden dar. Die folgenden Themen werden behandelt: der Fehlerbaum für das Sturmflutwehr als ganzes, die Stabilitätsanalyse des Pfeilerfundamentes mit Einschluss des ökonomisch optimalen Entwurfs sowie die Risikoanalyse des durch Erosion an den Rändern der Senkmatten verursachten Setzungsfliessens.

1. INTRODUCTION

Since half of the Netherlands is situated below mean sea level the need for an adequate safety system of the Dutch sea defences is obvious. The storm surge barrier in the south-western part of the Netherlands is one of the last large sea defence projects under construction. The barrier in the mouth of the Oosterschelde basin crosses three tidal flow channels (Roompot, Schaar and Hammen) over a total length of 3000 m. with a maximum water depth of 35 m. (Fig. 1).
The storm surge barrier consists of 65 large concrete piers with a submerged weight of 12.000 tons. The piers, prefabricated in a dry dock, were placed by means of a special lift-vessel as gravity offshore structure on the sand bottom, which is covered with filter mattresses. In between the piers steel gates can be lowered during severe storm floods from the North Sea. Under normal conditions the gates are lifted and allow the sea water to flow into the Oosterschelde basin with the tidal movements, in order to maintain the natural state and ecosystem of the estuary. To protect the subsoil and the filter layers against scouring a rubblemound sill was placed around the piers and up to a distance of 600 m. from the piers a bottom protection was applied (Fig. 2).
The barrier as a system has to meet very high safety requirements according to the governmental codes of acceptable flood excess frequencies. It must be emphasized that the quality of the barrier proceeds from the quality of the different structural elements, such as the concrete piers, the steel gates, the bottom protection and the granular foundation. To provide a consistent quality control of the overall system, probabilistic methods were applied with which the different structural elements can be evaluated at a comparable level of reliability.

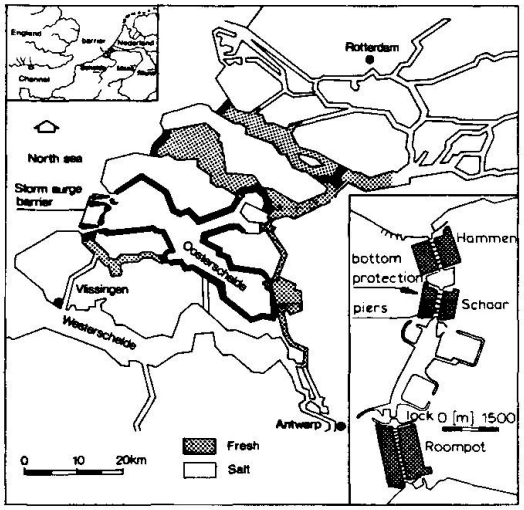

fig. 1 Location of the storm surge barrier.

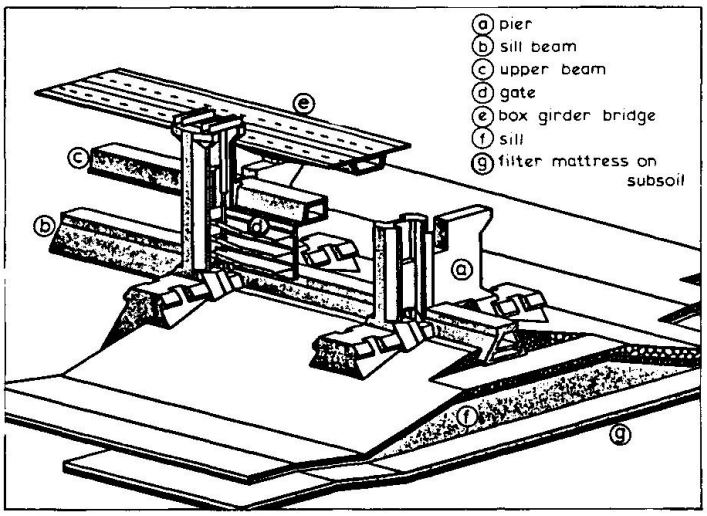

fig. 2 The storm surge barrier.

2. PROBABILISTIC APPROACH STORM SURGE BARRIER

Three steps can be distinguished in the application of probabilistic methods in the design and construction of the storm surge barrier (s.s.b.) [1].
The first step is based on the concept of the design excess frequency of storm surge water levels, according to the design codes for the overtopping height of the Dutch dikes, in which the water level appeared to be the main loading parameter. The s.s.b. however has to withstand, next to storm surge levels, other loading conditions such as water levels inside the basin (headloss in two directions), waves, currents (also in case of malfunctioning of the lowering system of the gates). Since the s.s.b. has to be designed for those loading combinations which potentially will yield most dangers to the structural reliability, the concept of design excess frequency for water levels has to be extended to each potential loading condition. This means that dependent on the structural element to be considered, the probability of all relevant loading parameters have to be taken into account.

The second step in the introduction of probabilistic methods is the performance of reliability analyses. In this type of analysis the uncertainties of both the loading parameters and the structural resistance parameters are accounted for. Since complete safety is unattainable the need for the assessment of an acceptable level of unsafety, expressed in terms of probability of failure, became apparent. For the s.s.b. as a whole a target probability of failure of 10^{-7} per annum (p.a.) is considered acceptable. This safety requirement is based upon the present probability of loss of live due to accidents in the Netherlands (order 10^{-4} p.a. per individu) and the number of fatalities after a possible storm flood catastrophe (order 1000).
To verify if the s.s.b. as a system satisfies the overall safety requirement, each of the components of the structure that contributes to the loss of stability of the s.s.b. has been evaluated. Fault tree - event tree analyses [1] proved to be a useful instrument to systematically assess the contributions of each component to the overall safety of the structure (Fig. 3).

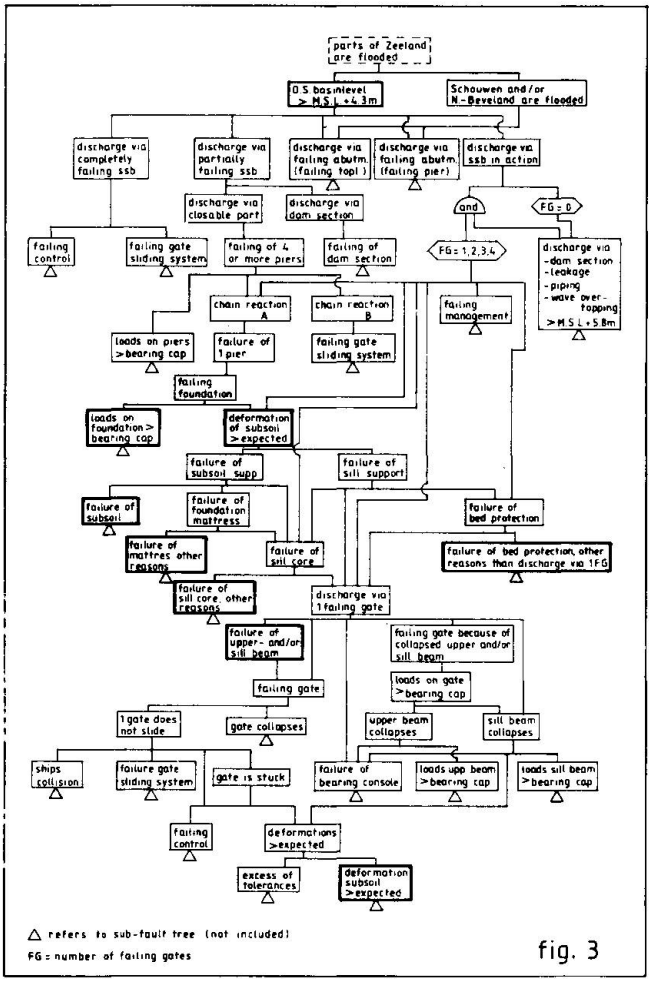

fig. 3

fig. 3 Main fault tree of the s.s.b.

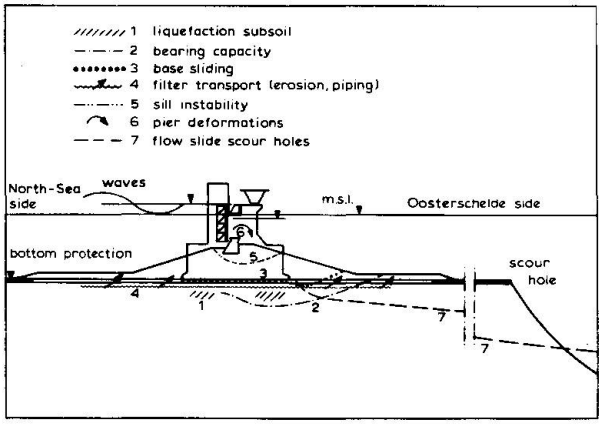

fig. 4

fig. 4 Presentation of the main geotechnical limit states.

The conditions at which the structural components start to fail are referred to as limit states. For the assessment of the reliability of each of these limit-states different probabilistic technics are available. In general it is endeavoured to model the failure mechanisms associated with the limit states of the components by way of amathematical relationship in which the basic strenght (m_j), the loading variables (s_i) and the geometric variables (g_k) are corporated. These relationships can be based on theoretical principles, model tests or on empirical data. Any limit state criterion may be expressed in terms of the basis variables by means of the reliability function Z according to:

$$Z = f(m_j, s_i, g_k) = o \qquad (1)$$

Current methods of probabilistic analyses of safety of structures belong to one of the following three categories, referred to as levels I to III [2].

Level III: concerns analysis of safety based on the use of the exact probability density functions of each of the variables involved in the reliability function.

Level II: concerns a number of approximation methods in which the reliability function is linearized at a selected point (or points).

Level I: includes semi-probabilistic methods where a sufficiently large distance between the strength - and the loading-function is created by the use of partial safety factors with respect to the characteristic value of the basic variables.

As third and last step in the probabilistic approach of the quality control, risk analyses for some structural components and construction operations on the site are performed. In this type of analysis also the effect of attaining the limit states, as far as it concerns economic damage, is evaluated. For some design or construction alternatives economic optimum solutions were derived, under the restriction that the overall target safety of the s.s.b. must be maintained.

3. GEOTECHNICAL LIMIT STATES

The main geotechnical limit states, indicated in the fault tree by thick lines, are depicted in figure 4.
The majority of the limit states concerns loadings under extreme storm conditions, that is when the s.s.b. is closed. However some limit states are critical even under daily tidal conditions with lifted gates. An example of this last type is the flow slide mechanism (liquefaction) due to gradually steepening of the slopes of the scour holes at the edges of the bottom protection.
For the evaluation of the limit states the conventionally applied geotechnical stability and deformation models are not always considered adequat, due to the complexity of the s.s.b., the lack of experience with similar offshore structures and the desired high level of structural quality.
In addition a great number of large scale model tests and finit element calculations were performed, all supported by an extensive geotechnical site investigation programme. The next paragraphs present some applications of probabilistic methods with respect to the quality control of a number of ultimate and serviceability limit states for the foundation design of the barrier.

4. PIER STABILITY AND OPTIMIZATION SILL GEOMETRY

During severe storms, when the gates will be lowered, the piers have to withstand high loadings due to the headloss and the wave action on the barrier. The resistance R of the piers with respect to geotechnical instability consists of two parts: first the passive earth pressure of the sill material at the back-wall of the pier R_p and second the sliding resistance at the base of the pier R_b (Fig.5). Since the horizontal load and associating moments are most uncertain, the stability is evaluated in terms of safety with respect to the total horizontal load (H). So the reliability function can be expressed as:

$$Z = m.\ (R_b + R_p) - H \qquad (2)$$

where m is a factor to account for the uncertainty of the calculation model.
The passive resistance R_p was determined using the Kötter-equations to estimate the coëfficiënt of passive earth pressure K_p.
Two modes of failure, concerning the modelling of the base sliding resistance R_b were evaluated. The first mode, referred to as the bearing capacity, regards curve-linear sliding plane passing through the subsoil. This failure mode is modelled by formulae for the bearing capacity of shallow foundations given by J. Brinch Hansen [3]. The second mode of failure, assuming a horizontal sliding plane between base and foundation, is modelled by a simple friction law:

$$R_b = V * \tan\delta_b \qquad (3)$$

where V is the total pier weight and δ_b the base friction angle.

For the bearing capacity mode of failure the vertical component of the passive pressure is ignored. No generation of excess pore pressure due to the cyclic loading in the foundation is expected, since the subsoil was compacted adequatly.

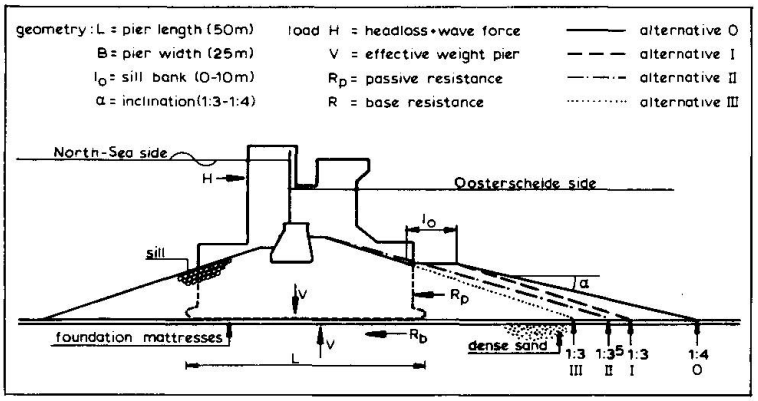

fig. 5 Design alternatives of sill geometry.

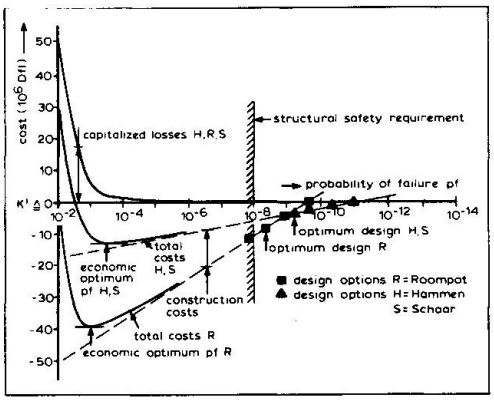

fig. 6 Determination economic optimum sill design.

First the safety requirement was assessed by a level I approach resulting in a minimum overal safety factor FS min ($FS=(R_b+R_p$ design/H design).
Next it was verified by level II analysis (advanced first order, second moment) if the level I safety requirement satisfies the target probability of failure of the foundation according to the fault-tree (p_f target = 10^{-8} p.a.).
From both level I and level II reliability analyses it turned out that the base sliding mode of failure was most critical [4]. Calculation results for different design alternatives show an almost perfect loglinear relationship between the actual safety factor FS and the probability of failure p_f:

$$FS = a * \log p_f + b \qquad (4)$$

where a and b are constants. The minimum safety factor (FSmin = 1.5) appeared to correspond very well with the target probability of failure 10^{-8} p.a.

In the final phase of the design it was considered if the original size of the sill (o-alternative) could be reduced in order to save on construction costs. Reduction of the sill size however implies a reduction of the pier stability since both the pier weight V and the passive resistance R_b will decrease.
Cost calculations for three design alternatives (I, II and III, Fig.5) show the following relationship between the total initial construction costs of the sill C and the associated probability of failure p_f.

$$C = C_o + c * \log p_f \qquad (5)$$

where C_o indicates the constant part of the initial costs, not influenced by the variation of the sill size, and c denotes a constant.
On the other hand also the risk associated with the increased probability of failure due to the sill reduction can be expressed in terms of costs. To this purpose the capitalized cost M of annual reservation (=fictive insurance premium) to avert the cost of repair due to unexpected failure during the service life of the structure (± 200 years), has been determined. The amount of the premium is given by the product of the probability of damage (=assumed to equal the probability of failure p.a.) and the associated economical loss if damage occurs:

$$M = \sum_{n=1}^{200} \frac{p_f * S}{(1+i)^n} \approx \frac{p_f * S}{i} \qquad (6)$$

where i is the rate of interest, corrected for inflation.
Minimization of the total costs R (=sum of the construction costs C and the capatalized damage cost M) produces the economic optimum sill design (ie. the optimum probability of failure). Fig. 6 shows the procedure for the four design options of respectively the sills in the Roompot channel and the Schaar/Hammen channels.

From the risk analysis [5] it turned out that the economic optimum probability of failure is higher than the target probability of failure (=p_f target). This means that p_f target, based on an acceptable level of probability of loss of live, is decisive. On the basis of the risk analysis it was decided to select design variant II for the Roompot and variant III for both the Schaar and the Hammen.

5. RISK ANALYSIS FLOW SLIDES DUE TO SCOUR

The s.s.b. is an obstacle in the tidal flow pattern. In consequence of this scour holes, up to a depth of 50 m below the sea bottom, will develop at the edges at both sides of the bottom protection. If the slopes of the scour holes get too steep they can become instable (Fig. 7). Depending on among other things the relative density of the sand either shearing of the scour slopes (to be modelled by a circular slip analysis) or flow slides may occur.

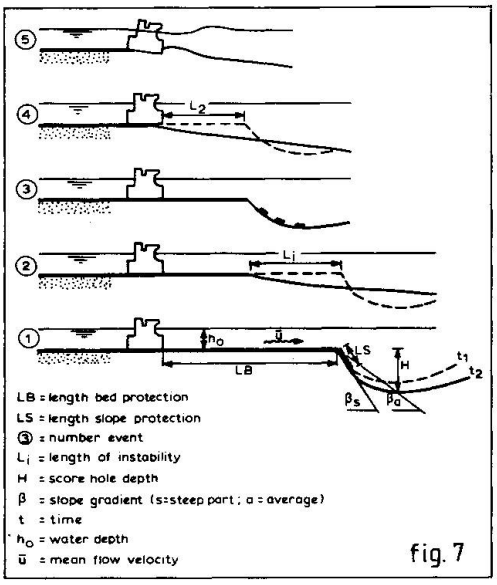

fig. 7

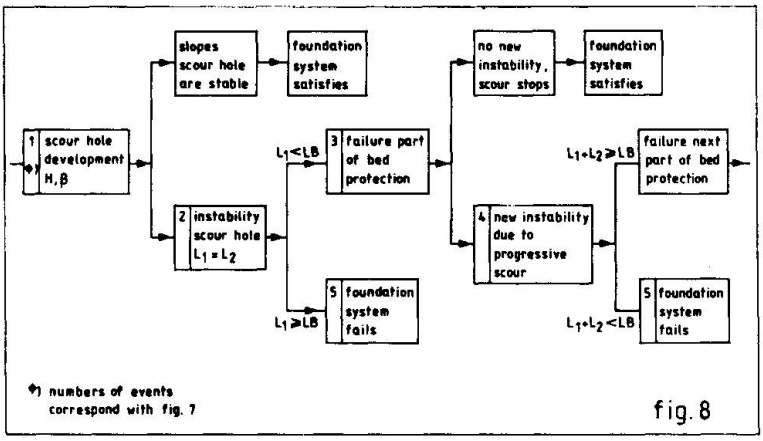

fig. 8

fig. 8 Simple event-tree of scour hole instabilities.

fig. 7 Progressive failure due to scouring.

A flow slide (or subsidence flow) is defined as a geotechnical instability where a saturated sand mass undergoes very large deformations ("flows") as a consequence of the development of excess pore water pressures and a simultaneous reduction of the shear strength, induced by the tendency of the sand to decrease in volume. Flow slides in the loosely packed Oosterschelde holocene sandlayers are of particular importance because they are associated with very flat slopes after failure. Risk analyses for different construction options were performed to decide which measures should be taken to improve the slope stability up to the desired level of safety. Each option provides information on the selected length of bed protection, the hydraulic conditions (water levels, currents), soil conditions (density), the construction schedule (time) and the maintenance program during the scour process (both during and after the construction period).
The risk analysis for evaluating the limit states in case of instabilities occuring at the scour hole, was performed in five steps [6]:

5.1. Prediction of scour hole development:

The scour hole is characterized by the maximum scour hole depth H and the slope gradient β (Fig. 7). From many hydraulic scale model tests, checked by several prototype tests, it was concluded that the growth of the scour depth can be described by the empirical formula [7]:

$$H_{max}(t) = (\alpha\bar{u} - u_{cr})^{1.7} * h_0 * 0.1 * (\rho_s/\rho_w - 1)^{-1.7} \qquad (7)$$

where ρ denotes the density of the sand particles s and the water w,
u_{cr} the critical transport velocity of the sand and α the dimensionless hydraulic scour factor (determined from hydraulic model tests); the other parameters are explained in fig. 7.

Due to the uncertainty of the different basic variables (especially the scour factor α) a significant coefficient of variation (order 20%) with respect to the prediction of the scour hole depth has to be counted with.
The slope gradient β can be described in a similar way as H; however the uncertainties are even greater. As a conservative assumption (that is with relatively steep slopes) a standard shape of the scour hole, which is only a function of H, is established. Starting from this principle the scour hole development for each section can be described adequatly by the scour depth as a function of time.

5.2. Assessment scour hole stability criteria:
The stability criteria for both the shearing mechanism and the flow slide are based upon empirical data, obtained from extensive observations of the slopes of the coast in the south western part of Holland during the last century. More than 1100 instabilities nearshore are reported, from which over 200 have been analysed in more detail. The profile measurements show a relation between the number of observed failures and the slope gradient (both the average and the steepest part) before failure occurred. Dependent on the type of soil (loosely packed holocene sand or dense pleistocene sands) the observed failures are divided into flow slides and shearing (sliding planes). Although a justified theoretical modelling of the flow slides, that can support the observed data is not available yet, the empirical data were used as black box prediction model.
To account for the length effect of the edges of the bed protection, the total length of 6 km. has been divided into statistically independent sections of 100 m. width. This somewhat conservative assumption meets the observations, which showed that the width of the zone affected by a flow slide or a shearing generally is in the order of 50 to 200 m.

5.3. Assessment of the damage length:
Given the event that an instability (shearing or a flow slide) occurs at the scour slopes, it is important to know what the damage consequences are. These consequences are expressed in the length (L) at which the adjacent bed protection looses its sand protection function.
The damage length L of the previously mentioned observed failures show a very great variation. For shearing this length varies from 0.5 to 2 H (H = max. depth of the channel or the scour hole) and for the flow slides from 0.7 to 8 H. The observed variation however could be explained by probabilistic back-calculations (first order-second moment) assuming that the volume of eroded sand equals the volume of sedimentated sand after failure. This hypothesis leads to a simple expression of L as a function of the stochastic variables H, β and some empirical geometry-factors.

5.4. Prediction probability of failure of the foundation:
The probability of failure of the pier foundation can be calculated straight forward from combination of steps 5.1, 5.2 and 5.3 according to the scheme of the simple event tree in fig. 8. The foundation fails (=definition) if the total damage length L after failure of the scour hole slopes exceeds the actual length of the bottom protection LB. It must be emphasized that also the damage effect of several succeeding smaller slope instabilities was taken into account (Fig. 7).
In practice however the actual probability of failure will be influenced by additional measures based on observed data during the scour process. If for example damage of the bed protection is detected, repairs will be carried out as soon as possible. In fact the quality of the inspection and maintenance system (o.a. frequency of monitoring, mobilization time for repair equipment) directly influences the probability of failure. In the risk analysis assumptions are made on this type of fuzzy information, directly translated in reduction of transmission probabilities.

5.5. Verification design and control measures:
After determination of the probabilities of the relevant events it has to be checked if the predicted contributions of the scour hole instabilities to failure of the s.s.b. system correspond with the target probability of safety according to the overall fault tree of the system. To judge the effectiveness of slope protection measures the probabilities of flow slide both with and without a protection with dumping layers on the scour slope are predicted.
From the risk analyses [6] it appeared that, apart from the shores of location Roompot East, slope protection measures are not necessary from the point of view of structural safety. For the Roompot East shore extra measures, consisting of a lenghtening of the bed protection in combination with a slope protection, are necessary to obtain the required safety level.

6. CONCLUSIONS AND RECOMMENDATIONS

Probabilistic methods proved to be a useful tool in the practice of the quality control of the design, the construction and the maintenance of the foundation of the complex s.s.b. offshore structure.
Relevant information for decision making can be obtained from probabilistic calculations. This information can vary from a simple check list of points of attention (as obtained from event-fault trees) to the selection of an economic optium design or construction alternative (as obtained from risk analyses).
Probabilistic methods can be used for the evaluation of a wide range of different types of geotechnical limit states dealing with a.o. stability, deformation, soil-structure interaction, flow slides and filter transport mechanisms.
Although the present state of knowledge of probabilistic methods deserves a wider practical implementation in geotechnics, further research is still necessary. This concerns among others the combined probability of failure of a structure as sociated with a number of simultaneous and partly correlated limit states, including the effect of auto-correlation of the basic system variables.

7. ACKNOWLEGDEMENT

The main part of the research presented herein was performed by order of the s.s.b. project organisation, in which Rijkswaterstaat, Dutch contractors and research institutes were involved. The author is much indebted to E.O.F. Calle of the Delft Soil Mechanics Laboratory for his comments on this manuscript.

8. REFERENCES

[1]. Vrijling, J.K. (1982), Design of concrete structures, Probability design method, Proc. Delta Barrier Symposium, Rotterdam, the Netherlands.
[2]. CIRIA (1976), Rationalisation of safety and serviceability factors in structural codes, CIRIA report 63, London.
[3]. Brinch Hansen, J (1970), A revised and extended formula for bearing capacity. Danisch Geotechnical Inst. Bull. 28.
[4]. Kooman, D. e.a., (1978), Probabilistic approach to determine loads and safety factors, Proc. Symposium on Foundation Aspects of Coastal Structures, Vol. I, paper 3.1, Delft.
[5]. Quelerij, L. de, and Vrijling, J.K. (1979), Economic optimization sill geometry, internal communication, Rijkswaterstaat, 31 DREO-M-79109, (in Dutch).
[6]. Davis, P.G.J. (1983), Stability problems of the scourholes at the edges of the bed protection of the storm surge barrier in the Oosterschelde, Polytechnisch Tijdschrift, Civiele Techniek 38, 1983,nr. 5, page 24-34, (in Dutch).
[7]. Huis in 't Veld, J.C. e.a. (1984), The closure of tidal basins, Chapter 2.4.9. Local scour (by Pilarczyk, K.W.), Delft University Press.

Safety of Earth Slopes: a Probabilistic Approach

Sécurité des talus de terre: une approche probabiliste

Sicherheit von Böschungen: ein probabilistischer Ansatz

M. Semih YÜCEMEN
Assoc. Professor
Yarmouk University
Irbid, Jordan

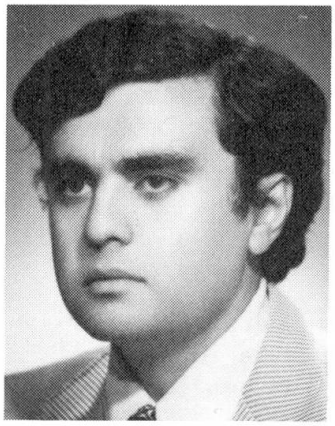

M. Semih Yücemen, born 1947, received his Ph.D. from the Univ. of Illinois. From 1973 to 1983 he was at the Middle East Technical Univ., Ankara, Turkey. He is now an Assoc. Prof. of Civil Engineering at Yarmouk Univ. He has published numerous technical papers on seismic hazard analysis, geotechnical and structural reliability.

Azm S. AL-HOMOUD
Civil Engineer
Irbid, Jordan

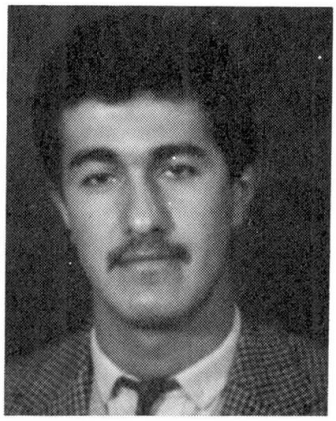

Azm S. Al-Homoud, born 1962, received his B.Sc. and M.Sc. degrees in Civil Engineering at the Yarmouk Univ., Irbid, Jordan, where he also worked as a teaching and research assistant for two years. He is now doing his compulsory military service. His research interest is in geotechnical reliability.

SUMMARY

A probabilistic model to assess the three-dimensional stability of earth slopes under long-term conditions is described. A landslide is studied in detail to illustrate the implementation of the proposed model. The slope formed after the occurrence of this landslide is also analysed, and the optimal alternative to improve its safety is selected in view of the associated failure probabilities and costs.

RÉSUMÉ

Un modèle probabliste pour évaluer la stabilité tridimensionelle des talus de terre à long terme est décrit. Un éboulement est étudié en détail pour illustrer l'application du modèle proposé. Le talus formé après l'éboulement est aussi analysé, et la meilleure alternative pour l'amélioration de sa sécurité est choisie, en vue des probabilités de ruine et des coûts.

ZUSAMMENFASSUNG

Es wird ein auf der Zuverlässigkeits-Theorie beruhendes Modell für die Überprüfung der dreidimensionalen Langzeit-Stabilität von Böschungen beschrieben. Die Anwendung des Modells wird an einem Beispiel gezeigt. Auch die durch den Erdrutsch neu entstandene Geländeform wird untersucht. Schliesslich wird die optimale Alternative zur Anhebung der Sicherheit untersucht auf der Basis von Versagenswahrscheinlichkeit und Kosten.

1. INTRODUCTION

In the past twenty years several landslides have been observed and reported along many Jordanian highways. One of these highways is the Irbid-Amman highway. Along this route a number of landslides have occurred at different locations in the past. Various researchers (e.g. Saket /2/) have analysed these landslides in detail with the purpose of estimating the values of the shear strength parameters at the time of failure. The existing slopes at the sites where these landslides have occurred were also analysed, and a set of recommendations were proposed to improve their stability. However, these studies were carried out within a deterministic framework. The uncertainties in the mechanical model and in soil properties were not accounted for explicitly. Also, there was no systematic basis for comparing various alternatives proposed to improve the safety of the existing slopes and thus select the optimal measure.

In this study, such a landslide is analysed based on the probabilistic three-dimensional slope stability analysis (PTDSSA) model developed by the authors. The formulation of this probabilistic model and the related assumptions are outlined in the first part of the paper. The analysis of the landslide through this model is presented in the second part of the study. To improve the reliability of the existing slope different remedial measures are compared. A risk-based optimization method is used in the selection of the optimal stabilization measure.

2. PROBABILISTIC 3-D SLOPE STABILITY MODEL

In our study, the PTDSSA model is developed by following the general framework outlined by Vanmarcke /3/. The details of the PTDSSA model can be found in /1/. Because of space limitation, here we shall only present an outline of the model.

The potential sliding soil mass centered at $x = x_o$ and bounded by vertical end sections at $x_1 = x_o - b/2$ and $x_2 = x_o + b/2$ is assumed to be a portion of cylinder with a finite length b (Fig. 1). For this soil mass the three-dimensional (3-D) safety factor, $F_b(x_o)$, is defined as follows /3/:

$$F_b(x_o) = \left(\int_{x_1}^{x_2} M_R(x)\, dx + R_e \right) \Big/ \int_{x_1}^{x_2} M_o(x)\, dx \qquad (1)$$

where, $M_R(x)$ and $M_o(x)$ are cross-sectional resisting and driving moments, respectively, and R_e is the contribution of the end sections of the failure surface to the resisting moment.

The probability of failure, $p_f(b)$, of a soil volume of width b and centered at a specified location along the slope axis is defined as follows:

$$p_f(b) = Pr(F_b \leq 1.0) \qquad (2)$$

Note that in this case the 3-D safety factor is treated as a random variable, since the location of the failure mass is fixed. On the other hand, the evaluation of the safety of an earth slope along its total length, B, is carried out by utilizing the level crossing concepts of random processes /1, 3, 4/. In this case, $F_b(x)$ forms a random process, since the location of the potential sliding soil mass is not fixed but random. A failure over a specified width of b will occur anywhere along the axis of the slope, whenever the random process $F_b(x)$ crosses into the unsafe domain defined by $\{F_b \leq 1.0\}$. Equations to compute the risk of failure at a specific location, $p_f(b)$, and the probability that a failure may take place at any location along the slope, $p_F(b)$, are

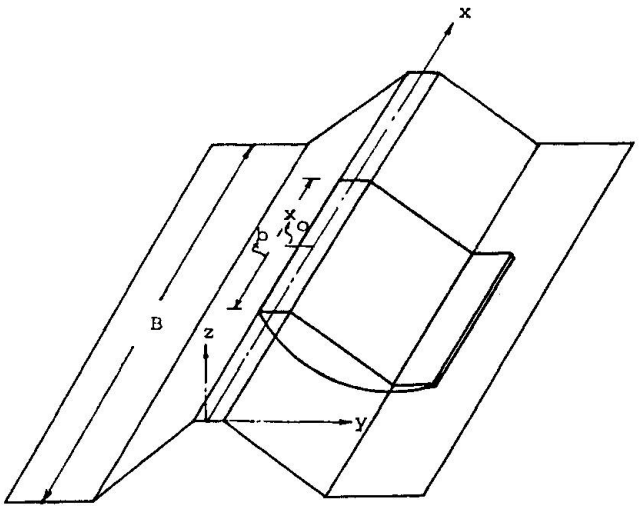

Fig. 1 Geometry of the sliding soil mass (from /3/)

derived and presented in /1/.

In Eq. 1 the most significant random function is $M_R(x)$. The ordinary method of slices is taken as the deterministic model of slope stability analysis and forms the basis for the computation of $M_R(x)$ and $M_o(x)$. Under the long-term conditions, the shear strength depends on the angle of friction, ϕ, cohesion, c, and the pore pressure, u. The spatial averages of these shear strength parameters are taken as the basic random variables, whereas the unit weight of soil and the geometric parameters are treated as deterministic basic variables, since the associated uncertainties are relatively small.

The proposed model takes into consideration all sources of uncertainties, quantifies them and systematically incorporates them into the assessment of the reliability of an earth slope. Besides the spatial variability of shear strength parameters in x, y, z directions, inaccuracies in the mechanics of the deterministic slope stability model as well as discrepancies between the in situ and laboratory-measured values of soil properties are taken into consideration. Random correction factors, denoted by N, are introduced to adjust for these inaccuracies and discrepancies.

The cross-sectional resisting moment, $M_R(x)$, with appropriate correction factors and consistent with the method of slices is expressed as follows /1/:

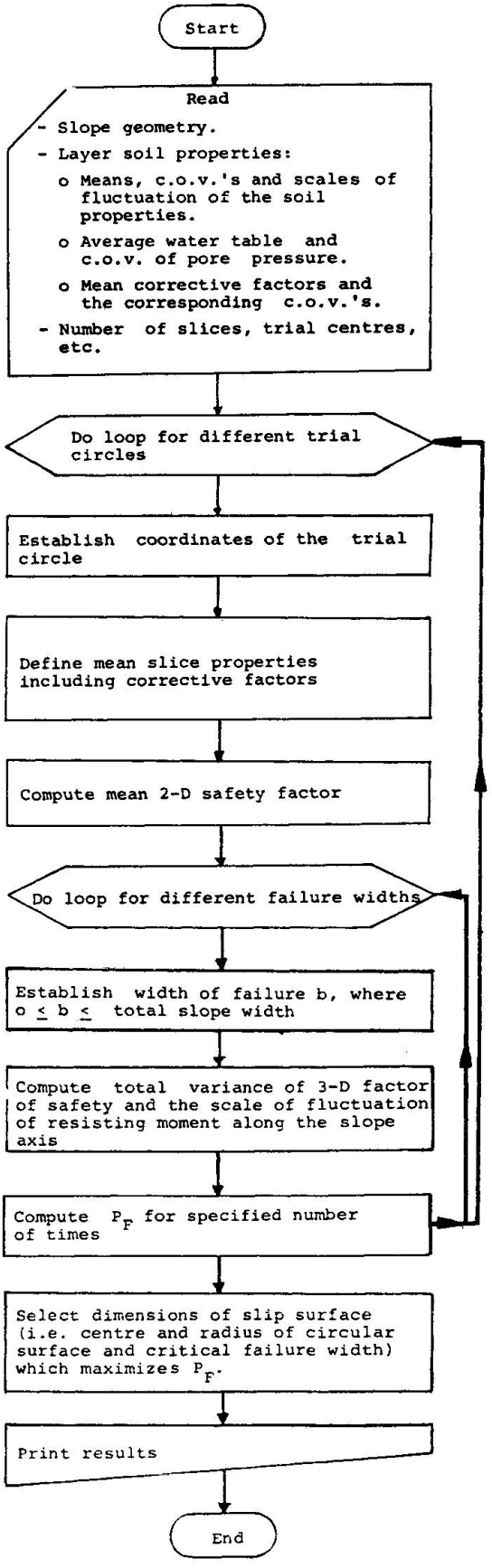

Fig. 2 Flowchart for the PTDSSA model

$$M_R(x) = N_m N_p r \sum_{i=1}^{m} \{ N_{c_i} c_i l_i + (W_i \cos\Theta_i - u_i l_i \cos^2\Theta_i) \tan (N_{\phi_i} \phi_i)\} \quad (3)$$

where, N_m and N_p are correction factors for the modeling error and the effect of progressive failure, repectively; l_i = length of the ith segment of the failure surface, m = number of slices, u_i = pore pressure acting on the ith slice computed from the average pore pressure distribution along the failure surface, W_i=weight of the ith slice, Θ_i = the inclination of the base of the ith slice to the horizontal axis; r = radius of the failure surface.

In Eq. 3, N_c and N_ϕ are correction factors accounting for the systematic uncertainties resulting from the discrepancies between laboratory and in situ conditions in the estimation of the values of c and ϕ. Each of these factors can be written as the product of component factors, $N_j(.)$'s, to accomodate for errors resulting from disturbance during sampling, size of specimen, rate of shearing, sample orientation and anisotropy /1, 5/.

The mean and variance of $M_R(x)$ is obtained by using the first-order approximation. In this case, the statistical parameters required are the means and point variances of the basic variables and of the correction factors. Also any type of existing correlations have to be quantified. The variance of the cross-sectional resisting moment, denoted by, $\tilde{M}_R^2$, will be composed of contributions from all of the component variables. In the computation of this variance, the spatial and other sources of correlations among the component variables are taken into consideration.

The degree of spatial correlation associated with the shear strength parameters is quantified by the scales of fluctuation in the x, y and z directions, denoted by λ_x, λ_y and λ_z, respectively. The scale of fluctuation, λ, which is introduced by Vanmarcke /3, 4/ is a convenient measure of the degree of correlation in a soil medium. Physically interpreted it represents the distance over which a soil property (in a certain direction) shows a relatively strong correlation.

The 3-D slope stability analysis requires the spatial averaging to be carried out over the soil volume, and this necessitates the consideration of 3-D correlation functions. However, in the proposed model the (volumetric) spatial averaging is carried out first over the arc length, then over the slope axis. Such a procedure simplifies the computations, since the knowledge of the 1-D correlation functions (or scales of fluctuation) in the x, y and z directions becomes sufficient.

It is to be noted that spatial averaging or integration have a smoothing effect, and thus cause a reduction in the variance. The degree of reduction depends on the degree of correlation, and in our study the dimensionless standard deviation reduction factor $\Gamma(.)$ is used to quantify this effect. For example, the standard deviation of the first term in Eq. 1, involving the integration becomes equal to "b $\tilde{M}_R$ $\Gamma(b)$", where, $\tilde{M}_R$ is the standard deviation of M_R, and $\Gamma(b)$ is the standard deviation reduction factor associated with the integration of M_R over a length of b. The exact functional form of $\Gamma(b)$ depends on the correlation function. However, by using the approximate relations proposed by Vanmarcke /3, 4/, it is possible to express $\Gamma(b)$ in a simple way based on the associated scale of fluctuation /1, 3, 4/.

The uncertainty in the driving moment M_o is neglected here, since the variables involved in the computation of M_o have comparatively small uncertainties. Thus, it is treated as a deterministic variable in Eq. 1.

The numerical computations associated with the PTDSSA model are to be carried out by using the computer program prepared for this purpose. The corresponding flow-chart is shown in Fig. 2.

3. ANALYSIS OF THE LANDSLIDE

3.1 Description of the Landslide

This landslide has occurred in early March 1967 at 37th km of the Sweileh-Jerash road. The failure was of a rotational nature. The total width of the slope was about 800 m whereas the width of the landslide was approximately 80 m. Prior to the movement, the slope had an inclination of 32° to the horizontal /2/. The slope cross-section before the landslide took place and the actual failure surface are shown in Fig. 3.

Undisturbed samples were taken throughout the soil deposit. The peak and residual strength parameters were measured from the triaxial and direct shear box tests, respectively. Based on the reported results of these tests the following mean values and inherent variabilities (δ) are computed:

$\bar{c}_p = 23.3$ kPa, $\bar{\phi}_p = 16.9^\circ$, $\bar{c}_r = 17.7$ kPa

$\phi_r = 11.5^\circ$, $\delta_{c_p} = \delta_{c_r} = 0.21$, $\delta_{\phi_p} = \delta_{\phi_r} = 0.06$

In Table 1, the mean correction factors and the corresponding coefficients of variation (c.o.v.) denoted by Δ, accounting for different sources of discrepancies between laboratory-measured and in situ values of c and ϕ are listed. These values are selected according to the guidelines given in /5/ and considering the soil properties reported for this site in /2/.

Correction Factors	$\bar{N}_j(c)$	$\Delta_j(c)$	$\bar{N}_j(\phi)$	$\Delta_j(\phi)$
Mechanical disturbance (N_1)	1.35	0.15	1.20	0.10
Specimen size (N_2)	0.73	0.10	0.93	0.05
Rate of shearing (N_3)	0.80	0.14	0.80	0.14
Anisotropy (N_4)	0.98	0.04	0.98	0.04

Table 1. Summary of the statistics of correction factors

There is no data available to calculate the scales of fluctuation for cohesion and angle of friction in the x, y and z directions. Therefore, estimates of these scales of fluctuation are obtained based on the ranges proposed in /1/. The selected values are: $\lambda_{c_x} = \lambda_{c_y} = \lambda_{\phi_x} = \lambda_{\phi_y} = 30$ m and $\lambda_{c_z} = \lambda_{\phi_z} = 1.5$ m. A sensitivity study carried out with respect to the scales of fluctuation indicated that within the range of reasonable values for the scales of fluctuation in the horizontal direction, the failure width is not sensitive to λ_x and λ_y /1/.

3.2 Assessment of Failure Probability

The stability analysis in terms of effective stresses is carried out for an approximate cross-section before the landslide took place, as shown in Fig. 3. Here the average peak strength parameters are to be used in the analysis, since this landslide is considered to be a first-time landslide. For the progressive failure effect the correction factor N_p, with $\bar{N}_p = 0.73$ and $\Omega_{N_p} = 0.10$ is applied, where Ω denotes the total c.o.v.

The exact position of the water table at the time of landslide was not known. However, the main cause of this landslide was indicated to be the heavy rain and consequent saturation of the soil /2/. In our analysis, the ground water table is assumed to be parallel to the natural ground surface with its top level

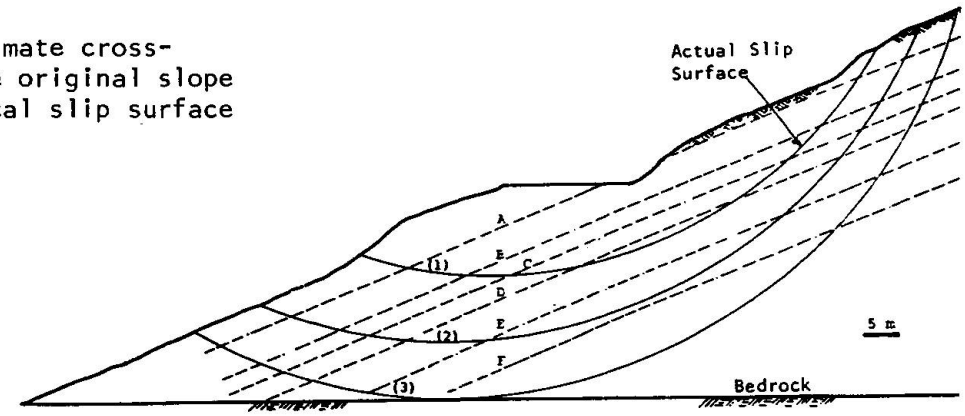

Fig. 3 Approximate cross-section of the original slope and the critical slip surface

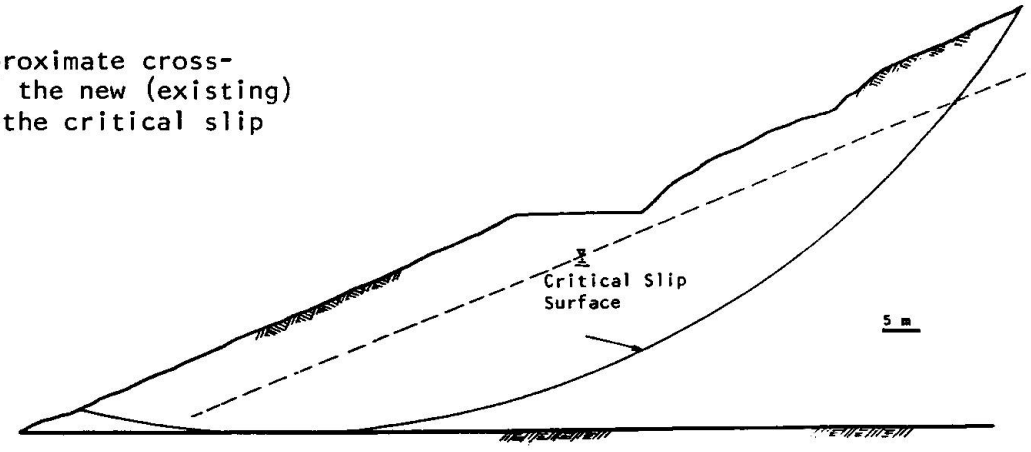

Fig. 4 Approximate cross-section of the new (existing) slope and the critical slip surface

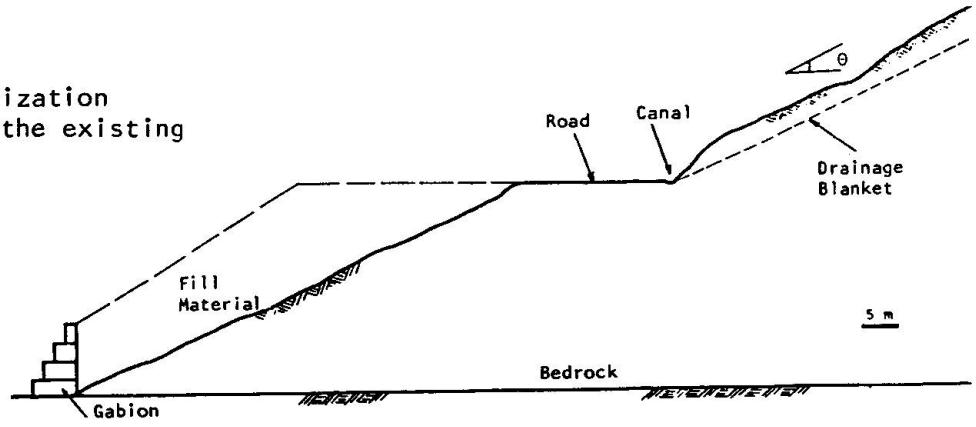

Fig. 5 Stabilization measures for the existing slope

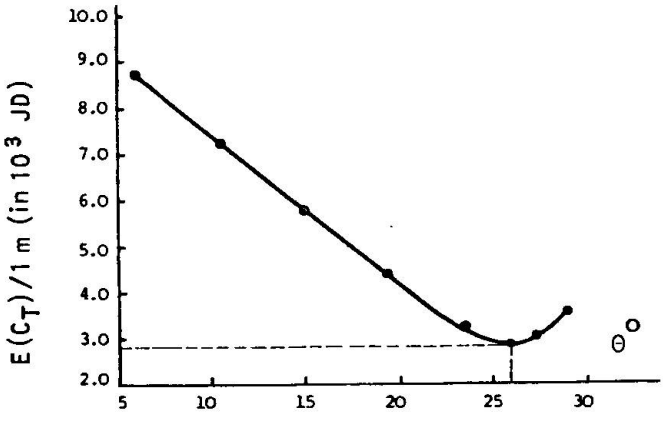

Fig. 6 Variation of the expected total cost with the slope inclination

at a certain distance from the ground surface. To account for the rather erratic fluctuations in pore pressure resulting from the rapid fluctuations in the ground water level (G.W.L.) a value of 0.3 is taken as the total uncertainty in pore pressure.

Considering the best estimate values of all parameters, an analysis is carried out on the actual slip surface for different mean water table levels. Computations are performed by using the PTDSSA computer program. High failure probabilities are computed for all water tables. On the other hand, ground water table level designated by B in Fig. 3 yields to a failure width of 77 m which is closest to the actual failure width of 80 m. So G.W.L. described by level B is taken to be our best estimate. The corresponding failure probability is 0.80, which is quite high and consistent with the observation of the landslide.

3.3 Assessment of the Safety of the Existing Slope

In this section we shall analyse the safety of that portion of the slope which has experienced a downward movement and moved out from the original slope mass. The width of the slope that experienced this movement was observed to be 80 m. However, the total slope width to be analysed in this section is taken to be 100 m considering the extensions at either sides of the failed soil volume. It should also be noted that for this existing slope, the residual shear strength parameters will be used, since the slope has already gone through a slide.

Figure 4 shows an approximate geometry of the existing slope. The existing slope is analysed using average residual strength parameters. The mean value and the c.o.v. of the correction factor that accounts for the progressive failure effect is taken to be 0.95 and 0.03, respectively. No change was made in the best estimates of the other parameters used in the analysis of the original slope. For the most critical slip surface and the mean ground water level shown in Fig. 4, the failure probability is found to be 0.96. This high failure probability implies that the slope is not in a safe state and remedial measures are needed to improve its safety.

3.4 Stabilization Measures for the Existing Slope

A set of remedial measures were suggested in /2/ to improve the safety of the existing slope. The first of these measures is the supply of adequate drainage to remove the surface water from the area and lower the G.W.L. If adequate drainage is achieved, then the G.W.L. will be shallow and we may reasonably assume that the pore pressure is zero in subsequent analysis. As a second remedial measure the resisting forces (or moments) against sliding will be increased by constructing a gabion wall at the toe of the original landslide and placing fill material behind the gabion as shown in Fig. 5.

The final remedial measure is the adjustment of the slope inclination, Θ, above the road level. For the purpose of selecting the optimal Θ value, different Θ values are assumed and the corresponding probability of total slope failure are calculated. For each alternative Θ value, the expected total cost is computed from the following equation:

$$E(C_T) = C_1 + C_2 + C_F\, p_F \qquad (4)$$

where, C_1 = (volume of fill) x (unit cost of fill), C_2 = (volume of the soil cut) x (unit cost of cut), $E(.)$ = expected value operator, C_F = cost of failure, p_F = probability of slope failure.

For the purpose of cost analysis, the cost of failure is assumed to be 30,000 JD per 1 m of slope width (this cost is due to road damage, delay, etc.). Also let the cost of fill material be 1 JD/m^3 and the cost of cutting to be 10 JD/m^3. By substituting these assumed costs into Eq. 4 we obtain the following

expression for the expected total cost per 1 m of slope width:

$$E(C_T) = 627.5 + 10\ V_c(\Theta) + 30{,}000\ p_F(\Theta) \quad (5)$$

where, $V_c(\Theta)$ = volume of the soil cut in order to achieve an inclination of Θ for the slope above the road level. A plot of the total expected cost versus slope inclination Θ is shown in Fig. 6. As observed from this figure, the optimum value of Θ is found to be 25.8^o, which means a reduction of 3^o in the original ground inclination above the road level (which is 28.8^o). The probability of slope failure for $\Theta = 25.8^o$ is 0.035. This failure probability appears to be high and further improvements may be required. In this case, it is necessary to specify the level of acceptable risk. Accordingly, additional improvements could be implemented by increasing the volume of the fill and/or decreasing the slope inclination.

It is to be emphasized that the costs used here were assumed just to show the procedure of selecting the optimum solution and may not reflect the actual costs.

4. CONCLUDING COMMENTS

The reliability of an earth slope depends closely on the various uncertainties involved in the stability analysis. The probabilistic model briefly discussed in this study evaluates the 3-D stability of slopes under long-term conditions taking into consideration the spatial variability (and correlations) of soil properties, as well as the uncertainties stemming from the discrepancies between laboratory-measured and in situ values of shear strength parameters. It also accounts for the effects of modeling errors and progressive failure. Consideration of the third dimension and the end effects are crucial for a realistic assessment of the safety of earth slopes. In the 3-D analysis, the critical and total slope widths become two new and important parameters.

Through the PTDSSA model a certain landslide that occurred along the Irbid-Amman highway is analysed in a systematic way including all sources of uncertainties. The failure width is predicted to be 77 m (versus 80 m of observed failure width) and the probability of slope failure is computed to be 0.80. These results agree well with those actually observed, supporting the predictive ability of the proposed probabilistic model.

To improve the safety of an existing slope, different remedial measures are compared and the optimal slope inclination is selected by using the failure probabilities associated with each alternative and based on the minimization of the expected cost criterion. Such an analysis shows one of the benefits gained through the probabilistic approach.

REFERENCES

1. AL-HOMOUD A.S., Probabilistic 3-D Stability Analysis of Slopes. M.Sc. Thesis. Dept. of Civil Engineering, Yarmouk University, Jordan, June 1985.

2. SAKET S.K., Slope Instabilities on the Jordanian Highways. Ph.D. Thesis. University of London, 1974.

3. VANMARCKE E.H., Probabilistic Stability Analysis of Earth Slopes. Engineering Geology. Vol. 16. 1980.

4. VANMARCKE E.H., Random Fields: Analysis and Synthesis. M.I.T. Press. Cambridge, Mass. 1983.

5. YUCEMEN M.S. and TANG W.H., Long-Term Stability of Soil Slopes: A Reliability Approach. Proc. 2nd ICASP. Aachen, Germany. Sept. 1975.

Assessment of Safety of Pipelines Subjected to Soil Liquefaction

Détermination de la sécurité de conduites dans des sols en liquéfaction

Sicherheit eingebetteter Rohrleitungen bei Erdbeben

Masaru KITAURA
Prof. Dr.
Kanazawa University
Kanazawa, Japan

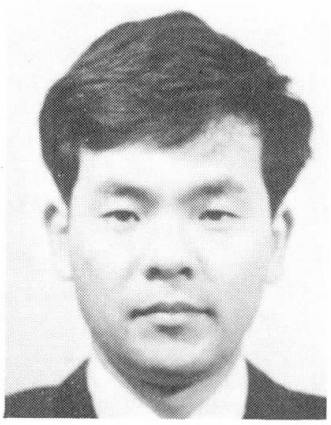

Masaru Kitaura, born 1944, received his M. Eng. at Kyoto University in 1969 and Dr. Eng. at Kyoto University in 1975. Since 1985, he is a professor of Civil Engineering at Kanazawa University. He is now studying earthquake-proof design for lifeline systems and optimum time for snow removal from wooden buildings.

Masakatsu MIYAJIMA
Research Assoc.
Kanazawa University
Kanazawa, Japan

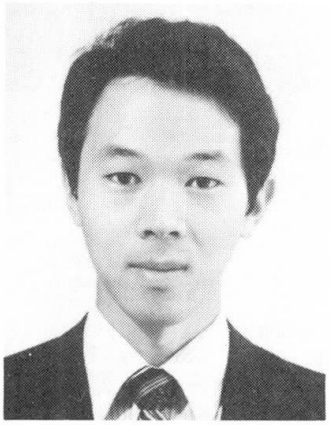

Masakatsu Miyajima, born 1956, received his M. Eng. at Kanazawa University in 1981. He has been employed at Kanazawa University since 1981. He is now studying the dynamic behavior of buried pipelines in relation to soil liquefaction.

SUMMARY

Lifeline systems have been frequently damaged by soil liquefaction. The present paper, firstly, describes the example of pipe failure subjected to soil liquefaction and the results of experimental and theoretical studies. Secondly, the factors concerned with pipe failure due to liquefaction and the safety on pipelines are discussed. It became evident from the present study that it was necessary to evaluate not only the liquefaction potential of the construction sites but also that in adjacent areas.

RÉSUMÉ

Les infrastructures subissent fréquemment des dommages lors de liquéfaction des sols. L'article décrit la rupture d'une conduite et les résultats d'études subséquentes, expérimentales et théoriques. Il mentionne les facteurs influençant la rupture de la conduite, lors de liquéfaction du sol, et traite de la sécurité des conduites. Il est nécessaire de considérer la liquéfaction possible du sol non seulement dans la zone de construction, mais aussi dans les zones environnantes.

ZUSAMMENFASSUNG

Der vorliegende Beitrag beschreibt, in welcher Art lebenswichtige Rohrleitungs-Systeme durch erdbebeninduzierte Bodenverflüssigung beschädigt werden können und stellt experimentell und theoretisch gewonnene Ergebnisse vor. Die für das Versagen und die Sicherheit von Rohrleitungen massgebenden Einflussgrössen werden diskutiert. Es ist offensichtlich, dass auch die Eigenschaft des Bodens ausserhalb der eigentlichen Einbettungsstrecke eine wesentliche Rolle spielt.

1. INTRODUCTION

The lifeline systems are becoming increasingly more important in the urban life. It is, however, well kown that the lifeline systems, especially buried pipeline systems, have been frequently damaged by the past earthquakes. For example, the Nipponkai-Chubu Earthquake of May 26, 1983 with magnitude 7.7 on the Japan Meteorological Agency scale caused extensively damage to the buried pipeline systems. A total of about 20 days was required for restoring the water supply and city gas pipelines in Noshiro City where was the middle of the hardest-hit area. It was also reported that the damage to underground pipelines were strongly influenced by soil liquefaction. The earthquake damage to pipelines were caused not only by seismic wave propagation but also by ground failure such as liquefaction, landslide, fault and so on. Dynamic behavior and failure criteria of the underground pipelines during liquefaction, however, have not almost been made clear. The present study deals with behavior of pipelines subjected to soil liquefaction and assessment of safety on the pipelines.

The present paper firstly describes the example of pipe failure subjected to soil liquefaction and the results of the experimental and theoretical studies. Secondly it points out the factors concerned with the pipe failure due to liquefaction and the safety on pipelines is discussed.

2. PIPE BEHAVIOR DUE TO SOIL LIQUEFACTION

2.1 Effects of Liquefaction-induced Lateral Spreading

2.1.1 State of earthquake damage

Permanent ground movement during the 1983 Nipponkai-Chubu Earthquke was measured by aerial photographs taken before and after the earthquke [1] . Figs. 1 and 2 show the permanent ground movement and pipe damage. A, B, C, D and E indicate the failure mode of the pipes in accordance with that

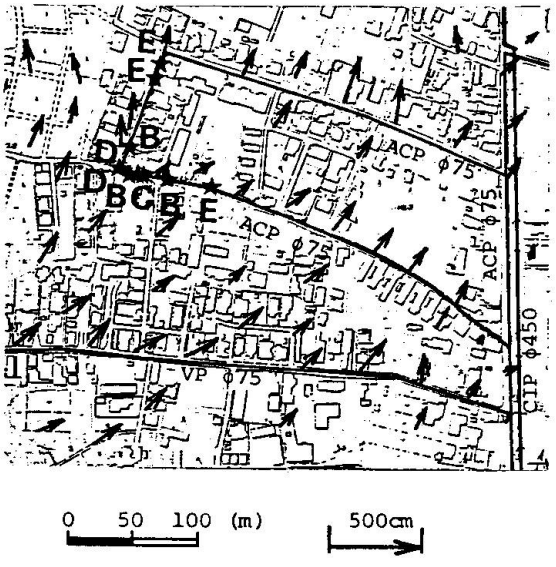

Fig. 1 Lateral spreading and pipe damage (Aoba-cho in Noshiro)

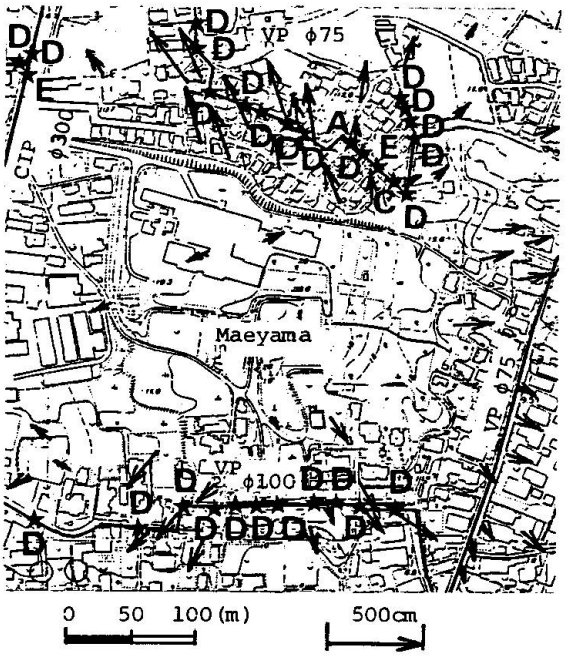

Fig. 2 Lateral spreading and pipe damage (Kawatogawa in Noshiro)

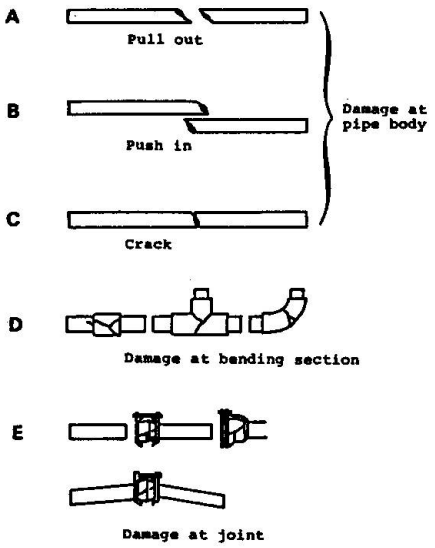

Fig. 3 Failure mode of pipe

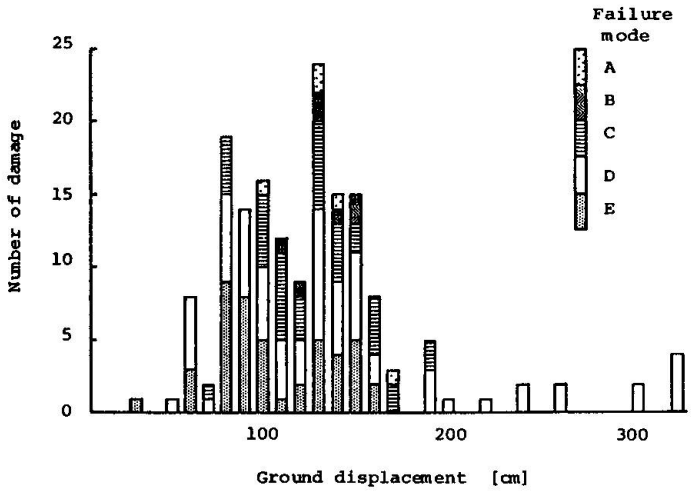

Fig. 4 Relationship between ground displacement and number of pipe damage

shown in Fig. 3 [2] . Length of arrows means the horizontal displacement of the permanent ground movement. Maximum displacement was about 5m in Noshiro City. Fig. 4 shows the relationship between the horizontal ground displacement and number of pipe damage in Noshiro City. This figure suggests that the much damage were caused at the sites where the horizontal ground displacement was greater than about 1m. Most of these areas were reported that the liquefaction occurred [3]. North slope of Maeyama hill in Kawatogawa area in Fig. 2, however, showed little sand volcano in spite that the large ground movement occurred. Based on these investigation data, the liquefaction-induced lateral spreading is classified into two types shown in Fig. 5. Type I is movement of competent surficial soils because of liquefaction of an underlying deposit (see Fig. 5 (a)), and type II is movement of surficial liquefied soils (see Fig. 5 (b)).

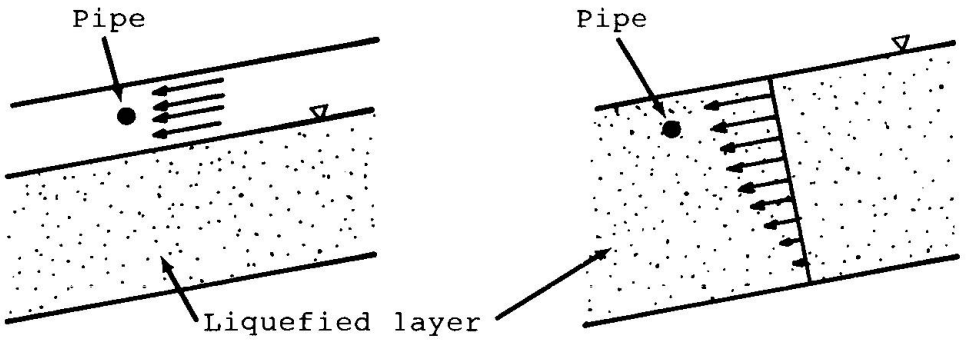

Fig. 5 Types of lateral spreading

2.1.2 Numerical example

An analytical model shown in Fig. 6 is proposed to study the effects of liquefaction-induced lateral spreading on the damage to the pipelines. A pipeline is modeled as a Winkler beam. Shape of horizontal ground displacement is assumed as a sinusoidal curve here and it is transferred to the buried pipeline through the soil spring. The basic differential equations governing the motion of a pipeline can be written for transverse movements:

$$EI\frac{d^4v_1}{dx^4} + K_y v_1 = 0 \qquad x \leqq 0$$

$$EI\frac{d^4v_2}{dx^4} + k_y v_2 = k_y \delta \sin\frac{\pi x}{l} \qquad 0 < x \leqq l$$

$$EI\frac{d^4v_3}{dx^4} + k_y v_3 = 0 \qquad l < x$$

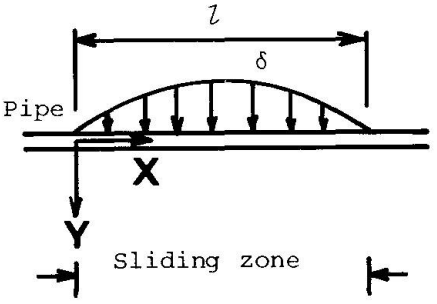

Fig. 6 Analytical model (Plane figure)

where, E is Young's modulus of the pipe material, I is geometrical moment of pipe inertia, δ is maximum displacement of the lateral spreading, K_y is soil spring constant for transverse motion, l is stretch of the liquefied zone and v_1, v_2, v_3 are transverse displacements of the pipe.

Fig. 7 shows the relationship between the maximum bending stress and the soil spring constant. The welded steel pipeline whose nominal diameter is 400mm is analyzed here. Table 1 shows dimensions of the steel pipe which is used in the present study. The maximum displacement, δ , in this case is 1m. Fig. 7 indicates that the maximum bending moment decreases in case that the soil spring constant is less than 17.6 kN/m^3 (1.8 x10^{-3} kgf/cm^3). That is, the horizontal movement of competent soil affects the pipe behavior rather than that of liquefied soil does. It is interesting to note that the smaller the ground stretch of lateral spreading is, the greater the maximum bending moment is. These results suggest the conclusion that the pipe behavior due to liquefaction-induced lateral spreading is strongly influenced by the ground stretch of the lateral spreading and soil spring constant. The numerical example also indicates that the type I mentioned above is more destructive on the pipe than type II in case that the maximum horizontal displacement has the same value.

Table 1 Dimensions of pipe

		Steel pipe
Outside diameter	(cm)	40.64
Thickness	(cm)	0.60
Young's modulus	(MPa)	205.80

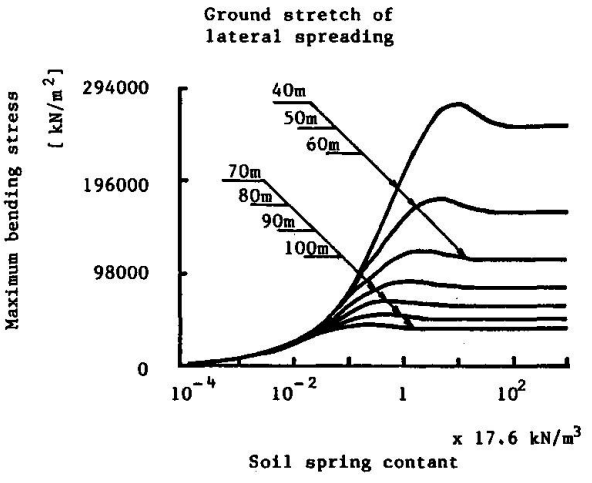

Fig. 7 Relationship between maximum bending stress and soil spring constant

2.2 Effects of Relative Movement Between Liquefied and Non-liquefied Ground

2.2.1 State of earthquke damage

One of the characteristics of the pipe damage due to the 1983 Nipponkai-Chubu Earthquake was that all of the damage to cast iron pipes (CIP) occurred at the liquefied site and most of them occurred at the joints of the pipes with large diameter of 400mm and 450mm. Fig. 8 indicates that such damage was caused at liquefied site near the boundary between the liquefied and non-liquefied sites.

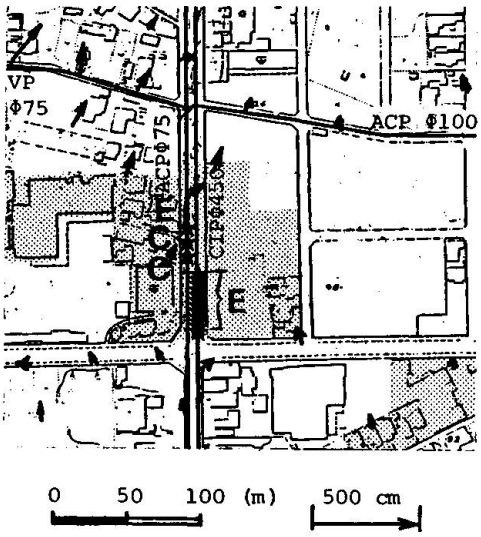

Fig. 8 Liquefied sites and pipe damage (Nagasaki in Noshiro)

2.2.2 Experimental study

We conducted the experiments employing the model pipe in order to investigate the pipe strain characteristics near the boundary between the liquefied and non-liquefied sites [4]. Fig. 9 shows the general view of experimental apparatus. The buried pipe model was a rubber stick with 20mm diameter and 1000mm in length. Its elastic modulus was 79.4 MPa (810 kgf/cm^2) and its weight per unit volume is 11.2 kN/m^3 (1.14 gf/cm^3). One end of the model pipe was fixed at the rigid arm setting on the sand box. The half of the model ground was very loose and the other was densified by compaction. Exciting frequency was 5Hz. Exciting acceleration was about 200gal and exciting duration time was 30 seconds.

Figs. 10 and 11 show the distribution of the maximum accumulated residual strains of the model pipe and that of mean vibrating strains, respectively. The shaded portion in these figures indicate the non-liquefied area. It can be seen in these figures that both pipe strains express the maximum value in the liquefied ground near the boundary between liquefied and non-liquefied areas. The great similarity can be seen in a comparison of the damage to CIP and the experimental results. It is considered that the following factors affect the strain characteristics: the buoyancy acting on the pipeline buried in liquefied site, difference of dynamic characteristics between liquefied and non-liquefied ground, ground settlement due to liquefaction and so on. It is conceivable that these factors could influence the pipelines near the boundary between liquefied and non-liquefied sites more than those at the liquefied site. Care should be taken of such case.

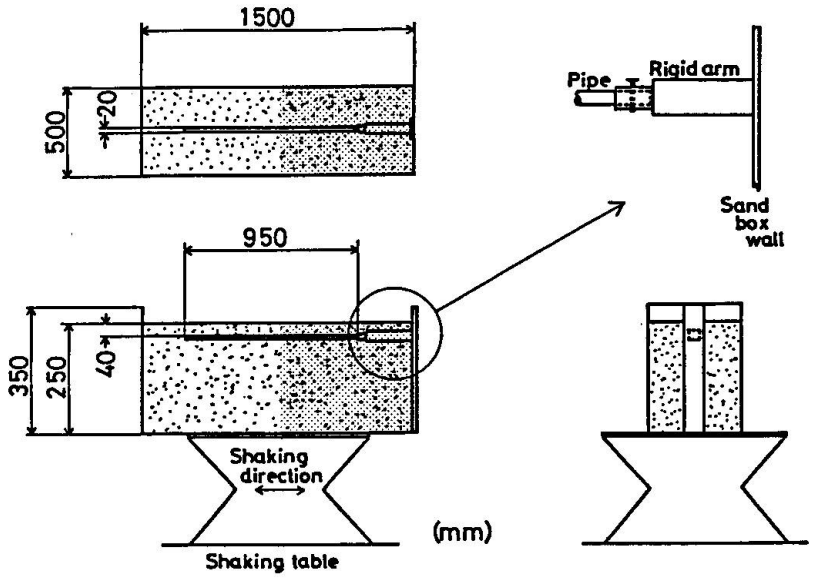

Fig. 9 General view of experimental apparatus

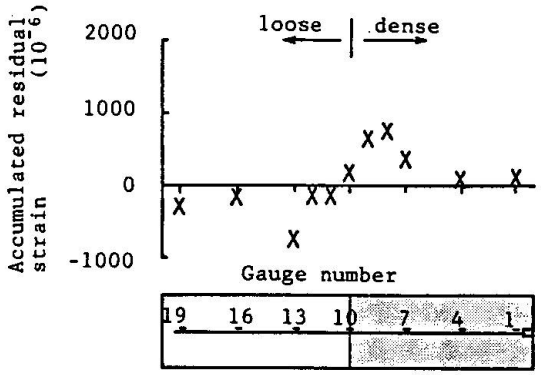

Fig. 10 Distribution of maximum accumurated residual strains of pipe

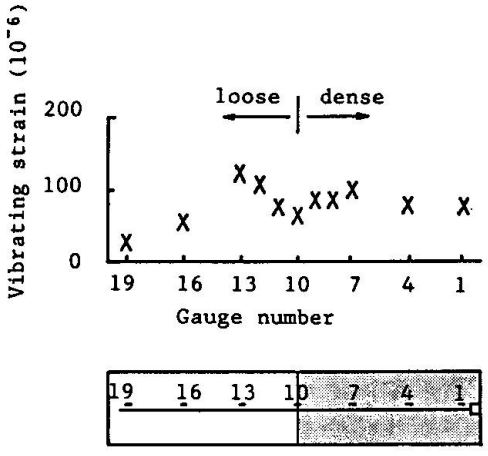

Fig. 11 Distribution of mean vibrating strains of pipe

3. SAFETY ON PIPELINES SUBJECTED TO SOIL LIQUEFACTION

The factors concerned with the failure of buried pipelines subjected to soil liquefaction are considered as follows.
(1) Large dynamic behavior of the ground during incomplete liquefaction.
(2) The forces due to the buoyancy and groundwater flow acting on the pipelines during complete liquefaction.
(3) Relative movement of the ground between the liquefied and non-liquefied ground.
(4) Large ground deformation due to soil liquefaction.
The present study theoretically and experimentally investigated the effects of the factors (3) and (4) based on the field investigation data of the earthquake damage. Factors (1) and (2) infuluence the pipelines at the liquefied sites in the liquefaction process. On the other hand, factor (3) affects the pipelines which go through the boundary ground between the liquefied and non-liquefied sites and as in factor (4), the scale of lateral spreading, that is scale of liuqefaction, influences the behavior of pipelines.

Most of guidlines and technical standards for earthquke-proof design for buried pipelines in Japan indicate how to predict the soil liquefaction. However, they do not predict how severely and how largely the liquefaction occurres, but they only predict whether or not the liquefaction does at a site. Therefore, in order to decide to take countermeasure for factors (3) and (4), it is very important to evaluate not only the liquefaction potential of the construction sites but also that in near areas.

ACKNOWLEDGEMENTS

The authors wish to acknowledge Professor T. Kobori for his kind advice throughout this study. For performance of the field investigation, the authors are grateful to the officers of Noshiro City Gas and Waterworks Bureau. A part of expense of this research was defrayed by a Grant-in Aid for science research from the Ministry of Education, Science and Culture in Japan (No. 60025017 and No. 60750417).

REFERENCES

1) KUBO, K., HAMADA, M. and ISOYAMA, R., Measurement of Permanent Ground Movement during the 1983 Nipponkai-Chubu Earthquke, Proc. of the 18th Conference on Earthquake Engineering, Japan Society of Civil Engineers, pp. 353-359, 1985 (in Japanese).

2) NOSHIRO CITY GAS AND WATERWORKS BUREAU, Report on the Damage to Water Supply Pipelines by the Nipponkai-Chubu Earthquke, 1983 (in Japanese).

3) TOHNO, I., YASUDA, S. and SHAMOTO, Y., Site Liquefaction and Damage Caused by the Nipponkai Chubu Earthquake, TSUCHI-TO-KISO, Japan Society of Soil Mechanics and Foundation Engineering, Vol. 31, No. 12, pp. 13-20, 1983 (in Japanese).

4) KITAURA, M. and MIYAJIMA, M., Dyanmic Behaviour of a Model Pipe Fixed at One End during Liquefaction, Proc. of Japan Society of Civil Engineers, No. 336, pp. 31-38, 1983 (in Japanese).

Leere Seite
Blank page
Page vide

Optimum Aseismic Design of Structures

Dimensionnement optimal de structures vis-à-vis des séismes

Optimale Bemessung von Bauwerken auf Erdbeben

Hiroshi KAWAMURA
Associate Professor
Kobe University
Kobe, Japan

Hiroshi Kawamura, born 1941, obtained B. Eng. and M. Eng. at Kobe University and D. Eng. at Nagoya University.

Takeshi TERAMOTO
Structural Engineer
Daiken Sekkei Architects
Tokyo, Japan

Takeshi Teramoto, born 1961, obtained B. Eng. and M. Eng. at Kobe University. His master's thesis covers the topic of this paper.

Akinori TANI
Research Associate
Kobe University
Kobe, Japan

Akinori Tani, born 1955, obtained B. Eng. and M. Eng. at Kobe University.

Minuro YAMADA
Prof. Dr.-Ing.
Kobe University
Kobe, Japan

Minuro Yamada, born 1930, has been professor of structural engineering at Kobe University, Japan, since 1964. Member, IABSE.

SUMMARY
A comprehensive and systematic procedure for optimum aseismic design of structures based on fuzzy set probabilistic theories is proposed. A case study is performed on an actual typical school building in reinforced concrete, at Kobe, Japan.

RÉSUMÉ
La contribution propose une procédure globale et systématique pour le dimensionnement optimal de structures, vis-à-vis des séismes, sur la base de la théorie probabiliste «Fuzzy Set». Une étude a été réalisée pour un bâtiment scolaire typique, en béton armé, à Kobe, Japon.

ZUSAMMENFASSUNG
Es wird ein umfassendes und systematisch aufgebautes Verfahren für die Bemessung von erdbebensicheren Bauwerken vorgestellt, welches auf der «fuzzy set»-Theorie beruht. Als Beispiel dient das Projekt eines typischen Schulhauses aus Stahlbeton in Kobe, Japan.

1. INTRODUCTION

The aseismic safety and quality of architectural structures should be assured from a comprehensive viewpoint. The Authors have already proposed an evaluation flow chart for seismic damages of structures [1] which is composed of three parts, i.e., EARTHQUAKE, STRUCTURE and DAMAGE as shown in Fig.1. By using this chart, the followings have become able to be performed easily; regional evaluation of seismic damages [1], aseismic reliability analysis [2] and fuzzy optimum aseismic design [3] of structures. The third fuzzy optimum design was carried out based on fuzzy set theory [4] and maximizing decision method [5] which enabled us to employ rationally multi-objective functions and subjective evaluations in the optimum aseismic design of structures [6][7].

In this paper, to make the fuzzy optimum design method mentioned above more real and practical, probabilistic expressions are applied to EARTHQUAKE in Fig.1, because occurrences and intensities of earthquakes belong essentially to natural scientific phenomena beyond human control. On the other hand fuzzy set conceptions are suitable to STRUCTURE and DAMAGE, because the design of structures and the evaluation of structural damages belong essentially to human decision making problems. The purpose of this paper is to propose such a new optimum aseismic design method of structures and to present a case study on a real type R/C building.

2. FUNDAMENTAL THEORY AND PROCEDURE

A probabilistic expression of EARTHQUAKE is able to be given by probabilistic density function of magnitude M and epicentral distance Δ[km], $f_e(M,\Delta)$, which is induced from the past observed earthquake occurrences [2]. When STRUCTURE is defined deterministically by a design parameter, γ , DAMAGE is calculated by a passage probability, p_x, which indicates the probability that a damage parameter, x , exceeds a critical one, x_c , more than one time in the future, i.e.,

$$p_x = p_r \left(x \geqq x_c \mid \gamma \right). \tag{1}$$

In this paper, the damage parameter, x , is calculated through the earthquake limit response analysis proposed by the Authors [1], and the passage probability, p_x , is computed by the following two methods for comparison:

(1) Method based on classical probability theory
The passage probability at the next earthquake, p'_x , is given by

$$p'_x = \iint_{\Omega} f_e(M,\Delta)\, dM\, d\Delta, \tag{2}$$

where Ω is the region with M above and Δ below the critical M-Δ curve on which $x = x_c$ as shown in Fig.2. When n_o is the expected number of earthquake occurrences in the next t_o years, the passage probability in the next t_o years, p_x , is given by

$$p_x = 1 - (1-p'_x)^{n_o}, \tag{3}$$

in which

$$n_o = n\, t_o / t, \tag{4}$$

where n is the total number of earthquake occurrences in the past t years.

(2) Method based on Benjamin's probabilistic model
By using Bayesian theorem Benjamin proposed a probability of observing n_o future Poission events in time t_o having observed n events in time t, $p[n_o \mid t_o, n, t]$ [8]. When zero is substituted into n_o in it, the non-passage probability in the region Ω where $x \geqq x_c$ (See Fig.2) in the next t_o years becomes $p[0 \mid t_o, np'_x, t]$. Therefore, the passage probability in the next t_o years is given by

$$p_x = 1 - p[0\ t_o, np'_x, t] = 1 - (1+t_o/t)^{-(np'_x+1)}. \tag{5}$$

Finally, an optimum aseismic design of structures is able to be performed by the following maximizing decision equation as shown in Fig.3:

$$m_D(\gamma^*) = \max_{\gamma} (m_\gamma \wedge m_{px}), \tag{6}$$

where m_γ and m_{px} are the membership functions of design parameter γ and passage probability p_x, respectively. Here, the membership functions are supposed to be the satisfaction degrees from architectural, structural and economical points of view. In the case study, here, number of shear walls γ is adopted as a structural design parameter, and damage factor DF, the maximum response displacement x_m and duration until fracture t_f are employed as damage parameters. The physical meanings of these characters will be explained later. Consequently, the total procedure of the proposed optimum aseismic design of structures is able to be shown in Fig.4. The maximizing decision is performed by means of and/or tree as shown in Fig.5 [3].

3. STRUCTURE

A case study is carried out in regard to the first story of a typical R/C school building at Kobe in Hyogo prefecture, Japan, which is the same structure as adopted in the past evaluation studies [1][2][3] (See Figs.6,7), and is idealized to be a one degree of freedom system. The calculation conditions are given as follows: yield shear force T_y, slipping shear force T_s, yielding lateral displacement x_y and hysteresis loop area $A(x_a)$ are calculated as follows [2][3];

$$\left.\begin{aligned} &T_y=[(1-x_1)x_1+2\beta_s p_a(1-2d_1)]\sigma_{bo}bh^2/H, \qquad x_y=\varepsilon_y/3(1-2d_1)h, \\ &T_s=(2\beta_s p_a-x_1)(1-2d_1)\sigma_{bo}bh^2/H, \qquad A(x_a)=(5T_y+9T_s)(x_a-x_y)/4, \end{aligned}\right\} \quad (7)$$

where $x_1=N/\sigma_{bo}bh$, (8) $\qquad \beta_s p_a=\sigma_{ay}bh/\sigma_{bo}a$. (9)

The restoring force characteristic of shear walls is considered as shown in Fig.9. Ultimate shear force T_u, displacement x_u and the i-th hysteresis loop area $A(x_i)$ are calculated as follows:

$$\left.\begin{aligned} &T_u=\sigma_{bo}Lt\ \sin\theta\cos\theta/2, \qquad x_u=0.002L/\cos^2\theta, \\ &A(x_i)/T_u x_u=(x_i/x_u)^2-(x_{i-1}/x_u)^2/2. \end{aligned}\right\} \quad (10)$$

Design parameter, γ, i.e., the number of shear walls is counted by a unit shear wall within a span between C_1, C_2 and C_3 columns in the span and ridge directions.

4. EARTHQUAKE

4.1. Earthquake Ground Motion Spectrum [1][2][3]

When M, Δ and predominant period T_G of surface ground are given, earthquake ground motion spectra are given as shown in Fig.10, and ground motion duration t_o[s] is calculated by $t_o=10^{0.5M-2.28}$. The average slip velocities faults of interplate- and intraplate-type earthquakes are assumed to be $\bar{d}$=15 and 50[cm/s], respectively. Out of the source region, the earthquake ground motion spectra are calculated by multiplying the values in Fig.10 by $(\Delta_B/\Delta)^2$.

4.2. Probabilistic Expression of Earthquake Occurrences

Cumulative distribution functions are approximated to the distributions of observed interplate- and intraplate-type earthquakes within the circles with radii 2000 and 200[km] round Kobe City in Japan, respectively. By differentiating them probability density distributions $f_e(M,\Delta)$ are calculated as follows [2]:

$$f_e(M,\Delta)=0.1583(e^{-M}-e^{-9})-1.322\cdot10^{-7}(\Delta-2000) \quad \text{for interplate-type,} \quad (11)$$

$$f_e(M,\Delta)=1.778\cdot10^{-6}(8-M)^6+1.573\cdot10^{-8}\Delta^2 \quad \text{for intraplate-type,} \quad (12)$$

and shown in Fig.11. Numerical calculations of M and Δ are carried out by the following meshes; ΔM=0.1, $\Delta\Delta$=100[km] for interplate-type earthquakes and ΔM=0.1, $\Delta\Delta$=10[km] for intraplate-type earthquakes.

5. DAMAGE

5.1. Earthquake Limit Response Analysis [1][2][3]

According to the principle of the maximum response, the momotonic maximum displacement x_m is given, when velocity and acceleration pulse spectra (v-pulse and α-pulse spectra) are in contact with the ground motion spectrum as shown in Fig.12, where the approximated bi-linear pulse response spectra are used for simplicity. T_1, T_2, v_{m1} and v_{m2} at the corners are calculated as follows:

Elastic response displacement:

$$T_1=4/\omega, \quad v_{m1}=\omega x_p/2, \quad (13) \qquad T_2=2/\omega, \quad v_{m2}=\pi\omega x_p/2, \quad (14)$$

Plastic response displacement:

$$T_1=4\mu_u\sqrt{\omega/2\mu_u-1}, \quad v_{m1}=\omega x_y\sqrt{2\mu_u-1}/2, \quad (15) \qquad T_2=2\mu_p/\omega\sqrt{2\mu_p-1}, \quad v_{m2}=\pi\omega x_y\sqrt{2\mu_p-1}/2. \quad (16)$$

where $\omega=\sqrt{k/m}$, (17) $T=2t_p$, (18); k is modulus of elasticity; m is mass; $\mu_p=x_m/x_y$ (19) in the velocity pulse spectrum, and $\mu_u=x_m/x_y$ (20) in the acceleration one. The physical meanings of these characters are shown graphically on the left hand side in Fig.12.

Response displacement x_a and the number of response cycles N_c are given at the crossing point of a finite resonance response acceleration capacity spectrum C^I_{RA} and the earthquake ground motion spectrum (See Fig.13) as follows [1][3]:

$$C^I_{RA}= A(x_a)/1.2\pi + 2T_a/3\pi, \quad (21) \qquad N_c=t_o/T_e, \quad (22)$$

where $T_e=2\pi/\sqrt{mx_a/T_a}$ is equivalent elastic natural period and T_a is restoring force amplitude.

5.2. Damage Parameters and Critical Values

One of damage parameters, the maximum displacement x_m is able to be calculated as the larger of the ones by pulse response analyses. Damage factor DF is calculated as follows [1][3]:

In the case of monotonic responses by pulse response analysis;

(1) DF of columns; $DF_{mc}=x_m/x_u$, (23)

where $x_u= \Phi_y H^2/6 + hH(\Phi_B - \Phi_y)/2$, (24) $\Phi_y=2\varepsilon_y/(1-2d_1)h$, (25)

$\Phi_B=0.004/(x_1-d_1)h$, (for concrete) (26)

$\Phi_B=150\Phi_y/(1-x_1-d_1)h$, (for reinforcing bar) (27)

(2) DF of shear walls; $DF_{mw}=x_m/x_u$ (28)

In the case of cyclic response by finite resonance response analysis;

(1) DF of columns; $DF_{cw}=N_c/N_B$ (29)

where $N_B=10^{8[1-x_1 h\Phi_a(0.004+d_1 h\Phi_a)]}$, (for concrete) (30)

$N_B=[300\Phi_y x 0.5^{3/4}/\{(1-2d_1)h\Phi_a-2\varepsilon_y\}]^{4/3}$, (for reinforcing bar) (31)

$\Phi_a= 2(x_a-x_y)hH + \Phi_y$. (32)

(2) DF of shear walls; $DF_{cw}=x_m/x_B$, (33) where $x_m=\mathrm{Max}(x_i)$.

In the both monotonic and cyclic cases, DF is assumed to be zero for elastic range of columns $x_m, x_a < x_y (=\Phi_y H^2/6)$, and non-cracked range of shear walls $x_m, x_i \leqq x_{cr} (= 2(1+1/6)\sigma_{bo}H/2\cdot 10^6)$. In the each case of monotonic or cyclic response the maximum values of DF is adopted as DF_m or DF_c, respectively. The duration until fracture t_f is calculated as follows:

$$t_f = \infty \quad \text{for DF} < 1, \qquad t_f = N_B T_e \quad \text{for DF} \geqq 1. \quad (34)$$

The effect of t_p derived from pulse response analysis on t_f are neglected here.

The critical values of DF_m, DF_c, x_m and t_f are assumed to be 1.0, 1.0, H/100 and

300[s], respectively. H is the clear height of columns. DF=1.0 means the fracture of structures. At the displacement, x_m=H/100, window glasses surrounded by alminium sashes are cracked. It is supposed that 300[s] is sufficient for refuge time.

5.3. Passage Prbability

The passage probabilities of DF_m, DF_c and x_m, i.e., P_{DFm}, P_{DFc} and P_{xm} are able to be derived from Eqs.(3),(5). As for t_f, the non-passage probability p_{tf} ($t_f \leqq 300$[s]) is also able to be given by using Eqs.(3),(5). Supposing that DF_m and DF_c are statistically independent, the passage probability of the damage factor p_{DF} is calculated as follows [2]:

$$P_{DF} = P_{DFm} + P_{DFc} - P_{DFm} \cdot P_{DFc} \quad . \tag{35}$$

6. FUZZY OPTIMUM ASEISMIC DESIGN

6.1. Membership Functions of Satisfaction Degree [3]

According to the architectural demand that buildings without shear walls are prefered and reffering to the real number of shear walls in the typical R/C school building shown in Fig.7, the satisfaction degree of the number of shear walls m_γ is supposed as the following membership function (See Fig.14):

for span direction; $\gamma \leqq 6$: $m_\gamma=0$, $6<\gamma \leqq 13$: $m_\gamma=1.24(\gamma-13)^2$, $\gamma>13$: $m_\gamma=1$. (36)

for ridge direction;$\gamma=0$: $m_\gamma=0$, $0<\gamma<4$: $m_\gamma=12.76(\gamma-4)^2$, $\gamma>4$: $m_\gamma=1$. (37)

Acoording to economic and mental demands, the satisfaction degrees of the passage probabilities, m_{DF}, m_{xm} and m_{tf} are supposed to have several patterns as shown in Fig.15 (a)-(e), which reflect the mentalities of cool, pessimistic, optimistic, emotional and ordinary man, respectively. The Authors adopted the satisfaction degree type in Fig.15 (e) and the following is assumed in this paper:

$$m_{xm}=-4(p_x-0.5)^3+0.5 , \tag{38}$$

where $p_x=p_{xm}$, p_{DF} and $\overline{p_{tf}}$

6.2. Maximizing Decision

Now, using the and/or tree such as shown in Fig.5, the maximum satisfaction degree $m_D(\gamma^*)$ has become able to be calculated. Calculations are performed in the following 16 cases:(1) Ridge and span directions of the building shown in Fig.7, (2) Interplate- and intraplate-type earthquakes, (3) Predominant natural periods of surface groud, T_G=0.1 and 0.8[s], (4) Classical probability theory and Benjamin's probabilistic model for passage probability. Figs.16,17 show the total distributions of satisfaction degrees of γ, p_{DF}, p_{xm} and $\overline{p_{tf}}$ with respect the number of shear walls, γ. The peak values of m in the hatched zone is $m_D(\gamma^*)$ and γ at the point is γ^* which are shown in Table 1.

7. DISSCUSSION AND CONCLUSIONS

As the result of applying fuzzy set and probability theory to the optimum aseismic design of a typical R/C school building, the following are made clear.

1)Using the simple evaluation procedure for aseismic damages of structures proposed by the Authors, it is possible to show clearly the relations among the satisfaction degrees of γ, DF, x_m and t_f by scanning the design parameter, γ.
2)In the cases of hard surface ground (T_G=0.1[s]), span direction and interplate earthquake, the maximum satisfaction degree is higher than in the case of soft surface ground (T_G=0.8[s]), ridge direction and intraplate earthquake, respectively. This tendency is reasonable and the same as the ones of the different type evaluations which the Authors have already carried out [1][2][3].
3)The final satisfaction degree is almost decided by the ones of the number of shear walls and the duration until fracture.
4)In the local range of γ, the satisfaction degree of the damage factor of the building decreases as γ increases. This tendency is against our experimental ones. This reason is that the damage factor is decided by two different damage factors of columns and shear walls, DF_c and DF_w.

5)In the case of the interplate-type earthquake the satisfaction degrees of the maximum displacement, and the duration until fracture by the method based on Benjamin's probabilistic model are lower than by the method based on classical probability theory, because the passage probabilities based on Benjamin's probabilistic model are higher than the ones based on the classical probability theory (See Figs.16,17). Even if zero is substituted into n in Eq.(6), there exist the passage probabilities p_{xm}, p_{DF} and non-passage probability $\overline{p_{tf}}$.
6)The reason why the number of shear walls in the ridge direction at the maximizing decision point is nearly zero is that its satisfaction degree is supposed according to the architectural demand that very few shear walls are prefered in the ridge direction.

9. REFERENCES

[1]KAWAMURA,H.,YAMADA,M.,TANI,A. and FUJITANI,H.:Regional Evaluation of Seismic Damages of Reinforced Concrete Buildings,Proc.8WCEE,Vol.IV,1984,pp.647-654.
[2]KAWAMURA,H.,YAMADA,M.,TANI,A. and TERAMOTO,T.:Aseismic Reliability of Buildings,Proc.ICOSSAR'85,Vol.II,May,1985,pp.II-187-196.
[3]KAWAMURA,H.,TERAMOTO,T.,TANI,A. and YAMADA,M.:Aseismic Design of Reinforced Concrete Buildings Based on Fuzzy Set Theory,Journal of Structural Engineering,Vol.32 B,A.I.J.,March,1986,(in Japanese)(to be published).
[4]ZADEH,L.A.:Fuzzy Sets,Information and Control,8,1965,pp.338-353.
[5]BELLMAN,R.A. and ZADEH,L.A.:Decision Making in a Fuzzy Environment,Management Science,Vol.17,No.4,Dec.1970,pp.B-141-164.
[6]FURUKAWA,K. and FURUTA,H.:A New Formuration of Optimum Aseismic Design Using Fuzzy Mathmatical Programing,Proc.8WCEE,Vol.V,1984,pp.443-450.
[7]WANG,G. and WANG,W.:Fuzzy Optimum Design of Aseismic Structures,Earthquake Engineering and Structural Dynamics,Vol.13,1985,pp.827-837.
[8]BENJAMIN,J.R.:Probabilistic Models for Seismic Design,Journal of Structural Division,ASCE,94,May,1968,pp.1175-1196.

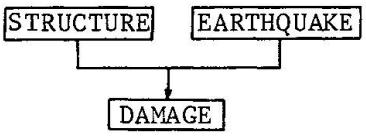

Fig.1 Outline of Evaluation Flow Chart for Aseismic Damages

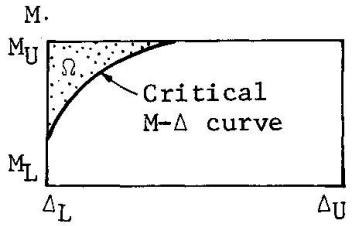

Fig.2 Region Ω and Critical M-Δ Curve

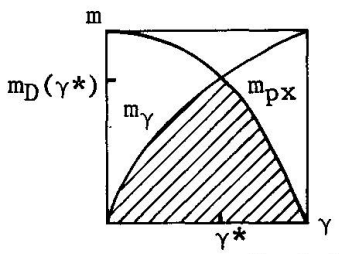

Fig.3 Maximizing Decision

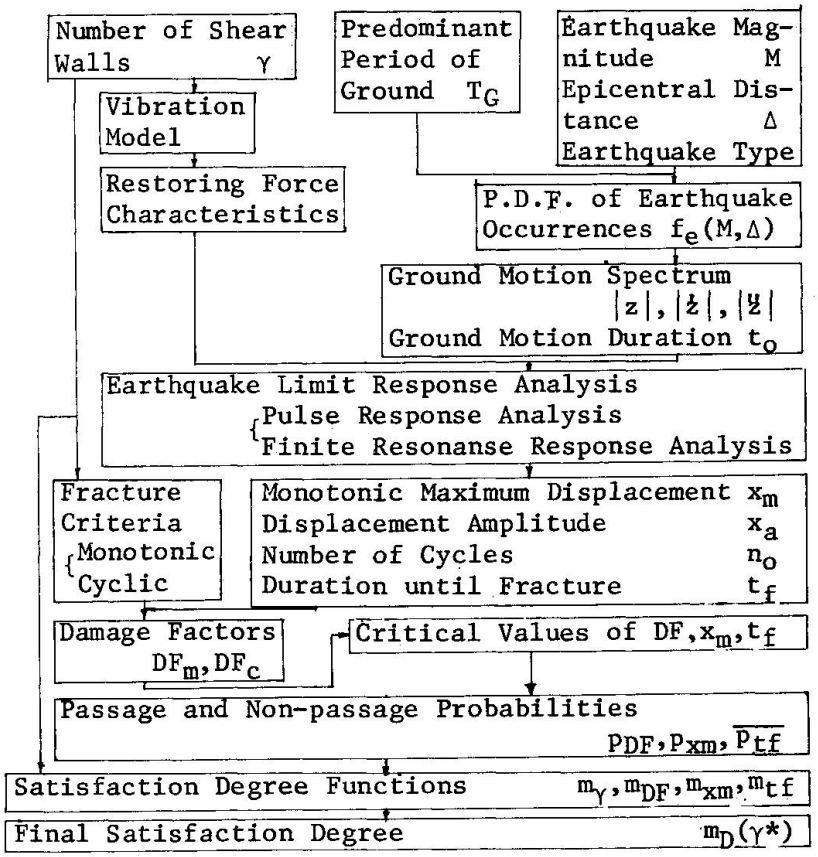

Fig.4 Flow Chart of Optimum Aseismic Design of Buildings

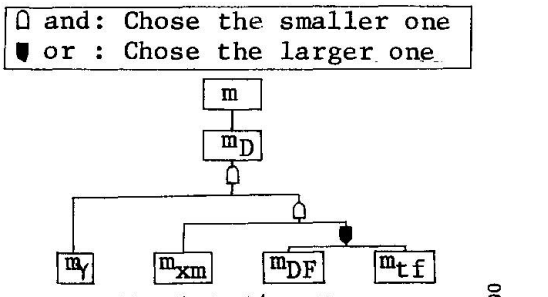

Fig.5 And/or Tree

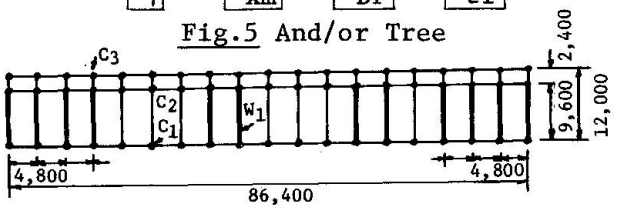

(a) Plan of C Block

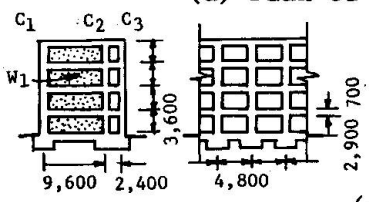

(b) Frameworks

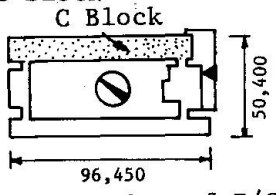

(c) Plot Plan of R/C School Building

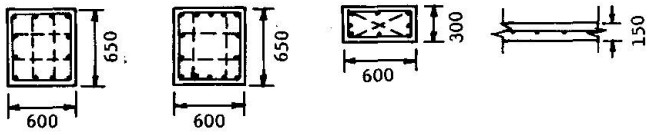

(d) Sections of Columns and Shear Walls

Fig.7 Structural Outline of C Block in Standard R/C School Building

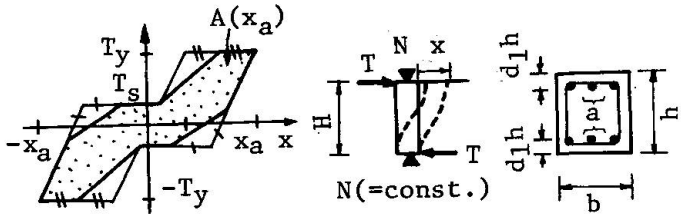

Fig.8 Restoring Force Characteristics of Columns [3]

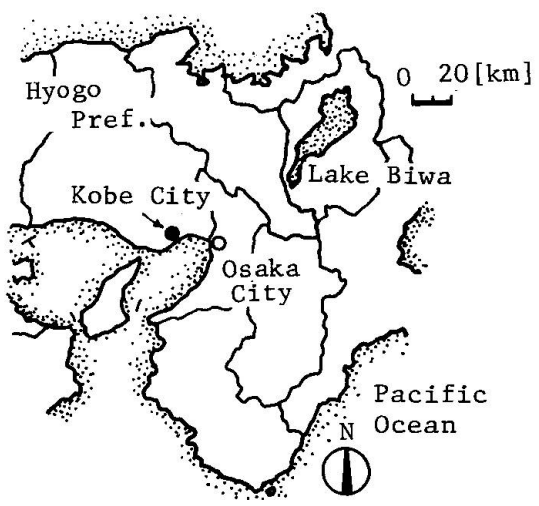

Fig.6 Location of typical R/C School Building (Kobe City, Hyogo Prefecture, Japan)

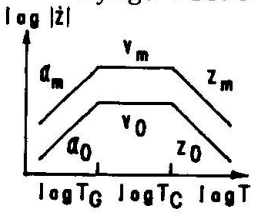

Within the Source Region

$\Delta_B = 10^{0.5M-2.1}$

$T_C = 0.5M-1.3-\log \bar{d}$

$f = (0.2\chi+0.4)/0.6$

$k = 0.5M-1.3$

Pulse Response Analysis

$a_m = \chi^2 \bar{d}/0.15$

$v_m = \chi T_G \bar{d}/0.3$ $(T_C \geq T_G)$

$v_m = \chi 10^k/0.3$ $(T_C < T_G)$

$z_m = T_G 10^k/0.6$

Finite Resonance Response Analysis

$a_0 = f a_m$

$v_0 = f v_m$

$z_0 = f z_m$

Fig.10 Earthquake Ground Motion Spectra [3]

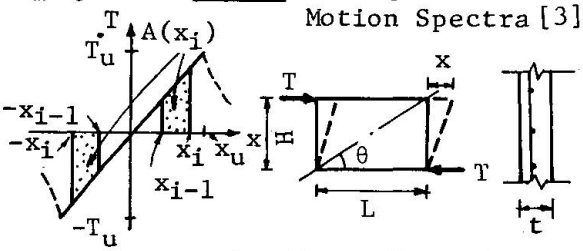

Fig.9 Restoring Force Characteristics of Shear Walls[3]

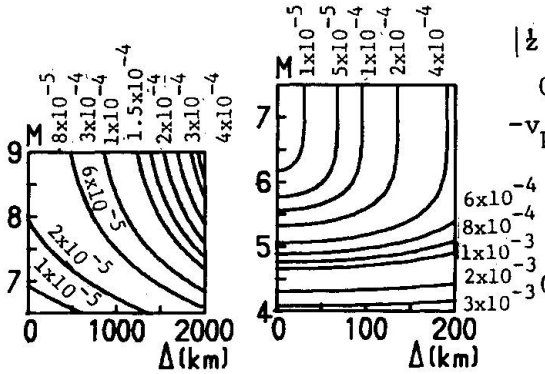

(Interplate) (Intraplate)

Fig. 11 Assumed Probability Density Distributions[2]

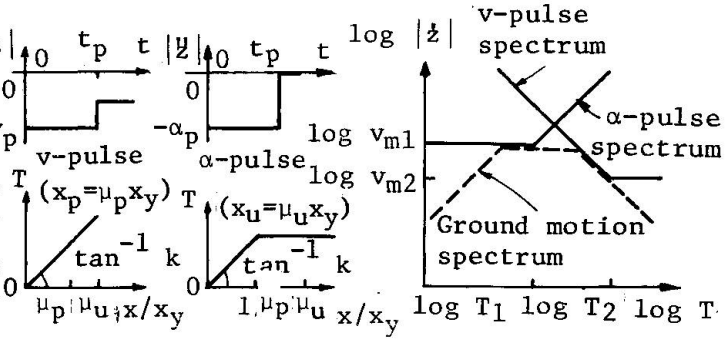

Elastic and Plastic Restoring Force Characteristics

Approximated Bi-linear Pulse Response Spectrum

Fig.12 Pulse Response Analysis[2][3]

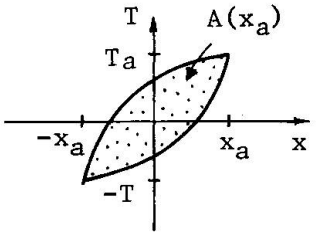

Hysteresis Loop

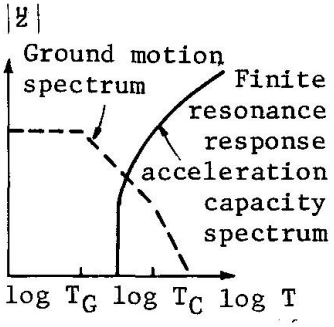

Fig.13 Finite Resonanse Response Analysis

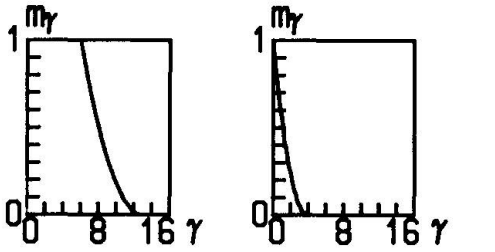

Span Direction Ridge Direction

Fig.14 Satisfaction Degrees of Number of Shear Walls

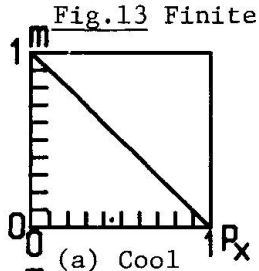

(a) Cool

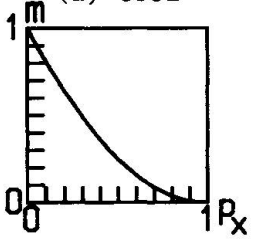

(b) Pessimistic

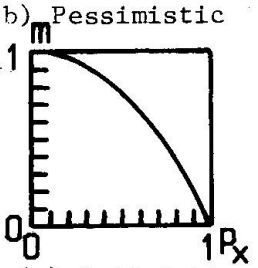

(c) Optimistic

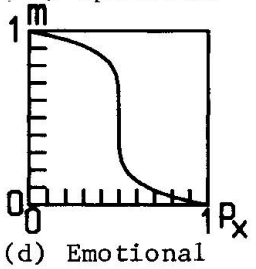

(d) Emotional

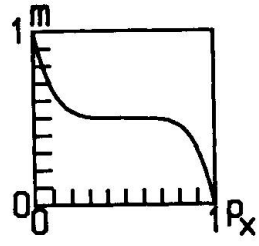

(e) Ordinary

Fig.15 Satisfaction Degrees of Passage Probability

0.1: T_G=0.1[s]
0.8: T_G=0.8[s]
S:Span direction
R:Ridge direction
Inter: Interplate-type earthquake
Intra: Intraplate-type earthquake

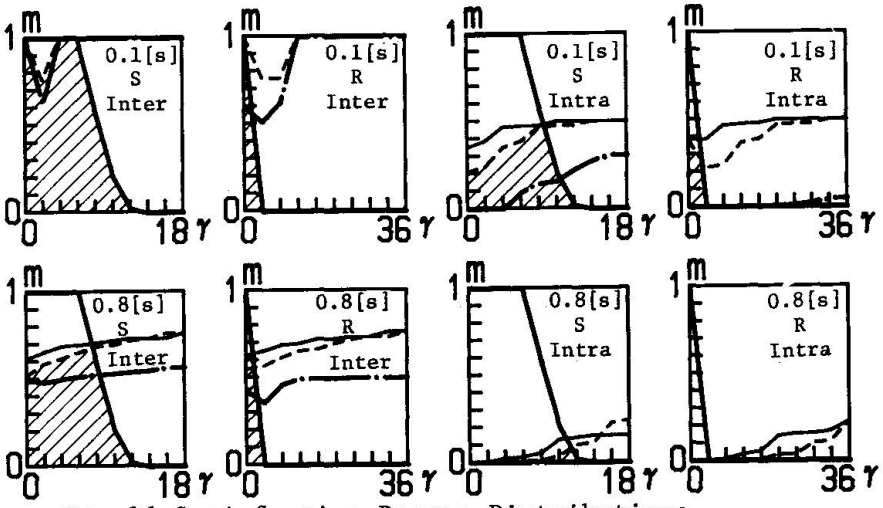

Fig.16 Satisfaction Degree Distributions Based on Classical Probability Theory

— Satisfaction degree of number of shear walls
-·- Satisfaction degree of damage factor
— Satisfaction degree of maximum displacement
-- Satisfaction degree of duration until fracture

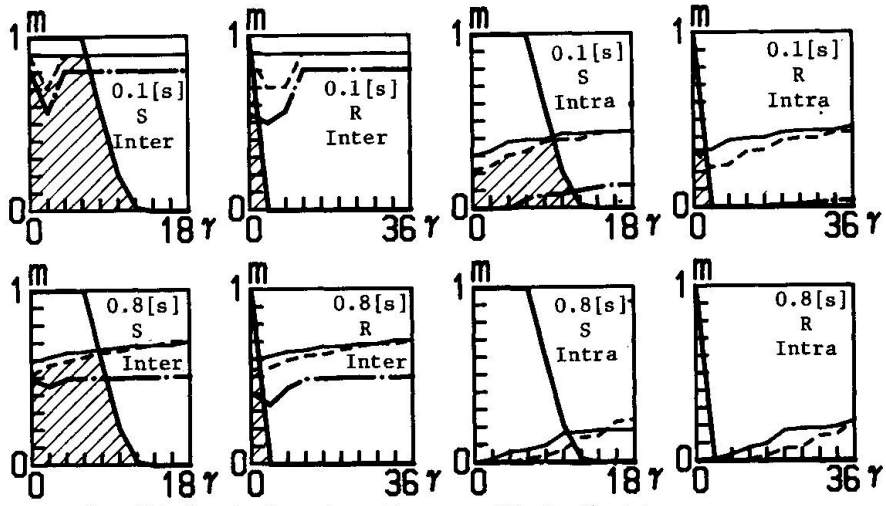

Fig.17 Satisfaction Degree Distributions Based on Benjamin's Probabilistic Model

Table 1 Values of Maximizing Decision Point of $m_D(\gamma^*)$

Probability theories \ Environment parameters	T_G [s]	Interplate-type Span	Interplate-type Ridge	Intraplate-type Span	Intraplate-type Ridge
Based on Classical Probability Theory	0.1	1 (0,4-6)	1 (0)	0.46 (8)	0.38(0)
	0.8	0.65 (6)	0.55(0)	0.03 (0)	0(0-36)
Based on Benjamin's Probabilistic Model	0.1	0.90(0,4-6)	0.90(0)	0.38 (8)	0.32(0)
	0.8	0.62 (6)	0.54(0)	0.07(10)	0(0 36)

Fatigue Reliability Level of Railway Bridges in China

Fiabilité des ponts de chemins de fer en Chine du point de vue de la fatigue

Zuverlässigkeit von chinesischen Eisenbahnbrücken in Bezug auf Ermüdung

Zhen-Ben TENG
Assoc. Prof.
North. Jaotong Univ.
Beijing, China

Born 1929, graduated from Harbin Technical University, China. He is Assoc. Professor of Civil Engineering at North. Jaotong University, China. His research interest is design of structures.

Yao-Kun ZHO
Assoc. Prof.
North. Jaotong Univ.
Beijing, China

Born 1931, graduated from Dong-Bei Technical Institute, China. She is Associate Professor of Civil Engineering at the North. Jaotong University, China.

SUMMARY

In this paper, the fatigue reliability level of railway bridges designed by the Chinese Railway Bridge Design Code is calibrated by level II reliability analysis on the basis of available load spectras, laboratory data and field observations of stress histories.

RÉSUMÉ

Le comportement à la fatigue et la sécurité des ponts de chemins de fer, calculés selon les normes chinoises pour les ponts-rails, sont étudiés à l'aide de l'analyse de la fiabilité, et sur la base des cas de charges connus, des données de laboratoire et d'observations sur des ouvrages existants.

ZUSAMMENFASSUNG

Das Zuverlässigkeits-Niveau in Bezug auf Materialermüdung von Eisenbahnbrücken, welche aufgrund der chinesischen Normen bemessen wurden, wird mit Hilfe der Zuverlässigkeits-Theorie überprüft. Dabei werden vorhandene Lastspektren, Labor-Ergebnisse und an Bauwerken beobachtete Spannungs-Geschichten berücksichtigt.

1. INTRODUCTION

In order to contribuite to development of probability based limit state design of railway bridge structures in China, the fatigue reliability level of railway bridges designed by the Chinese Railway Bridge Design Code is calibrated by first-order, second-moment procedure on the bases of available load spectras, laboratory data and fied observations of stress histories.
Accoding to the CRBD Code the bridge structures are designed for fatigue assuming that all cyclic loads cause stress equal to that induced by the maximum live load namely Chinese Railway Live Load shown in Fig.1. If the maximum stress falls above the fatigue limit for constant amplitude cycling the allowable number of cycles, $2 \cdot 10^6$, for the maximum stress is obtained from an allowable wöhler curve. If it falls below the fatigue limit, the structure is said to have an infinete life.
Field mesurment of actual live load defeine variable amplitude stress range histograms. With the equation of the Wöhler curve, $N=C\Delta\sigma^{-K}$, and the formulas for the comulative damage of the Palmgren-Miner hypothesis, an equivalent stress range of constant amplitude $\Delta\sigma_e$ that produces the same degree of fatigue damage as the variable amplitude stress ranges it replaces.
The fatigue reliability level of bridge structures designed by the present chinese code is calibrated by reliability indices.

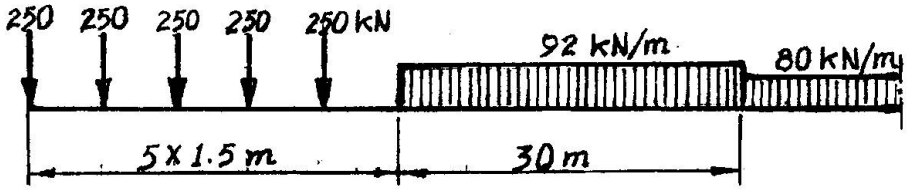

Fig.1. CR design live load

2. DISTRIBUTION OF STRESS RANGES UNDER TRAFFIC LOADS

In order to examine the real traffic conditions on various lines, the stresses under traffic loads were measured on 13 railway bridges. The survey concerning the bridges studied is given in Table 1.
At selected sports of the bridge structure, the stress was recoded by means of strain gauges on magnetic tape for tests of long duration. The stress-time history was further processed in the laboratory.
The recodings show quite regular stress fluctuations under the passage of the passenger train, they are much more random under the freight train. The locomotives of both train types cause predominant stress peaks. The frequency of occurrence of stress ranges is defined by a histogram in which the height of the bar represents the percentage of stress ranges within an interval represented by the width of the bar. The frequency-of-occurrence data can be presented in a more general way by dividing the height of each bar by the width of the bar to obtain a probability density curve.
Let $\Delta\sigma$ be a random variable denotiong stress range. The study of

field data showed that the distribution of the applied stress range $\Delta\sigma$ may be conveniently modeled with the beta-distribution. This particular form of the distribution with specified upper and lower limits for the stress range is appropriate. The beta-density curve can be skewed by changing the parameter values. Three types of stress range pattens are suggested, corresponding to "light", "medium" and "heavy" loading conditions, respectively. The statistics of these three stress range distribution used in the calibration are given in Table 2.

Railway	Material	span (m)	Bridge componested	Number of days	Number of trains
ZG	Reinforced concrete	16	main girders	2.5	140
SF	Pretensioned concrete	16	main girders	3	120
BB	Pretensioned concrete	31.7	main girders	2	95
HC	Reinforced concrete	4.5	main girders	2	95
NL	Reinforced concrete	16	main girders	4	105
L I	Post-tensioned concrete	23.8	main girders	2.5	101
L II	Reinforced concrete	8	main girders	2	110
LL	Post-tensioned concrete	31.7	main girders	3	90
JG	Post-tensioned concrete	31.7	main girders	2	92
JP	Post-tensioned	31.7	main girders	2	108
FS	Post-tensioned concrete	31.7	main girders	2	128
PY	Steel trusses	48	truss chords cross beams stringers	7	490
XG	Steel girders	24	main girders cross beams stringers	7	340

Table 1 Survey of tested bridges

The question arises as to how to treat theoretically such distribution of stress ranges in order to assess the cumulative fatigue damage under the random stress range. The method of equivalent damage has been shown one of the most effective.
Based on the linear damage accumulation hypothesis of Palmgren-Miner and the fatigue strength lines accoding to $N = C\,\Delta\sigma^{-k}$, the equiva-

lent stress range $\Delta\sigma_e$ can be obtained

$$\Delta\sigma_e = [E(\Delta\sigma^k)]^{1/k} \quad (1)$$

where $E(\Delta\sigma^k) = \int_0^\infty \Delta\sigma^k f(\Delta\sigma)d\Delta\sigma$

and $f(\Delta\sigma)$= the probability density for the random variable $\Delta\sigma$. For a beta-distribution with a maximum value of $\Delta\sigma_{max}$, a minimum of o, and shape parameters q, r, the m-th statistical moment of $\Delta\sigma$ becomes

$$E(\Delta\sigma^k) = \Delta\sigma_{max}^k \cdot \frac{\Gamma(q+r)\Gamma(k+q)}{\Gamma(q)\Gamma(k+q+r)} \quad (2)$$

where $\Gamma(\cdot)$ represents the gamma function. Thus the equivalent stress range for a beta-distributed stress range becomes

$$\Delta\sigma_e = \Delta\sigma_{max}\left[\frac{\Gamma(q+r)\Gamma(k+q)}{\Gamma(q)\Gamma(k+q+r)}\right]^{1/k} \quad (3)$$

Noting that $\Delta\sigma_{max} = (\Delta\sigma_{max}/\Delta\sigma^c_{max})\cdot\Delta\sigma^c_{max} = \alpha\,\Delta\sigma^c_{max}$, substituting $\Delta\sigma^c_{max} = (\Delta\sigma^c_{max}/\Delta\sigma_{cR})\cdot\Delta\sigma_{cR} = \gamma\Delta\sigma_{cR}$ and introducing the equivalent stress factor $\varphi = \Delta\sigma_e / \Delta\sigma_{max}$, we obtain

$$\Delta\sigma_e = \Delta\sigma_{cR}\cdot\alpha\cdot\gamma\cdot\varphi \quad (4)$$

where $\Delta\sigma_{eR}$ = the computed stress range due to design loading;
$\Delta\sigma^c_{max}$ = the computed stress range due to actual traffic loading;
$\Delta\sigma_{max}$ = the measured stress range due to actual traffic loading
α = the ratio of actual traffic to theoretical stress, accounting for stress reduction due to participation of elements disregarded in the design, impact values different from design values, stress dissipation, etc;
γ = the ratio of actual stress range to design stress range;
φ = $[\Gamma(q+r)\Gamma(k+q)/\Gamma(q)\Gamma(k+q+r)]^{1/k}$ = equivalent stress factor.

It is to be noted that α, γ and φ can be treated as random variables. From the above formula, mean and coefficient of variation of equivalent stress range $\Delta\sigma_e$ are obtained as follows

$$\overline{\Delta\sigma_e} = \Delta\sigma_{cR}\cdot\bar{\alpha}\cdot\bar{\gamma}\cdot\bar{\varphi} \quad (5)$$

$$V_e = (V_\alpha^2 + V_\gamma^2 + V_\varphi^2)^{1/2} \quad (6)$$

Mean values and coefficients of variation of these random factors were determined from the results of tests, measurements and engineering judgements. These are summarized in Table 3.

loading	q and r of beta-distribution q r	upper limit of stress range $\Delta\sigma_{max}$	mean $\overline{\Delta\sigma}$	standard deviation $S_{\Delta\sigma}$	coefficient of variation $V_{\Delta\sigma}$
Light	1 6	0.7 $\Delta\sigma_{cR}$	0.175 $\Delta\sigma_{cR}$	0.101 $\Delta\sigma_{cR}$	0.577
Medium	4 4	0.7 $\Delta\sigma_{cR}$	0.350 $\Delta\sigma_{cR}$	0.170 $\Delta\sigma_{cR}$	0.334
Heavy	4 1	0.7 $\Delta\sigma_{cR}$	0.560 $\Delta\sigma_{cR}$	0.114 $\Delta\sigma_{cR}$	0.204

Remak $\Delta\sigma_{cR}$=the stress range due to Chinese Railway Live Load.

Table 2 Statistics of stessrange distributions

Loading	$\Delta\sigma_e$	V_α	V_γ	V_φ	V_e
Light	$0.225\ \Delta\sigma_{cR}$	0.15	0.12	0.40	0.444
Medium	$0.387\ \Delta\sigma_{cR}$	0.15	0.11	0.40	0.441
Heavy	$0.581\ \Delta\sigma_{cR}$	0.15	0.10	0.40	0.439

Table 3 Statistics of $\Delta\sigma_e$

3. RANDOM FATIGUE RESISTANCE

Under the condition of a constant stress range, the fatigue life of a structural component or detail has been observed to exhibit considerable variability and, therefore, should be described with a random variable.

Since the data seldom are sufficient to define the probability distributions, we nomally must rely on assumed distributions which arise from relevant physical arguments. The weibull and lognormal distribution have been widely used in fatigue studies.

The results of a series of tests for the same value of $\Delta\sigma$ in the number of load cycles until fracture are assumed to follow a lognomal distribution. Use of the lognormal distribution has been based primarily on arguments of mathematical expelience.

If fatigue strength $\Delta\sigma$ is assumed to be lognormal, the least square line is the median of $\Delta\sigma$ for a given N, denoted as $\tilde{\Delta\sigma}$. The mean value of $\Delta\sigma$ is estimated as $\ln \bar{\Delta\sigma}$.

The coefficient of variation of $\Delta\sigma$ should incoporate all sources of uncertainty inherent to the fatigue behavior of the structural detail in service. In addition to inherent scatter in the laboratory test data, these would include errors in the stress analysis, the effects of fabrication and workmanship, sampling and measurment.

The value of uncertainty in the fatigue resistance $V_{\Delta\sigma}$ may be evaluated in terms of the individual sources of uncertainty and combined systematically through statistical methods. An estimate for $V_{\Delta\sigma}$ may be obtained by first-order statistical analysis

$$V_{\Delta\sigma} = \frac{1}{K^2}\left(V_c^2 + V_N^2 + V_g^2\right)$$

where V_c = the uncertainty in the intercept of the Wöler curve; this should include the uncertainty in the effect of fabrication and quality of workmanship;

V_N = scatter in the fatigue life data about the Wöler curve;

V_g = the inaccuracy of the fatigue model

The objective in calibration is to check the reliability level in fatigue design covered by the present code. In the calibration the fatigue strength of structural members and details are taken as fatigue resistances. In the fatigue limit state, resistance is expressed in terms of stress ranges. In the CRBD Code calibration several characteristic detailes and members are selected. They are often used in bridge structures constructed in China. In the FOSM methods of reliability checking a random variable is usually characterized by two values, such as the mean and the coefficient of variation. The resistances are characterized by their nominal values, the ratios of mean to nominal, $\bar{\Delta\sigma}/\Delta\sigma_n$, and the coefficient of variation $V_{\Delta\sigma}$.

The values of $\bar{\Delta\sigma}/\Delta\sigma_n$ and $V_{\Delta\sigma}$ used in calibration are calculated on the basis of information provided by various specialized research

groups in China, and adopted from engineering judgment. The adopted statistics of fatigue resistance are listed in Table 4.

Detials and mumbers	$\Delta\sigma/\Delta\sigma_n$	K	V_N	$(V_c^2+V_g^2)^{\frac{1}{2}}$	$V_{\Delta\sigma}$
Continuous manual longitudinal fillet welds parallel to the diraction of stress.	1.02	-2.78	0.359	0.4	0.193
Beam flange with cover plate-not welded across plate ends.	1.00	-2.97	0.271	0.4	0.163
Transverse stiffener fillet welded to beam web.	1.01	-2.75	0.509	0.4	0.235
Plate transverse butt welded to beam flange.	1.02	-3.17	0.428	0.4	0.185
Post-tensioned concrete beam.	1.00	-3.50	0.201	0.4	0.167

Table 4. Statistics of fatigue strength

4. RELIABILITY INDICES

In order to conduct calibration of fatigue reliability level of bridge structures designed by present code, which is the purpose of this study, the First-Order, Second-Moment procedure is thought to be appropriate. In the FOSM procedure the degree of reliability is characterized by a reliability index which is defined, in general, as

$$\beta = \frac{\bar{Z}}{\sigma_Z} \tag{7}$$

in which $Z = g(X_1, \ldots, X_n)$ is the fomulation variable corresponding to the limit state $g(X_1, \ldots, X_n)=0$, X_i are the basic random variables in the formulation of the problem; $\bar{Z}$ and σ_Z are the mean and the standard deviation of Z, respectively.
The reliability index for fatigue may be obtained by formulating the limit state

$$Z = \ln(\Delta\sigma/\Delta\sigma_e) = 0 \tag{8}$$

where $\Delta\sigma$ = the fatigue strength and $\Delta\sigma_e$ =the equivalent stress range. In practice the mean and standard deviation of Z can be takan as the first-order approximations

$$\bar{Z} = \ln(\overline{\Delta\sigma}/\overline{\Delta\sigma_e}) \tag{9}$$

$$\sigma_Z = (V_{\Delta\sigma}^2 + V_e^2)^{1/2} \tag{10}$$

where $\Delta\sigma$, $V_{\Delta\sigma}$ =mean and coefficient of variation of fatigue strength, and $\Delta\sigma_e$, V_e =mean and coefficient of variation of equivalent stress range, respectively. Thus the reliability index is given by

$$\beta = \frac{\ln\left(\frac{\overline{\Delta\sigma}}{\overline{\Delta\sigma_e}}\right)}{(V_{\Delta\sigma}^2 + V_e^2)^{1/2}} \qquad (11)$$

The typical details of welded plate girders and prestressed concrete girders of railway bridges designed occording to the CRBD Code were calibrated using Eq. (11). The calculated values of the fatigue reliability indices β are given in Table 5.

Category of bridge Described in table 4	Total uncertainty $(V_{\Delta\sigma}^2 + V_e^2)^{1/2}$	Traffic load factor $\overline{\Delta\sigma_e}/\Delta\sigma_{eB}$		
		Light	Medium	Heavy
		0.225	0.387	0.581
1	0.484	3.58	2.48	1.64
2	0.473	3.63	2.49	1.62
3	0.502	3.49	2.36	1.55
4	0.481	3.59	2.47	1.62
5	0.474	3.66	2.53	1.67

Table 5 Calculated values of the reliability indices β

5. CONCLUSIONS

The primary objective of this paper is to check for the fatigue reliability level of actual traffic on railway bridges designed by the present CRBD Code. As a result, it is shown that the ranges of reliability indices are found to be from 1.5 to 3.6 for fatigue design situation. The level of is affected very much by coefficients of variation of loads and resistance, especially if they are large.

Other design situations such as the ultimate limit state and the second serviceability limit state were not considered in this calibration collection of statistical data of loads and resistance of bridge structures and calibration of them with reliability indices are strongly needed in China for future probability based limit state design of railway bridge structures.

6. REFERENCES

1. FRYBA L., Railway bridges subjected to traffic loads and their design for fatigue. Rail International, October 1980.

2. CRRA, Axle-loads and stress distributions of railway bridges in China. Repot of Chinese Reilway Research Academy, December 1983. (in Chinese)

3. Ministry of Railway, Chinese Reilway Bridge Design Code. 1973. (in Chinese)

4. MBRA, A collection of experimental data for fatigue. Repot of Metallurgical Bulding Research Academy. 1978, (in Chinese).

5. ANG A.H.-S. and Munrse W.S., Practical reliability basis for structural fatigue. ASCE National structural Engineering Conference, April 1975.

6. GURNEY T.R. and MADDOX S.J., A Re-analysis of Fatigue Data for Welded Joints in Steel. Research Rpt. NO. E/44/72, The Welding Institude, Cambridge, England, Jan. 1972.

7. ALBRECHT P. and FRIEDLAN I.M., Fatigue-Limit Effect on Variable-Amplitude Fatigue of Stiffeners. Journal of the structural Division, ASCE, Vol. 105, NO.ST12, December 1979.

8. TENG Z.-B. and ZHo Y.-K., Method of bridge design code calibration. Repot of Northern Jaotong University, May 1983. (in Chinese)

Acceptable Risk Levels for Fatigue Design of Concrete Structures

Niveaux de risque acceptables pour le dimensionnement à la fatigue de structures en béton

Akzeptierbares Risiko-Niveau für die Bemessung von Betonbauten auf Ermüdung

R.F. WARNER
Prof. of Civil Engineering
Univ. of Adelaide
Adelaide, Australia

R.F. Warner was born in 1935. He obtained his doctorate from Lehigh University. With research interests in the behaviour of concrete structures, he has published text books on the design of prestressed and reinforced concrete.

SUMMARY

A method is proposed for determining acceptable risk levels for the fatigue design of concrete structures. The safety level for fatigue failure is found by calibrating back to the safety level for flexure failure. The underlying assumption is that the expected cost of failure should be approximately equal for fatigue and flexure.

RÉSUMÉ

Une méthode est proposée afin de déterminer les niveaux de risque acceptables pour le dimensionnement à la fatigue de structures en béton. Le risque d'une rupture due à la fatigue est comparé au risque d'une rupture par flexion. L'hypothèse retenue est que le coût prévisible de la rupture soit à peu près semblable dans les cas de fatigue et de flexion.

ZUSAMMENFASSUNG

Eine Methode für die Bestimmung akzeptierbarer Versagenswahrscheinlichkeiten für die Bemessung von Stahlbetonbauten gegen Ermüdung wird vorgeschlagen. Die Wahrscheinlichkeit des Ermüdungsbruchs wird an der Wahrscheinlichkeit eines Biegebruchs kalibriert. Dabei wird vorausgesetzt, dass die Versagenskosten für diese beiden Brucharten etwa gleich sein sollten.

1 INTRODUCTION

Before any new, improved structural design procedure can be introduced into a code of practice, an appropriate margin of safety for design has to be chosen, and partial safety coefficients which will provide this safety margin then have to be evaluated. The problems of choosing an appropriate margin of safety and evaluating the corresponding safety coefficients also arise whenever the design of an unusual, one-off structure is undertaken in circumstances to which routine code design procedures are not applicable. With a new generation of limit states codes being introduced progressively in a number of countries, many code writers are currently involved in the tasks of establishing target safety margins for structural design and evaluating the corresponding safety coefficients.

Despite much recent theoretical research into structural reliability theory, the most frequently used method for evaluating design safety coefficients is still by back-calibrating to an existing design procedure which has been shown by extensive previous use to be safe and economic. Back calibration consists essentially of adjusting the safety coefficients in the new design procedure so that, for a number of carefully selected, representative design cases, the resulting designs are very similar to those which are obtained from the existing method. Of course, the back-calibration method can only be used if a well-tried design procedure is already at hand. This is not the situation in the design of concrete structures for fatigue. Indeed, the problem of design for fatigue, as distinct from analysis of fatigue life and fatigue resistance, has received surprisingly scant research attention. Consequently, there is very little guidance presently available to the designer with regard to the safety margins and partial safety coefficients which should be used in fatigue design.

This paper describes a procedure for determining the appropriate risk level for use in the fatigue design of reinforced concrete and prestressed concrete structures. The procedure is called cross-calibration, since it relies on a quantitative comparison of the safety requirements for fatigue with those of another limit state (in this case flexure) which has already been back-calibrated to an existing design method (the ultimate strength method) with a history of successful use. The basis for the quantitative comparison is expected cost of failure.

2. LIMIT STATE FORMAT FOR FATIGUE

In the usual limit states design format [6], a comparison is made between a measure of load intensity S, and a measure of structural resistance R. The margin of safety may be defined as the difference between R and S:

$$Z = R - S \qquad (1)$$

All three quantities R, S and Z must of course have the same dimension, which for an ultimate limit state may be force, moment or possibly stress. In fatigue design, R and S may be chosen in a variety of ways: they may refer to the stress intensity at a potential fracture point, to the number of cycles to failure, to accumulated damage in a critical region of the structure, or even to the degradation in static strength of the structure as the result of fatigue damage [6]. Given the limited amount of design data currently available on fatigue of concrete structures, the cycle format appears to be the most promising and the one most readily adaptable to useful design calculation.

Once the design format has been chosen, simple first-order reliability concepts can be applied in a routine manner. The actual fatigue life N_R of a member subjected to a specified load spectrum shows considerable variability and is

best treated as a random variable. For design, a characteristic fatigue life N_{Rk} is chosen to correspond to a specific failure probability P_k:

$$P[N_R < N_{Rk}] = P_k \tag{2}$$

A design value N_{Rd} is defined by means of a safety coefficient γ_{RN}:

$$N_{Rd} = \frac{1}{\gamma_{RN}} N_{Rk} \tag{3}$$

The number of cycles of load which the structure will be designed to resist is denoted by N_S. This may be regarded either as a design constant (such as $2X10^6$) or as a random variable [1]. In the latter case, a characteristic value N_{Sk} has to be chosen:

$$P[N_S < N_{Sk}] = 1 - P_k \tag{4}$$

and hence by means of a partial 'load' factor γ_{SN}, a design value can be defined:

$$N_{Sd} = \gamma_{SN} N_{Sk} \tag{5}$$

Experimental studies of fatigue failure suggest that fatigue life N is best considered on a logarithmic scale. The safety margin Z is therefore defined here in terms of the transformed variables:

$$\bar{N}_S = \log N_S \tag{6}$$

$$\bar{N}_R = \log N_R \tag{7}$$

$$Z = \bar{N}_R - \bar{N}_S \tag{8}$$

The reliability index β then can be defined as follows [4]:

$$\beta = \frac{\mu(Z)}{\sigma(Z)} = \frac{\mu(\bar{N}_R) - \mu(\bar{N}_S)}{\sqrt{\sigma^2(\bar{N}_R) + \sigma^2(\bar{N}_S)}} \tag{9}$$

The nominal probability of failure P_f is related to β by the properties of the normal distribution [4].

Various problems are involved in the evaluation of the safety coefficients γ_{RN} and γ_{SN}, once the reliability index β has been chosen. For example, in dealing with the fatigue life N_R the load spectrum has to be taken into account, usually by some form of cumulative damage calculation. Such matters have been discussed elsewhere [6]. The purpose of the present paper is to deal with the problem of determining an appropriate margin of safety, ie of evaluating β or, equivalently, P_f.

3. CROSS-CALIBRATION AND EXPECTED COSTS

The cross-calibration procedure proposed here is based on a comparison of the safety requirements for fatigue design with those for design for flexure. It is assumed that the latter has already been back-calibrated to the existing ultimate strength design procedures in current use. The quantitative basis for the comparison is expected cost of limit state entry. The probability of occurrence of an event E_j, such as entry into a limit state, will be written as $P[E_j]$. The cost of event E_j, should it occur, is $C[E_j]$, and the expected cost of E_j is defined as:

$$EC[E_j] = P[E_j].C[E_j] \tag{10}$$

A range of consequences, Q_{ij}, follow on from an event E_j, and each consequence has an associated cost $C[Q_{ij}]$. If the consequences all occur simultaneously, then we have:

$$C[E_j] = \sum_i [Q_{ij}] \tag{11}$$

and the expected cost of E_j becomes:

$$EC[E_j] = P[E_j] \sum_i C[Q_{ij}] \tag{12}$$

However, if there exists a range of alternative, mutually exclusive consequences Q_{ij} with costs $C[Q_{ij}]$ and associated probabilities $P[Q_{ij}]$, then we have:

$$C[E_j] = \sum_i P[Q_{ij}].C[Q_{ij}] \tag{13}$$

$$EC[E_j] = P[E_j] \sum_i P[Q_{ij}].C[Q_i] \tag{14}$$

As we shall be concerned only with fatigue and flexure failure, the indices 1 and 2 will be used to refer to these limit states, respectively. Thus, E_1 and E_2 are the events of fatigue failure and flexure flexure.

In order to evaluate the target design probability for fatigue, $P[E_1]$, the criterion of equal expected costs for fatigue and flexure failure is applied:

$$EC[E_1] = EC[E_2] \tag{15}$$

This leads to the following expression for the target design probability for fatigue:

$$P[E_1] = P[E_2] \frac{C[E_2]}{C[E_1]} \tag{16}$$

Nominal probabilities of failure for use in the design of concrete, steel and timber members have recently been evaluated by Leicester [2], by a process of back-calibration to existing Australian design codes. Extreme values obtained by Leicester for the safety index β, together with the corresponding nominal probabilities of failure, $P[E_2]$, for the flexural design of concrete members, are summarised in Table 1.

4. CONSEQUENCES AND COSTS OF LIMIT STATES ENTRY

If estimates can be made of the consequences and hence relative costs of fatigue failure and flexure failure, Eq 16 can be used in conjunction with the information in Table 1 to evaluate $P[E_1]$, the nominal probability of failure for use in fatigue design.

If event E_j represents the entry of a member into a strength limit state, the consequences which need to be considered include the following:

Q_{1j}: damage to, or destruction of, the structural member;
Q_{2j}: damage to, or destruction of, non-structural attachments;
Q_{3j}: damage to the contents of the structure;
Q_{4j}: injury and possible loss of life;

Q_{5j}: inconvenience, including loss of income, during the period that the structure is out of service.

r	β_2		$P[E_2]$ ($\times 10^{-6}$)	
	min	max	min	max
0	3.37	3.85	337	60
0.25	3.60	4.25	159	11
0.50	4.08	5.08	21	0.2
0.75	4.00	4.39	32	5
1.00	3.93	3.93	48	48

Table 1 Values of β_2 and $P[E_2]$ for flexure failure (obtained by back calibration [2]).

Note: r is the ratio of wind load to total load, ie wind plus dead plus live loads.

It will be assumed that the cost associated with each of these consequences is a simple multiple of the original cost C_0 of the structural member:

$$C[Q_{ij}] = f_{ij} \cdot C_0 \tag{17}$$

This assumption is probably very reasonable for some of the consequences listed (eg i = 1,2) but rather arbitrary for others (i = 3,4,5). Nevertheless, anything but the simplest approach is unwarranted. Since the consequences being considered can occur simultaneously, we use Eq 12 to express the expected cost of limit state entry as:

$$EC[E_j] = P[E_j] \cdot C_0 \sum_i f_{ij} \tag{18}$$

By introducing a factor F into Eq 16 to take account of the multiplying factors f_{ij}, we obtain the following expressions:

$$P[E_1] = P[E_2] \cdot F \tag{19}$$

$$F = \frac{\sum_i f_{i2}}{\sum_i f_{i1}} \tag{20}$$

The events leading to failure and the consequences of failure are greatly affected by the structural details of the member, as well as by its use and, where relevant, the occupancy and contents of the overall structure. Of particular structural importance is whether or not the member is statically indeterminate.

Considering first the case of a statically determinate member, we can reasonably assume that flexural failure leads to collapse, with destruction of any attached non-structural members and contents. In contrast, the consequences of fatigue failure in a determinate concrete flexural member are likely to be far less serious. The reason for this is that fatigue failure occurs progressively in a concrete flexural member by successive fracture of the tensile steel elements (prestressing wires or reinforcing bars). In practice there are many individual elements which make up the total tensile steel area, and so the process of fatigue failure is not sudden but gradual, with warning of deterioration given by increasing deflection and widening cracks.

In order to obtain a range of relevant cost values we consider two main structural cases, one with, and the other without, serious consequences of collapse. In Table 2, estimated values for the cost factors f_{ij} are included for the various conditions.

i	Consequences of failure: serious j=1 fatigue	serious j=2 flexure	not serious j=1 fatigue	not serious j=2 flexure
1	2	2	2	2
2	1	10	2	2
3	1	50	1	10
4	1	150	1	1
5	10	10	10	10
$\sum_i f_{ij}$	15	222	16	25

Table 2 Cost factors f_{ij}

In the case of flexure failure a factor of 2 is used in Table 2 for the costs associated with repair or replacement (Q_{12}). Although the damage from fatigue failure (fracture of several steel elements in the critical section) is not as severe as for flexure failure, repair is likely to be complicated. Furthermore, fatigue damage is likely to have been initiated in other steel elements and in other critical cross-sections. The cost of repair has therefore been chosen as equal to that for flexure failure. Damage to any non-structural attachments is likely to be severe in the case of flexural failure, and it seems appropriate to choose f_{22} to correspond to the full cost of replacement. These can only be evaluated accurately for a specific example and a rather arbitrary range is given in Table 2. In the case of fatigue failure, collapse does not occur, so that there is likely to be little or no damage to non-structural attachments. The situation regarding damage to contents is similar to that for non-structural attachments. Damage is likely to be zero for fatigue failure and substantial for flexure failure.

Although the likelihood of injury will depend very much on the use and occupancy of the structure, the consequences of fatigue failure remain minimal because collapse is avoided. On the other hand, flexural failure in a determinate member is always potentially serious. The values chosen for f_{42} are intended to reflect this. The situation is rather different with regard to the out-of-service costs, which will be incurred irrespective of the reason for the structure not being able to coninue to function. Out-of-service time is also of importance, but this will depend on the repair process rather than on the cause of failure. Similar values for f_{51} and f_{52} have therefore been introduced into Table 2. From the entries in Table 2, a range of values for the factor F of from 10 to about 250 is obtained for statically determinate members.

In the case of statically indeterminate members, the consequences of flexure failure become less severe because attainment of the moment capacity in a critical cross-section does not any more imply structural collapse, but rather localised yielding of the reinforcing steel with increased deformations and deflections, possibly with some permanent set. The situation is now more comparable with that of fatigue failure, for which the consequences are rather similar. The cost of repair in each case is probably about equal to the cost of replacement. However, there is little point in considering the indeterminate

case in detail because current and proposed design procedures [3] rarely allow for different safety levels according to the degree of statical indeterminacy.

The general figures given in Table 2 are clearly very approximate and even speculative. However, more accurate figures can always be obtained if a specific design case is investigated. It must also be remembered that gross approximations are introduced into the safety treatment for flexural design. As we have just seen, even the influence of statical indeterminacy is at present ignored in the choice of the safety margin for flexural design. For statically determinate members with important and expensive installations and contents, and subject to high occupancy, the cost factors in Table 2 would suggest a value of the ratio F (Eq 20) as follows:

$$F = 20$$

For less important members, the value of F drops markedly:

$$F = 2 \text{ to } 10$$

In the case of indeterminate structures with high levels of built-in indeterminacy, the factor F would also be quite low and similar to the previously quoted range for less important members.

In order to obtain an independent estimate of the factor F, it is possible to use data provided by the Nordic Committee on Building Regulations (NKB). In choosing target failure probabilities, the NKB considers the consequences of failure in three categories, namely not serious, serious, and very serious. Three failure types are considered:
(1) ductile failure with strength reserves due to strain hardening;
(2) ductile failure without reserve capacity; and
(3) brittle failure and instability.

If fatigue failure in a concrete member is identified with first wire or bar fracture, then it is reasonable to treat this as a type 1 failure category, while normal flexure failure for a determinate member could well be regarded as category 2. Assuming the consequences of failure to be serious or very serious, and then taking the corresponding NKB nominal probability levels as quoted in Ref [4], we obtain a range of values for $P[E_1]$ of from 10 to 100 times $P[E_2]$, ie

$$F = 10 \text{ to } 100$$

This range includes the values obtained from the previous considerations.

5. SAFETY COEFFICIENTS FOR FATIGUE DESIGN

With the nominal probability level $P[E_1]$ evaluated, and hence also the corresponding value of β determined, it is possible to estimate values for the partial safety coefficients from the basic limit states requirement:

$$N_{Sd} < N_{Rd} \qquad (21)$$

If N_S is treated as a design constant rather than a random variable, γ_{SN} is set equal to unity and the following expression is obtained from the usual second order theory:

$$\gamma_{RN} = \frac{\mu(N_R) - 1.64\,\sigma(N_R)}{N_s} \qquad (22)$$

In order to obtain numerical values for γ_{RN}, the design safety coefficient for fatigue, estimates must first be obtained for the coefficient of variation of N_R. It is not the purpose of this paper to discuss the evaluation of γ_{RN}; however this question has been discussed specifically in regard to fatigue in Ref [6].

6 CONCLUDING REMARKS

The proposed back-calibration procedure is open to the criticism that gross and highly approximate estimates of the costs and consequences of entry into the relevant limit states have to be made, in order to obtain numerical values for $P[E_1]$ and hence for the safety index β and the partial safety coefficients. While this is certainly correct, it must be considered in context. There are gross approximations implied in the use of the safety coefficients for flexure, and the error introduced in the present treatment of fatigue reliability is probably not excessive when compared with the errors implied by the gross approximations made in the safety treatment for flexure, which is the best documented of the design limit states.

It should be emphasised that the probability of failure dealt with in simple first order reliability theory is a nominal quantity only, and has nothing directly to do with actual, observed frequencies of failure of real structures. In practice, failure usually occurs in a great majority of cases due to gross error. The important question regarding the relevance of analyses based on nominal probabilities of failure cannot be entered into here. Although it has been argued that design procedures derived from nominal failure probabilities are applicable, even when gross errors govern the rate of occurrence of failure in real situations, the question is far from settled in the opinion of the present author. The main argument which can be raised in defence of the method used here is one of consistency: The proposed cross-calibration procedure will at least give consistency with other limit states design procedures, such as for flexure and shear, for which it has been possible to use back-calibration procedures.

7. REFERENCES

1. GRUNDY P., Fatigue as a Design Limit State. Proceedings IABSE Fatigue Colloquium, Lausanne, IABSE Reports Vol 37, Zurich, 1982.

2. LEICESTER R., Guidelines for conversion to limit states design codes, Part III, Examples of load factors for limit states codes, Working Document, Standards Association Australia, 1982.

3. STANDARDS ASSOCIATION AUSTRALIA (SAA), Draft Australian Standard for Concrete Structures, Document DR85137, Standards Association Publication, May, 1985.

4. THOFT-CHRISTENSEN P., BAKER M.J., Structural reliability theory and its applications, Springer Verlag, Berlin, 1982.

5. WARNER R.F., Fatigue of Partially Prestressed Concrete Beams, Proceedings, IABSE Fatigue Colloquium, Lausanne, IABSE Reports Vol 37, Zurich, 1982, pp431-438.

6. WARNER R.F., Design of concrete structures for fatigue reliability, Bulletin, Disaster Prevention Research Institute, Vol 35, Kyoto University, 1985.

Probabilistic Appraisal of Safety Factors in Design Codes

Apprécation probabiliste des facteurs de sécurité dans les normes de calcul

Wahrscheinlichkeitstheoretische Einschätzung von Sicherheitsfaktoren in Normen

Toshiyuki SUGIYAMA
Associate Professor
Yamanashi University
Kofu, Japan

Toshiyuki Sugiyama, born in 1954, graduated and received his Dr. Eng. degree from the University of Tokyo. He is now engaged in teaching and research on structural engineering, particularly the application of reliability theory at Yamanashi University.

Yozo FUJINO
Associate Professor
University of Tokyo
Tokyo, Japan

Yozo Fujino, born in 1949, graduated from the University of Tokyo, and received his Ph.D. degree at the University of Waterloo, Canada in 1977. After teaching at the University of Tsukuba, he is now at the University of Tokyo.

Manabu ITO
Professor
University of Tokyo
Tokyo, Japan

Manabu Ito, graduated in 1953, and received his Dr. Eng. degree from the University of Tokyo. He has been engaged in teaching and research on bridge engineering and structural dynamics at the same university.

SUMMARY
This contribution discusses the reliability level for the determination of safety factors in structural codes. The first part is concerned with the target safety level of a component of a structural system, taking into account the variability of loads and uncertainties due to gross errors. The latter part of the paper discusses the balance of safety levels of different components in a structural system using a long-span suspension bridge as an example.

RÉSUMÉ
L'article traite du niveau de fiabilité pour la détermination de facteurs de sécurité dans les normes de construction. La première partie concerne le niveau de sécurité optimal pour un élément du sysstème structural, considérant la variation des charges et l'incertitude possible due à de grossières erreurs. La deuxième partie envisage l'équilibre des niveaux de sécurité de divers éléments dans un système structural, à partir de l'exemple d'un pont suspendu de grande portée.

ZUSAMMENFASSUNG
Der Beitrag befasst sich mit dem Zuverlässigkeits-Niveau für die Festlegung von Sicherheitsfaktoren in Tragwerks-Normen. Zunächst befasst er sich mit dem anzustrebenden Sicherheits-Niveau von Bauteilen, wobei sowohl die Streuungen der Lasten als auch die Unsicherheiten aus groben Fehlern berücksichtigt werden. Sodann wird am Beispiel einer weitgespannten Hängebrücke die Ausgewogenheit des Sicherheits-Niveaus verschiedener Bauteile eines Tragsystems erörtert.

1. INTRODUCTION

One of the most important items in reliability-based code making is to determine the target sefety level. It is often believed in code calibration that the uniform safety level for different loads or their combination is desirable[1]. However, it seems that the situation is not necessarily so in the current design codes. For example, the safety factor or safety level for dead plus live loads is, in most of the codes, taken higher than that for the environmental loads such as wind or earthquake effects[2].

The target safety level is basically determined such that the total cost including the initial and failure costs is minimized. It should be noted that the variability of the loads would considerably affect the initial cost in securing the required safety level, and hence the optimal safety level can be expected to depend on the load variability.

The history of structures indicates that incompleteness of engineer's knowledge or human error has been one of the major causes of the structural failures[3]. It would be true that the traditional safety factor has been expected to cover not only randomness of resistance and load, but also partly to cover the above mentioned uncertainties which are called as 'gross errors' in this paper. Certain gross errors cannot be completely excluded in the present design and construction processes, although their occurrence may be kept below a prescribed level by means of quality control and inspection.

Under these considerations, in the first part of this paper the target safety level of a component of structural system is assessed, taking into account the variability of loads and uncertainties due to gross errors.

Many of civil engineering structures are regarded as a system of several components. The safety levels or safety factors should not be necessarily the same for different load combinations or different structural components[4]; the appropriate safety factors for each component should be chosen depending upon its cost and consequence of its failure. In the second part of this paper, the balanced allocation of safety factors in a structural system is discussed on the basis of the economic optimization. A long-span suspension bridge is used therein as an example.

2. TARGET SAFETY LEVEL

2.1. Target safety level by cost minimization principle

2.1.1 Evaluation of total cost

Total cost C_T of civil engineering structure may be expressed by

$$C_T = C_I + P_F C_F \tag{1}$$

where C_I and C_F represent the construction plus maintenance cost and failure cost of the structure (component), respectively, while P_F is the probability of failure[5]. According to the principle of total cost minimization, the design of structure attaining the minimum total cost is regarded as optimum.

It is assumed in this study that both the structural resistance R and the load effect S, treated as random quantities, are log-normally distributed. Then the probability of structural failure P_F is given by

$$P_F = \Phi(-\beta) \tag{2}$$

where $\Phi(\cdot)$ is the cumulative distribution function of the standard normal distribution and safety index β is

$$\beta = \{\ln(\bar{\nu}\sqrt{1+V_S^2}/\sqrt{1+V_R^2})\}/\sqrt{\ln\{(1+V_R^2)(1+V_S^2)\}} \quad (3)$$

$$\bar{\nu} = \bar{R} / \bar{S} \ : \text{ central safety factor} \quad (4)$$

$\bar{R}$: mean of R, V_R: coefficient of variation of R,
$\bar{S}$: mean of S, V_S: coefficient of variation of S

In general, initial construction cost C_I increases with the increase of the safety factor ν. The following function proposed in Refs. [6] and [7] is used:

$$C_I(\nu) = C_I(\nu_0)\{1+b(\nu/\nu_0-1)\} \quad (5)$$

where ν_0 is the value adopted in the current code and 'b' is a constant. Then the total cost is obtained as

$$C_T = C_I(\nu_0)\{1+b(\bar{\nu}/\bar{\nu}_0-1)+P_F C_F^*\} \quad (6)$$

Failure cost of structure should be evaluated taking account of the direct loss and the indirect loss associated with social and economical effects caused by failure. Because its evaluation is very difficult at present, the dimensionless failure cost C_F^* is assumed to be constant in this study.

Design resistance R_d and design load S_d are assumed to be the fractile values, corresponding to 10% lower and upper fractile, respectively. Furthermore, the following design format is used:

$$R_d / \nu \geqq S_d \quad (7)$$

Then substituting eq. (2) into eq. (6) and satisfying the condition $dC_T/d\beta = 0$, the optimal safety level βopt can be obtained.

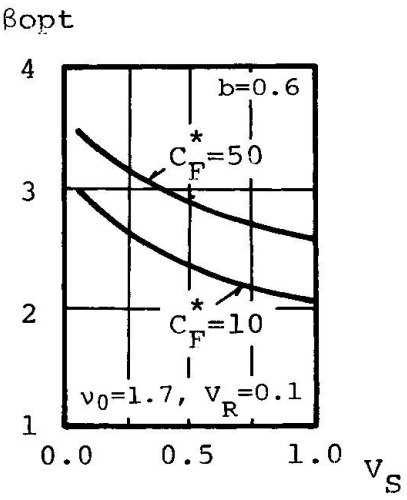

Fig.1 Optimal safety level β_{opt}

2.1.2 Numerical results and discussions

Fig. 1 shows the calculated optimal safety level βopt as a function of the coefficient of variation, V_S of load effect. It is found that the value of βopt for the small V_S is significantly larger than βopt for the large V_S. This result suggests to assign a relatively high target safety level to the structures subject to the less variable load effects. The reason for being obtained this result is that the safety index β does not effectively increase with the increase of the central safety factor when the value of V_S is large. In other words, the large initial cost is required to achieve high safety level for this case.

2.2 Target safety level in presence of gross errors

2.2.1 Probabilistic model

It is well recognized that structural safety depends not only on statistical uncertainties but also uncertainties due to gross errors such as human errors. Then the effect of the latter uncertainties on structural reliability is investigated by use of the simple probabilistic model defined as below[3].

Assume that the structural resistance R decreases to R_u because of the existence

of uncertainties due to gross errors and that R_u is defined as

$$R_U = R \times U \tag{8}$$

where U is the random variable whose probability density function is

$$f_U(x) = P\delta(x-\phi) + (1-p)\delta(x-1) \tag{9}$$

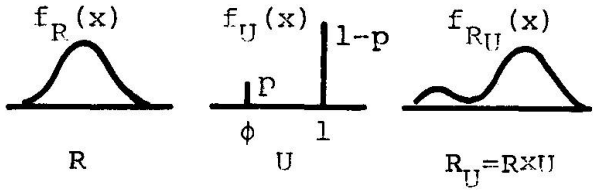

Fig.2 Structural resistance deterioration model

in which $\delta(\cdot)$ is Dirac's delta funcion. In this modeling it is considered that the resistance reduction occurs with probability p and that structural resistance R deteriorates to $(1-\phi)R$ as shown in Fig. 2. The probability of failure with log-normally distributed R and S is expressed as

$$P_F^* = \text{Prob}[R_U < S] = pP_{F_U} + (1-p)P_{F_n} \tag{10}$$

in which

$$P_{F_U} = \Phi(-\beta_n - \ln\phi / \sqrt{\ln\{(1+V_R^2)(1+V_S^2)\}}) \tag{11}$$

$$P_{F_n} = \Phi(-\beta_n) \tag{12}$$

βn in eqs. (11) and (12) is the 'apparent' or 'operational' safety index and is the same as that defined by eq.(3). If the values of p and ϕ in eqs. (10) and (11) are given, P_F^* can be calculated by eq. (10).

2.2.2 Values of parameter p and ϕ

We attempt herein to estimate the reasonable range of parameters p and ϕ from the surveys on bridge failures[8]. Suppose that all of structures are designed so as to attain the target safety level βn. Under this condition, the ratio 'a' which leads to the relation between the number of failure caused by uncertainties due to gross errors and that caused by statistical ones is defined from eq. (10) as

$$a = pP_{F_U} / (1-p)P_{F_n} \tag{13}$$

According to the structural failure data in Ref. [8], it can be found that the ratio 'a' takes the values between 0.25 and 2.4. On the other hand, many civil engineers and investigators consider that the actual failure probability of civil engineering structures may be higher than operational one[9], which is generally said to be about $10^{-4} \sim 10^{-6}$. Taking account of these situations, the ratio 'a' is assumed here to take the value between 0.25 and 10.0. Consequently, the fluctuation range of parameter p is $4.1 \times 10^{-3} \sim 1.4 \times 10^{-1}$ for $\phi = 0.7$ under the conditions that $V_R = 0.1$, $V_S = 0.2$ and $\beta_n = 3.0$.

2.2.3 Numerical results and discussions

The apparent β_n to attain the probability of failure $P_F^* = 1.35 \times 10^{-3}$ ($\beta^* = -\Phi^{-1}(1.35 \times 10^{-3}) = 3.0$) is calculated under the conditions that $\phi = 0.7$ and $P = 4.1 \times 10^{-3} \sim 1.4 \times 10^{-1}$ and are presented in Fig. 3. Fig. 3 shows that the case dominated by less variable load effects requirs higher target β_n to attain the same safety level. This means that the probability of failure of the structure subject to less variable loads is strongly increased by the existence of the gross errors. In other words, uniform apparent safety level results in the less safety margin against the uncertainties due to gross errors in the case of the small variance of load effects.

2.3 Target safety level taking account of both total cost minimization and uncertainties due to gross errors.

In this section, target safety level taking account of both total cost minimization and uncertainties due to gross errors is discussed. Substituting eq. (10) instead of eq. (2) into eq. (6) and applying the principle of total cost minimization, βn, opt is calculated. The parameter values used are;

C_F^*=10 and 50, ν_0=1.7, V_R=0.1, V_S=0.05∿1.0,

ϕ=0.7, p=4.1x10^{-3}∿1.4x10^{-1}, b=0.6

Fig. 4 shows the optimum apparent safety level βn, opt calculated as a function of the coefficient of variation of load effect. As expected, βn,opt is larger than that presented in Fig. 1. And it is also found that βn,opt is considerably higher for smaller coefficient of variation V_S of the load effect. This result agrees with that obtained from Fig. 1 and Fig. 3. Accordingly, it can be concluded that relatively higher safety level to the less variable load effects should be assigned and consequently that it is not necessary to provide large difference between load factors according to the variability of load effects.

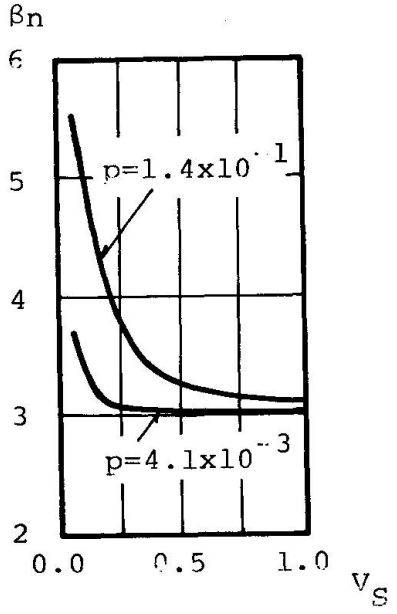

Fig.3 Apparent safety level β_n

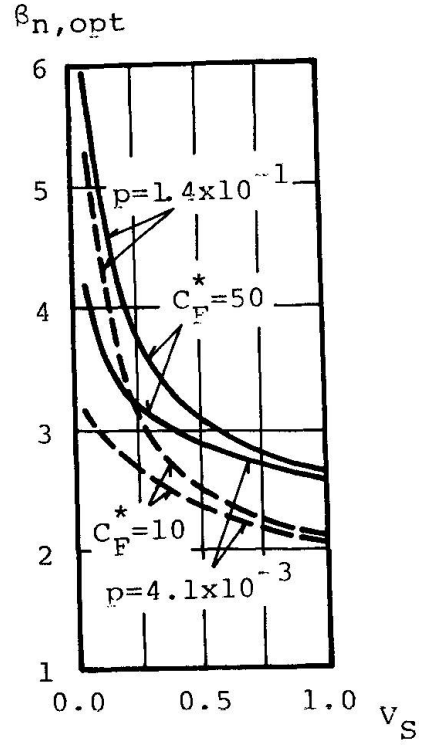

Fig.4 Optimal apparent safety level $\beta_{n,opt}$

3. BALANCE OF SAFETY FACTORS IN A STRUCTURAL SYSTEM

Many of the civil engineering structures are consisted of different components and have various failure modes. Hence they are to be treated as structural systems. Long-span suspension bridge is certainly one of the typical structural systems. Its superstructure is composed of towers, cables and stiffening girder. In towers and cables of a long-span suspension bridge, dead load effect exceeds 90% of the total design load effect. On the other hand, the design of the principal members of stiffening girder is controlled by the wind load, at least in our Japanese practice. This is especially true for the truss type of girders because of the large wind force. The dead load has a very small variation under elaborate quality control, but the wind load and the performance of the suspension bridge under wind action is very much uncertain. This observation leads to smaller safety factor for the towers and cables and to larger safety factor for the stiffening girder. The current design specification for long-span suspension bridges seems opposite; approximately the safety factor of 3.0 for the ultimate strength of the cable and less than 2.0 for the stiffening girder[10].

In this section, balanced allocation of the safety factors in a system is studied again from an economical point of view. Only two components in the suspension bridge, namely cables and stiffening girder are investigated herein.

3.1 Evaluation of total cost

In a similar manner as in section 2, the total cost of each component is expressed as

$$C_{TC}=C_{IC}+P_{FC}C_{FC}\ ,\quad C_{TG}=C_{IG}+P_{FG}C_{FG} \tag{14}$$

in which subscript 'C' and 'G' stand for the cables and girder, respectively.

Then the total cost C_T of the structure is given by

$$C_T=(C_{IC}+P_{FC}C_{FC})+(C_{IG}+P_{FG}C_{FG}) \tag{15}$$

The random variables, i.e., structural resistance, dead and wind loads are assumed log-normally distributed and then the probability of failure P_{FC} and P_{FG} can be obtained from eq. (2). C_{IC} and C_{IG} are assumed to be the form of eq. (5). Break of the cable leads to the collapse of the suspension bridge;failure of the stiffening girder does not necessarily mean the collapse of the whole structure. Considering this, it is reasonable to assume C_{FC} is larger than C_{FG}. The sum of C_{IC} and C_{IG} is assumed to keep constant.

3.2 Numerical results and discussions

Numerical computations are carried out in order to find the optimal set of safety factors ν_C and ν_G.

Under these observations as well as the design caluculation used in the proposed Akashi Straits Bridge, the longest bridge of the Honshu-Shikoku project, the following values are subjectively chosen and used in the example calculation:

$\nu_0=1.7$, $C_{IC}:C_{IG}=2:1$, $C_{FC}:C_{FG}=2:1$, $C_{IC}:C_{FC}=1:100$, $V_{RC}=V_{RG}=0.1$,

$V_D=0.1$ (dead load effect), $V_W=0.3$ and 0.5 (wind load effect)

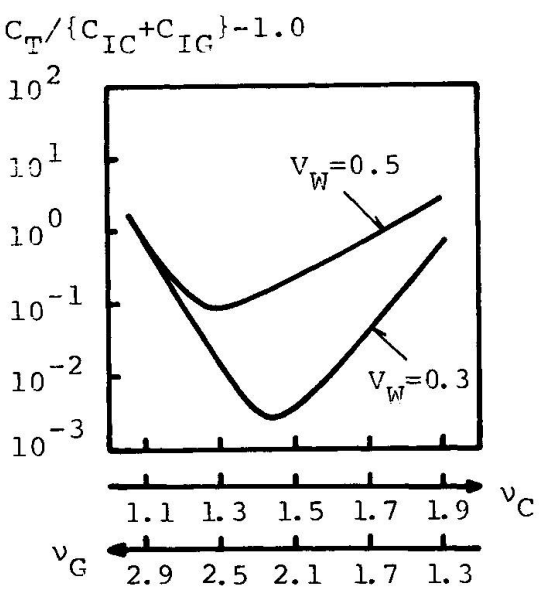

Fig.5 Total cost vs. Safety factors ν_C and ν_G

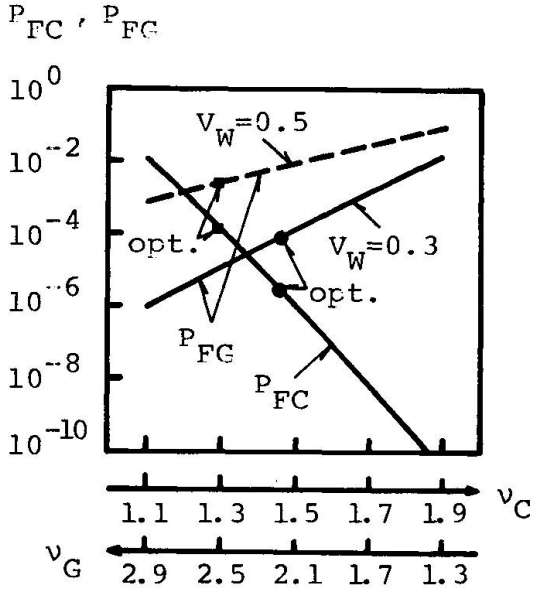

Fig.6 P_{FC} vs. ν_C and P_{FG} vs. ν_G

The dimensionless total cost $C_T(\nu_C, \nu_G)/\{C_{IC}(\nu_0) + C_{IG}(\nu_0)\} - 1.0$ and probability of failure P_{FC} and P_{FG} were calculated as the function of ν_C and ν_G as shown in Fig. 5 and Fig. 6, respectively. It can be found that the optimal safety factor $\nu_{C,opt}$ is noticeabley smaller than $\nu_{G,opt}$, while the optimal value of P_{FC} corresponding to $\nu_{C,opt}$ is smaller than optimal P_{FG} corresponding to $\nu_{G,opt}$. Although P_{FC} decreases remarkably as the increase of ν_C, further increase of ν_C is not profitable refering to Fig. 5. The combination of ν_C and ν_G in the current design specificaitons for long-span suspension bridges contradicts with the above findings. Although the parameter values need to be more carefully chosen, reconsideration of the selection of safety factors might be desirable.

4. CONCLUDING REMARKS

The target safety level of a structural component as well as structural system has been discussed. Introducing a gross error model, the optimal safety level of a structural component was calculated on the basis of cost optimization.

The resluts show that it is reasonable to assign relatively higher safety level to the less variable load effects. This implicitly supports the situation of safety level in the current design code.

Employing a long-span suspension bridge as a structural system example, the optimal allocation of the safety levels for different components was studied. The numerically higher safety level for the components subject to less variable load effects is found optimal in this example as well; namely, the higher safety level for the cable and the lower for the stiffening girder. The reconsideration of the safety factors in the current design practice of long-span suspension bridges is suggested on the basis of these findings.

REFERENCES

[1] RAVINDRA, M.K. and R.V. GALAMBOS: Load and Resistance Factor Design for Steel , Proc. of ASCE, Jour. of the Structural Division, Vol. 104, No. ST9, pp. 1337-1353, Sept., 1978.

[2] ELLINGWOOD, E., T.V. GALAMBOS, J.G. MACGREGOR and C.A. CORNELL: Development of a Probability-Based Load Criterion for American National Standard A58-Building Code Requirements for Minimum Design Loads in Buildings and Other Structures, U.S. Dept. of Commerce, SP-577, pp. 1-222, June, 1980.

[3] NOWAK, A.S.: Effect of Human Error on Structural Safety, ACI Journal, pp. 959-972., 1979.

[4] LIND, N.C., L.I. KNAB, and W.B. HALL: Economic Study of the Connection Safety Factor; Proc. of Third Specialty Conference on Cold-formed Steel Members, pp. 951-966.

[5] TURKSTRA, C.J.: Theory of Structural Design Decisions, Solid Mech. Division, Univ. of Waterloo, SM Study, No. 2, pp. 1-124, 1970.

[6] LIN, S.: Reliability-based Design Code for Highway Bridges, Master Thesis, Univ. of Tokyo, pp. 1-100, March, 1980 (in Japanese).

[7] LIND, N.C.: Approximate Analysis and Economics of Structures, Proc. of ASCE, Jour. of the Structural Division, Vol. 102, No. ST6, pp. 1177-1196, June, 1977.

[8] SMITH, D.W.: Bridge Failures, Proc. of ICE, Vol. 60, Part 1, pp. 367-382, Aug., 1976.

[9] BROWN, C.B.: A Fuzzy Safety Measure, Proc. of ASCE, Jour. of the Eng. Mech. Division, Vol. 105, No. EM3, pp. 855-871, June, 1979.

[10] HONSHU-SHIKOKU BRIDGE AUTHORITY; Design Specifications for Superstructure, August, 1977.

Probability-Based Working Stress Design Code

Dimensionnement probabiliste sur la base de contraintes admissibles

Probabilistisch hergeleitetes System von zulässigen Spannungen

Hyo-Nam CHO
Professor
Korea Military Academy
Seoul, Korea

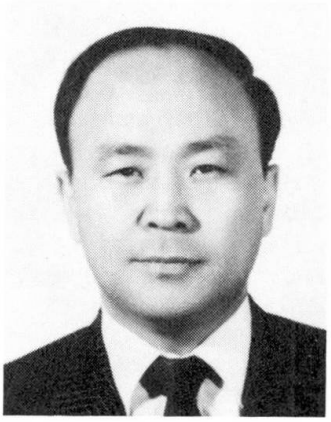

Hyo-Nam Cho received his B.S. degree from KMA in 1967, and M.S. and Ph.D. degrees in civil engineering from Michigan State Univ. in 1972. His active research areas are structural optimization and structural reliability. He was visiting professor at Cornell Univ. in 1985. He is professor of structural engineering at KMA.

SUMMARY

Reliability of reinforced concrete structural members is evaluated by using an advanced second moment reliability method. Then, a practical method for code calibration is shown in this paper. A set of allowable stresses for reinforced concrete is proposed based on the rational target reliability indices.

RÉSUMÉ

La fiabilité des éléments de structure en béton armé est calculée sur la base de la méthode de fiabilité du deuxième ordre. Une méthode pratique de calibrage de la norme est présentée. Des contraintes admissibles pour les constructions en béton armé sont recommandées sur la base d'indices de fiabilité déterminés.

ZUSAMMENFASSUNG

Die Zuverlässigkeit von Stahlbeton-Tragelementen wird aufgrund einer verfeinerten Methode der Zuverlässigkeitstheorie ermittelt. Eine praktische Methode zur Kalibrierung von Normen wird vorgestellt. Schliesslich wird ein Satz von zuverlässigen Spannungen für die Bemessung von Stahlbeton angegeben, der sich auf das angestrebte Zuverlässigkeits-Niveau stützt.

1. INTRODUCTION

Recent advances in structural code development are primarily directed toward probability-based framework of limit state design (LSD) or load and resistance factor design (LRFD). However, little attention has been paid to the systematic development of a probability-based working stress design (PBWSD) code, despite the fact that WSD is still predominantly used in design practice in those countries such as Korea and Japan among others.

PBWSD code, like LSD or LRFD codes[5,9,13], could employ up-to-date advanced first order second moment (AFOSM) reliability methods, and thus can be drafted as an equivalent probability-based code which provides essentially identical and consistent reliability. On the one hand, it is generally recognized that WSD has some serious drawbacks compared to LSD or LRFD-multiple factor design methods. It appears that the most serious drawback of WSD is the missing of the flexibility that the presence of many adjustable load factor gives, and the feeling about the overloading safety of each variable load. And thus, in the long run, LSD or even more advanced or higher level reliablity based design codes in the future should be considered as the prototype structural code for the next generation. On the other hand, it is expected that it will take more than a decade for most practitioners to abandon WSD and become familiar with LSD or LRFD in design practice especially in those countries such as Korea or Japan. Therefore, for the transition decade to come the current WSD code should be remodeled as a pobability based equivalent design method corresponding to the LRFD or LSD code.

This paper presents a practical procedure for the calibration of the PBWSD code for reinforced concrete, reports the investigations of the structural reliability by the current code and then proposes pobability-based safety provisions for the WSD code.

2. CURRENT CODE AND DESIGN PRACTICE

R.C. design standards in Korea are almost similar to the ACI code, and specify two alternative design methods, that is, the strength design method and WSD which are not probability-based. Although the current code recommends the use of the strength design method in design practice, the majority of engineers still prefers to use WSD and sticks to the concept of safety in terms of allowable stresses or traditional notional safety factors. Virtually no engineers in practice have a little understanding of modern structural reliability or safety concepts. From a probabilistic point of view based on a series of investigations, the safety provisions of the current R.C. design standards are irrational and invariably too much conservative, and, in general, result in uneconomical designs although some safety provisions are too low or fluctuating too much. For inatance, in case of the usual sustained service design loads (dead + sustained live load), the allowable stresses are given as a fraction of nominal strength of materials, whereas, for safety checking with the load combination with transient loads such as wind or earthguake loads, the exceedence of 1/3 of the allowable stresses is provided in the code primarily based on the experiences and judgements as in usual traditional WSD codes.

3. RELIABILITY BASIS FOR WSD CODE

3.1 Simplified procedure for Parameters

Almost every prlbability-based code model employs advanced or practical Level II AFOSM reliability methods for the derermination of safety parameters in the code calibration procedure. AFOSM methods are well known and established

reliability methods, and the detailed concepts and the procedure of which are published in the major reports [9,16,18], papers [6,7,10,11] and texts [12,20]. No detailed or even brief procedures or equations will be presented in this paper.

Once a LRFD format code is drafted by employing an AFOSM Level II methods [9,15], then nominal safety factors, n', for each limit state can be obtained directly from the safety factor parameters (ϕ, γ_{si}) of the LRFD code. In this paper, a simplified procedure for determining ϕ, γ_{si} is also briefly presented as reference. Suppose we choose the following format as a LRFD limit state equation [8,9];

$$\phi \bar{R} = \Sigma \gamma_{si} \bar{S}_i \tag{1}$$

where, $\bar{R}, \bar{S}_i$ = mean resistance and ith load effects

$$\phi = \exp(-\alpha_R \beta_o V_R) \tag{2a}$$

$$\gamma_{si} = 1 + \alpha_{si} \beta_o V_{si} \tag{2b}$$

in which V_R, V_{si} ; coefficients of variation of R & S_i
α_i ; direction cosine of design point on failure surface
β_o ; target reliability index

Also note that, in terms of the total load factor design format, the safety parameters are :

$$\phi \bar{R} = \gamma_s \bar{S} \tag{3}$$

where, $$\gamma_s = 1 + \alpha_S \beta_O V_S = 1 + \frac{V_S^2 \beta_O}{\sqrt{\gamma_s^2 V_R^2 + V_S^2}} \tag{4}$$

Note that, by definition, the central safety factor $n_0 = \bar{R}/\bar{S} = \gamma_S/\phi$. If we make use of the relationship between γ_s and γ_{si}, which can be derived directly [3] as:

$$\gamma_{si} = 1 + \frac{\rho_i V_{si} \beta_o}{(1+\Sigma\rho_i)\sqrt{\gamma_S^2 V_R^2 + V_S^2}} \tag{5}$$

where, $\rho_i = \bar{L}_i/\bar{D}$, in which $\bar{L}_i$=ith variable load, $\bar{D}$=dead or permanent load, then the safety parameters ϕ, γ_{si} of a LRFD code can be determined from Eq.(3)-(5) provided that the total load factor γ_s is evaluated iteratively by using Eq.(4).

Once ϕ, γ_{si} corresponding to a target reliability index β_o are evaluated, then the nominal safety factor n' can be obtained in terms of the mean-nominal ratio of resistance and load effects ($\eta_R = \bar{R}/R'$, $\eta_S = \bar{S}/S'$) as follows.

$$n' = \frac{\eta_S}{\eta_R} n_o \tag{6}$$

The nominal values of R' and S' may be obtained from the characteristic values of basic random variables.

3.2 Allowable Stresses

Allowable stresses in WSD are usually expressed as a fraction of material strengths by using "notional safety factor", n, newly defined in this paper. It is evident that the notional safety factor of WSD is, in general, different from the nominal safety factor, n', of limit state codes defined according to failure modes [3] as in the previous section (for instance, $n = (M_y/Mn)\,n'$).

3.2.1 Flexural Member

-1. Bending : Although the allowable stress of steel of a R.C. beam can be simply expressed as $f_{sa} = f_y/n'$, the allowable stress of concrete can not be given as f_c'/n'. And thus, in this paper, a simple but rational way of determining the allowable stress of concrete which results in under-reinforced section (in the limit state sense) but a balanced section (in the WSD sense)

is presented. Suppose we prefer to proportion a R.C. beam so that the reinforcing ratio of the section takes near 1/2 p_{max} or optimum ratio p_o as an under-reinforced section. Then, the allowable stress of such a section can be derived by using balanced section formula [3], that is,

$$p_b = \frac{f_{ca}}{2f_{sa}}\left(\frac{f_{ca}E_s/E_c}{f_{sa}+f_{ca}E_s/E_c}\right)$$

as
$$f_{ca} = p_b f_{sa} + \sqrt{p_b^2 f_{sa}^2 + 2p_b f_{sa}^2 E_s/E_c} \qquad (7)$$

where, $p_b = \frac{1}{2} p_{max}$ or p_o (optimun steel ratio)

$f_{sa}=0.85f_c'm/n'$, in which m is the effective strength ratio.

-2. Shear: It is clear that the allowable shear stress of concrete can be directly obtained from $\tau_a = \tau_{ci}/n'$ or $\tau_a = \tau_{ca}/n'$ respectively for one way or two way action, and the allowable stress of shear reinforcement as $f_{sa}=f_y/n'$.

3.2.2 Compression Member

In case of pure compression, the allowable stress of concrete and steel are simply given as $f_{ca} = 0.85f_c'/n'$, $f_{sa} = f_y/n'$, respectively, but, due to the complexity of reliability analysis of general columns subject to compression with bending, the outline of the reliability procedure for those columns can not be presented herein, although this study made use of the previous study [4, 8] which is not rigorous but approximate and practical. The essential part of the column design provisions for the PBWSD is to construct the allowable linear interaction diagram based on the limit state interaction diagram by using the nominal safety factor as proportional reduction factor. However, the more rational way of provisioning R.C. columns in the PBWSD is to adopt the limit state column design procedure by simply taking the permissible resistances as $P_a = P_n/n'$, $M_a = M_n/n'$, and thus using the column interaction equation or diagram along with the service load effects(P,M).

3.2.3 Retaining Wall

The limit states of the stability for retaining walls are overturning, sliding and bearing capacity, which can be formulated in terms of dead weights, soil pressures and surcharge loads. Once the parameters for each limit state corresponding to the selected set of target reliability indices are obtained, then the nominal safety factor,n',for each stability limit state of retaining walls can be obtained from the corresponding parameters [3]. Also, note that the allowable stresses of R.C. retaining walls can be obtained by following the same way as in the case of flexural members but with different load effects and target reliability indices.

4. CALIBRATION OF PBWSD CODE

4.1 Statistical Uncertainties

Statistical uncertainties of resistances as shown in Table 1 are evaluated from the best available data in Korea [1,2,3,4]. However, uncertainties of load varibles are chosen as conservative values mainly based on the engineering judgements and experiences as well as the available foreign data [8,9,14], because the statistical load data at present are not available and the research on stochastic load models is still going on in Korea.

4.2 Reliabilities of R.C. Members Designed by the Current Code

Figure 1 shows the reliability index of the various R.C. structural members designed by the current WSD code, As shown in the figure, the reliability of

Table 1 Resistance & Load Statistical

Action	Type	V_R	V_{SD}	V_{SL}	V_{SL}	V_W	$\bar{R}/R_n$	$\bar{D}/D_n$	$\bar{L}/L_n$	$\bar{L}/L_{In}$	$\bar{W}/W_n$
Bending	Beams	0.16	0.10	0.26	0.50	0.37	1.12	1.05	1.20	0.50	0.90
	2-way Slabs	0.16	0.24	0.35	0.50	0.37	1.12	1.05	1.20	0.50	0.90
	Footings	0.18	0.10	0.26	0.50	0.37	1.12	1.05	1.20	0.50	0.90
Shear	Beams(Flex.)	0.17	0.10	0.26	0.50	0.37	1.09	1.05	1.20	0.50	0.90
	2-way Slabs	0.17	0.24	0.35	0.50	0.37	1.09	1.05	1.20	0.50	0.90
	Footings	0.19	0.10	0.26	0.50	0.37	1.09	1.05	1.20	0.50	0.90
Compress-ion	Tied Col.	0.17	0.10	0.26	0.44	0.37	1.05	1.05	1.20	0.50	0.90
	Spiral Col.	0.17	0.10	0.26	0.44	0.37	1.05	1.05	1.20	0.50	0.90
Stability (Retain-ing Wall)	Overturning	0.09	-	0.26	V_{Ss}=0.20		1.19	0.99	1.34	S/S_n=1.14	
	Sliding	0.14	-	0.25	V_{Ss}=0.16		1.18	0.99	1.34	S/S_n=1.14	
	Bearing Cap.	0.44	0.06	0.21	V_{Ss}=0.08		1.17	0.99	1.34	S/S_n=1.14	

various R.C. members is, in general, invariably conservative, and fluctuate to a considerable degree depending on mean live to dead load ratio ($\rho = \bar{L}/\bar{D}$). It can be easily observed that a design by the current WSD code results in the irrational and uneconomical proportioning, and the reliability is fairly sensitive to the variation of the load ratio, which is the inevitable pitfall of WSD with single safety parameters.

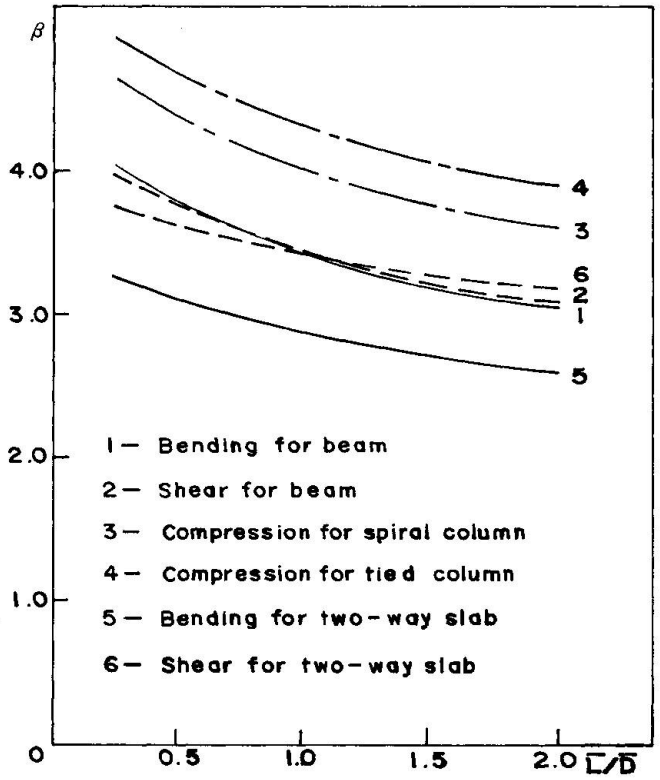

Fig.1 Reliability Indices of R.C. Members Designed by the Current WSD Code (β v.s. $\bar{L}/\bar{D}$)

4.3 Selection of Target Reliability Indices

No established procedure for the rational selection of target reliability indices, however, is available so far, although various approaches have been suggested in the several procedure reports such as CIRIA report 63 [16] and NBS SP-577 [9] , and a few papers [17,19] among others. The socio-economic criteria approach adopted by the CIRIA report still needs further investigation, but the method of calibration against the current practice used by the NBS report may not also provide optimal target reliability indices due to the lack of rationale behind the selection criteria. A research on the selection of optimum target reliability based on sensitibity analysis and optimization method is still on the way. In the mean time the approach proposed in this study is, therefore, based on the concept of the desired hierarchy of safety level along with the engineering judgement and experiences as well as foreign practices together with the trade-off between theory and practice, and may be briefly stated as follows:

- Set up the desired hierarchy of safety levels for each limit state of each structural component (e.g. slab < beam < column < footing , flexure < shear , tied < spiral).

- Consider the reliability level of the current practice, and review the rationality of the current reliability based on engineering judgements.
- Based on the deviation of β_o between limit states used in the foreign codes, and by the judgement, select the tentative β_o for each limit state.
- Curry out the calibrations and examine the results whether it is reasonable or acceptable after a few cycle of adjustment, and then select the final set of desired target reliability indices.

Table 2 shows the results of selected reliability indices obtained by the above arguments

Table 2 Allowable Stresses and Nominal Safety Factors

Action	Type	Target Reliability Indices	Allowable Stresses*				n'	n	γ_o
			Concrete		Steel				
			Cur.	Pro.	Cur.	Pro.			
Bending	Beams	3.0(2.5)	0.40	0.45	0.50	0.55	1.84	1.79	0.70
	2-way Slabs	2.8(2.5)	0.40	0.45	0.50	0.55	1.95	1.89	0.63
	Footing	4.0(3.5)	0.40	0.40	0.50	0.45	2.39	2.32	0.69
Shear	Beams(Flex.)	3.2(2.7)	0.47	0.50	0.50	0.50	2.02	2.02	0.69
	2-way Slabs	3.0(2.7)	0.42	0.45	0.50	0.45	2.14	2.14	0.63
	Footings	4.2(3.7)	0.42	0.40	0.50	0.40	2.65	2.65	0.69
Compression	Spiral Col.	3.5(3.0)	0.25	0.35	0.40	0.40	2.46	2.46	0.70
	Tied Col.	4.0(3.5)	x85%	x90%	x85%	x90%	2.65	2.65	0.69
Stability (Retaining Wall)	Overturning	4.0	-	-	-	-	1.80	-	-
	Sliding	3.5	-	-	-	-	1.90	-	-
	Bearing Cap.	3.0	-	-	-	-	3.60	-	-

* allowable stresses = (factors in concrete and steel)x(nominal strength)

4.4 Proposed Safety Provisions for WSD Code

Table 2 shows essential parts of the summary of the calibration results of the safety parameters for the following PBWSD format:

$$R_a'(f_{ca}, f_{sa}) \geq \gamma_o \sum S_i' \qquad (8)$$

, where γ_o ; load combination factor for the combinations other than D+L, which is the ratio of n' for $(D+L_I+W)$ and n' for $(D+L)$.

At first, the nominal safaty factors, n', the corresponding notional safety factors, n, and the load combination factor, γ_o, are calculated, as shown in Table 2, by following the procedure of Eq.(1)-(6) with the selected target reliability indices shown in Table 2 and the uncertainties shown Table 1. It can, thus, be seen that γ_o shown in the last column result in near 0.7 except γ_o of slabs (=0.63). It can, then, be concluded that a bit conservative value γ_o=0.7 could be satisfactory as the load combination factor in practice $(0.7x(D+L_I+W))$. Next, it can, also, be admitted that the factors for the calculated allowable stresses are to be rounded up as the proposed nominal values as shown in Table 2 for the convenience of the use in practice. Note that in the calibration of the nominal safety factors and allowable stresses, the weighted error minimization which is widely accepted in the code calibration is used in this study, and an optimum degree of complexity in the matrix of safety factors is considered as shown in Table 2.

4.5 Comparision with the Other Codes

First, following observations can be made by comparing the proposed PBWSD provisions with the current WSD provisions as shown in Table 2. The allowable stresses of the current code provisions which are obtained, mainly from the engineering judgements and experiences are significantly different in a number of cases from those of the proposed PBWSD provisions as shown in Table 2. For instance, the proposed allowable concrete stress of column is $0.35f_c'$, while

the current is $0.25f_c'$, which indicates 40% difference, and in the case of stability of retaining walls, the proposed nominal safety factors are significantly less than the current ones with more than 20% reduction. The comparison of allowable stresses indicates that the traditional safety provisions of the current WSD code are irrational and yield uneconomical designs in a number of cases, and thus have to be revised in order to confirm with the corresponding main LRFD code provisions.

Next, in order to check the consistency of the reliability of the proposed PBWSD according to the variation of the variable load ratios, β V.S. $\bar{L}/\bar{D}$, the curves are plotted for the PBWSD provisions with the corresponding LRFD provisions [3], as shown in Fig. 2. Figure 2 shows that the variation of the curves of the LRFD at β_o are fairly insensitive to the variation of $\bar{L}/\bar{D}$, while those of the curves of the PBWSD are fairly sensitive, which is anticipated in the case of WSD code with single safety factor for each limit state. However, if we consider that the range of the variation of load ratio, $\bar{L}/\bar{D}$, for general R.C. building structures falls within 0.5-1.5, it can be seen that the deviations of the reliability indices, in most cases, are nothing but less that $\pm$ 0.2. This, also, indicates that the PBWSD provides practically consistent reliability-based design criteria.

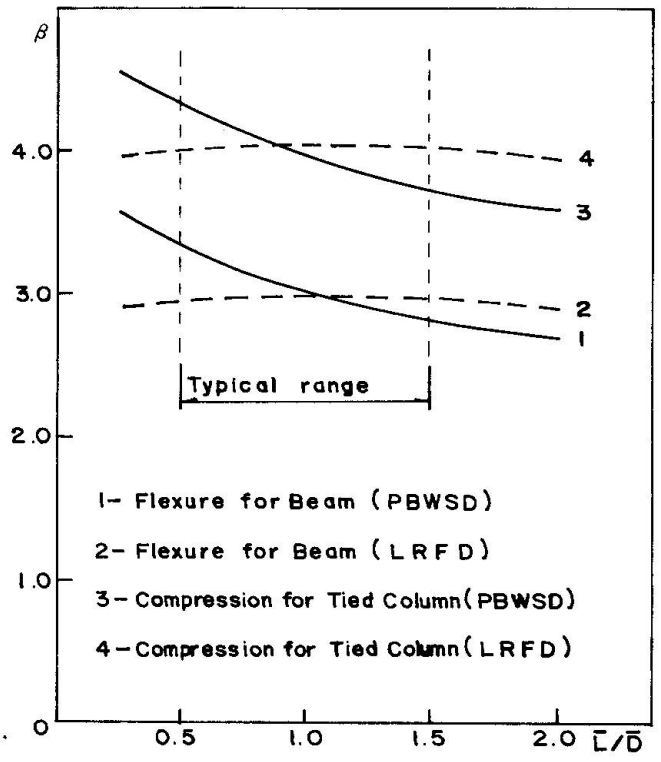

Fig. 2 Comparison of the Consistency of Reliability

5. CONCLUSIONS

The following conclusions can be drawn based on this study.

-1. The current WSD codes should be remodeled as the PBWSD by using the practical AFOSM reliability method and the simple code calibration procedure proposed in this study.

-2. Thus, the irrational allowable stresses of the current code can be replaced by a reasonably complex matrix of the rational allowable stresses which yields economical designs in a number of cases.

-3. The PBWSD can be used as an alternative design method for practitioners during the transition decade to come in Korea, which provides approximately as identical and consistent reliability as the corresponding primary LRFD code.

-4. More elaborate and systematic studies on the selection of optimal target reliability indices remain as further research area.

6. REFERENCES

1. CHO H.N., A Study on LRFD Reliability Based Design Criteria of R.C. Flexural Member. Proceeding of KSCE(Korean Society of Civil Engineers), Vol. 1, No. 1, Dec. 1981, pp. 21-32.
2. CHO H.N., A Study on Reliability Based Design Criteria for Reinforced Concrete Bridge Superstructures. Proceeding of KSCE , Vol. 2, No. 3, Sep. 1982, pp. 87-101.
3. CHO H.N. and CHUN C.M., A Study on Revision of Current R.C. Standard Code Based on Reliability Design Theory. Korea Science Foundation Report No. 84/ 1984.
4. CHO H.N. and MIN K.J., A Study on Reliability Based Design Criteria for Reinforced Concrete Columns. Proeeding of KSCE Vol. 3, No. 1, Mar. 1983, pp. 25-33.
5. Common Unified Rules for Different Types of Construction and Material. CEB Bulletin No. 116E/1976.
6. CORNELL C.A., A Probability-Based Structural Code. Journal of the American Concrete Institute, Vol. 66, No. 12, 1969, pp. 974-985.
7. DITLEVSEN O., Generalized Second-Moment Reliability Index. Journal of Structural Mechanics, Vol. 7, 1979, pp. 435-451.
8. ELLINGWOOD B., Reliability Basis of Losd and Resistance Factors for Reinforced Concrete Design. NBS Building Science Series 110, U.S. Dept. of Commerce, Feb. 1978.
9. ELLINGWOOD B. et al., Development of a Probatility Based Load Criterion for American National Standard A58. National Bureau of Standards Publication 577, Washington, D.C./1980.
10. First Order Reliability Concepts for Design Codes. CEB Bulletin No. 112, July 1976.
11. LIND M.C and HASOFER A.M., Exact and Invariant Second-Moment Code Format. Journal of the Engineering Mechanics Div., ASCE, Vol. 100, No. pp. 111-121.
12. MADSEN H.C, KRENK S. and LIND N.C., Methods of Structural Safety. Prentice-Hall, Inc., Englewood Cliffs/1986.
13. OHBDC (Ontario Highway Bridge Design Code), Ontario Ministry of Transportation and Communication, Downsview, Ontario/1983
14. Probabilistic Basis for Design Criteria in Reinforced Concrete. Reinforced Concrete Research Council, ASCE Bulletin No. 22/1985.
15. RACKWITZ R. and FIESSLER B., Structural Reliability under Combined Random Load Sequences. Computers & Structures, Vol. 9, 1978, pp. 489-494.
16. Rationalisation of Safety and Serviceability Factors in Structural Codes. CIRIA Report No. 63, London/1977.
17. RAVINDRA M.K. and LIND N.C., Theory of Structural Code Optimization. Journal of the Structural Div., ASEC, Vol. 99, 1973, pp. 541-553.
18. Recommendations for Loading and Safety Regulations for Structural Design. NKB-Report, No. 36, Copenhagen, Nov. 1978.
19. SIU W.W., PARAMI S.R. and LIND N.C., Practical Approach to Code Calibration. Journal of the Structural Div., SACE, Vol. 101. 1975, pp. 1469-1480.
20. THOFT-CHRISTENSEN P. and BAKER M., Structural Reliability Theory and Its Applications, Springer-Verlag, Berlin/1982.

Risk Analysis and Protective Island Design for Ship Collisions

Analyse de risque et projet d'îlots protecteurs contre les collisions de bateaux

Risiko-Analyse und Entwurf von Schutzinseln gegen Schiffskollisionen

Karsten HAVNØ
Senior Hydraulic Engineer
Danish Hydraulic Institute
Hørsholm, Denmark

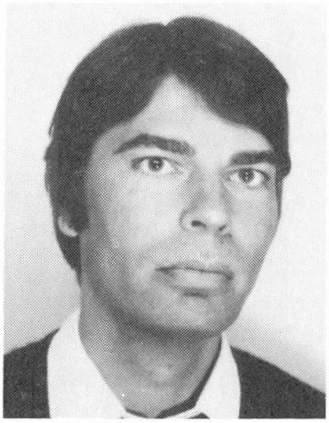

Michael KNOTT
Senior Structural Engineer
Greiner Engineering Sciences
Tampa, FL, USA

SUMMARY

The paper describes a combined approach for assessment of collision risks and optimization of protective structure designs. A mathematical model has been developed which simulates with all 6 degrees of freedom the collision scenarios and resulting impact forces. In its most general form the model can describe the deformations of both vessel and protective structure simultaneously. The risk analysis and the optimization of island designs have been applied to the new Sunshine Skyway Bridge, across Tampa Bay, Florida, which is used as an example in the contribution.

RÉSUMÉ

La contribution décrit une approche combinée pour l'évaluation des risques de collisions et l'optimisation du projet de constructions protectrices. Un modèle mathématique a été developpé; il simule, avec six degrés de liberté, les scénarios de collisions et les forces d'impact qui en résultent. Dans sa forme la plus générale, le modèle peut décrire simultanément les déformations du bateau et des constructions protectrices. Les analyses de risques et l'optimisation du projet d'îlots protecteurs ont été appliqués au pont Sunshine Skyway, Tampa Bay, Floride, et est présenté comme exemple dans cette contribution.

ZUSAMMENFASSUNG

Der Artikel beschreibt einen kombinierten Ansatz für die Beurteilung von Kollisionsrisiken und die Optimierung des Entwurfes von Schutzkonstruktionen. Ein mathematisches Modell wurde entwickelt, welches das Kollisionsgeschehen mit allen sechs Freiheitsgraden und die zugehörigen Stosskräfte simulieren kann. In der allgemeinsten Form lassen sich die Deformationen sowohl des Schiffs als auch der Schutz-Konstruktion beschreiben. Das Modell wurde auf das Projekt der neuen Sunshine Skyway Brücke über die Tampa Bay in Florida angewendet, welche auch im vorliegenden Beitrag als Beispiel dient.

1. INTRODUCTION

On May 9, 1980 during an intense early-morning thunderstorm, the empty 40,000 dwt bulk carrier M/V Summit Venture struck one of the anchor piers of the two parallel bridge structures. A 396m section of the southbound main span collapsed, and 35 lives were lost in vehicles which fell into the bay. The Florida Department of Transportation is currently replacing the existing bridge with a new 6.705 km-long replacement structure. The new structure (Fig. 1.1) has a 365.8m single-plane, cable-stayed, segmental concrete main span. In the background of Fig. 1.1 can be seen the existing parallel bridges, one of which was partially destroyed by the ship collision.

The Skyway Bridge failure, and other similar bridge failures around the world, has resulted in an increased awareness in the international engineering community of the need to include ship impact as a major design condition in bridges and offshore structures located in busy marine waterways. The IABSE Colloquium on "Ship Collision with Bridges and Offshore Structures" /1/ in Copenhagen, 1983 established the state-of-the-art of the current understanding of ship impact within the profession.

2. PIER PROTECTION SYSTEM

2.1 Risk Analysis

The final selection of the pier protection system to be constructed for new bridges was based on the results of detailed studies of numerous alternative protection systems using risk analysis and cost-effectiveness techniques /2/.

The risk analysis methodology results in an assessment of the annual frequency of ship collision with any part of the bridge structure (either pier or spans) and the annual frequency of bridge collapse. The methodology involves the complex organization of a large body of data into a series of calculations involving various statistical and probability procedures. Factors included in the analysis are:

- Frequency and vessel size distribution of the ship/barge fleet passing under the bridge
- Probability of vessel aberrancy
- Geometric probability of collision based on vessel sailing paths, vessel dimensions, and bridge geometry
- Impact strength of the bridge pier and span components
- Impact force of the ship/barge based on vessel displacement and speed
- Local weather conditions, currents, tides, and pilotage standards
- Costs associated with bridge repair and replacement, port interruption, motorist interruption, and loss of human life costs.

Pier No. (N&S)	Unprotected (Years)	Protected (Years)
1	80	-
2	138	3442
3	262	1458
4	552	1106
5	1492	2984
6	2804	8000
Total	38	427

Table 2.1 Return Periods of Bridge Collapse.

The recommended protection system consists of 1) physical protection of the first six piers on each side of the channel using a combination of dolphins and islands to protect the main pier and dolphin protection around the remaining piers, (Fig. 2.1), 2) a motorist warning system on the bridge structure, and 3) an electronic navigation device to be carried aboard the vessels by the local harbor pilots. The remainder of this paper will discuss the method of analysis used to evaluate the main pier artificial island to protect the main pier from potential ship collisions.

Fig. 1.1 Construction of the new Sunshine Skyway Bridge.

Once the results of the analysis of the unprotected structure have been evaluated, a protection system can be developed. Table 2.1 summarizes the results of the Skyway analysis for the main span portion of the bridge with the physical protection system described below.

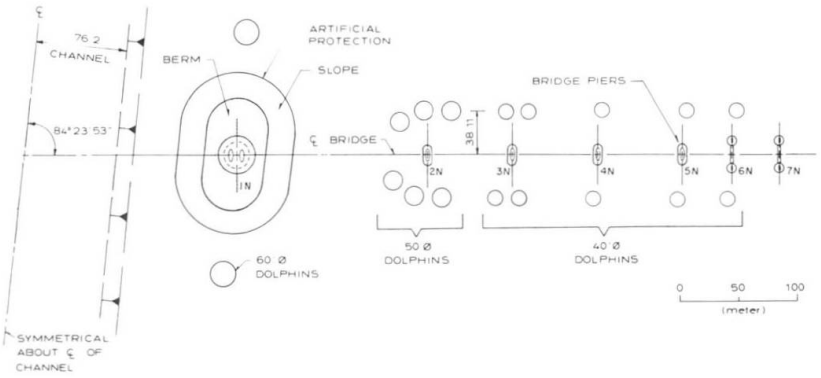

Fig. 2.1 Protection System for the new Skyway Bridge.

2.2 Protection with Artificial Islands

By ship collision, impact energy is mainly absorbed through the deformation of the island material and deformation of the ships bow. In front of the ships bow, a force is transmitted through the island material and part of this might might be transmitted to the bridge pier.

Both mathematical and physical models can be constructed to represent the situation with deformable ship and deformable island. However, it is often adequate for design purposes to assume a rigid vessel, and hence a situation, where only the island is deforming. For the Skyway Pier Protection study, the rigid vessel impact was studied both in a mathematical and a physical model, and the applicability of the rigid approach was verfied with a mathematical model which includes the description of the ships deformation, /3/.

The second part of this paper mainly concerns the mathematical modelling, but also gives comparisons with the physical model results.

3. MATHEMATICAL MODEL FORMULATION

3.1 General Formulation of Equations of Motion

The equations of the vessel's motion are expressed by using two Cartesian frames of reference:

1. A fixed Cartesian frame, Frame I, with horizontal x- and y-axes and a vertical z-axis.
2. A Cartesian frame, Frame A, which is fixed relative to the vessel, with origin in the vessel's centre of gravity and x_A- and y_A-axis coinciding with the vessel's longitudinal and transversal axis, respectively. The angular displacements of the rotational motion around this frame axis are denoted RZ, RY and RX.

The relationship between coordinates of the two frames becomes

$$\begin{vmatrix} x \\ y \\ z \end{vmatrix} = \begin{vmatrix} X_G \\ Y_G \\ Z_G \end{vmatrix} + \begin{vmatrix} C_{11} & C_{12} & C_{13} \\ C_{21} & C_{22} & C_{23} \\ C_{31} & C_{32} & C_{33} \end{vmatrix} \begin{vmatrix} X_A \\ Y_A \\ Z_A \end{vmatrix}, \text{ where}$$

C_{11} = cosRY cosRZ
C_{12} = sinRX sinRY cosRZ - cosRX sinRZ
C_{13} = cosRX sinRY cosRZ + sinRX sinRZ
C_{21} = cosRY sinRZ
C_{22} = sinRX sinRY sinRZ + cosRX cosRZ
C_{23} = cosRX sinRY sinRZ - sinRX cosRZ
C_{31} = -sinRY
C_{32} = sinRX cosRY
C_{33} = cosRX cosRY

and X_G, Y_G and Z_G denote the translatory displacements of the vessel's centre of gravity.

3.2 Formulation of Earth Pressure with Rigid Vessel Assumption

A mathematical formulation of the earth pressure forces on a vessels bow which penetrates an island was formulated by the Danish Geotechnical Institute in connection with the Danish Great Belt Bridge study.

The formulation, which is based on analytical considerations and physical model tests, yields a force perpendicular to the vessel bow; Account is made for higher earth pressures which occur when the ship bow is at the slope of the island, andthe formation of a sand bank which forms at the front of the bow as the vessel pushes into the island.

In the numerical integration, the ship's bow is mathematically divided into a number of slices. For each slice, the contact force is estimated for the centerpoint in that slice, and also the resulting friction force is calculated, see Fig. 3.1.

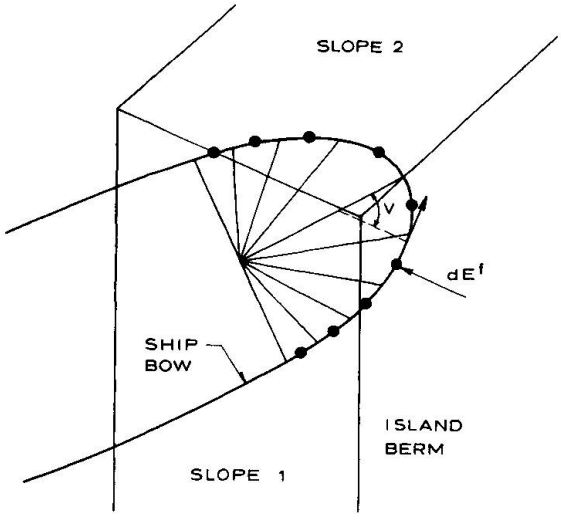

Fig. 3.1 Ship bow discretization

The vertical position of the point of impact is estimated from the assumption, that the earth pressure varies linearly with depth in the wet and the dry part of the island, respectively.

3.3 Formulation for Deformable Vessel Assumption

At a certain depth below the islands surface, the earth pressure will exceed the strength of the vessel, which deforms. This phenomena has been incorporated in a more general mathematical formulation with the above presented earth pressure description for the upper (undeformed) part of the ships bow, and a force formulation according to plastic bow deformation for the lower part. The division between the two descriptions is assumed to follow the plane within the island, where the earth pressure equals the ship strength.

The shape of this plane can be estimated from the soil characteristics, and will generally appear as in Fig. 3.2.

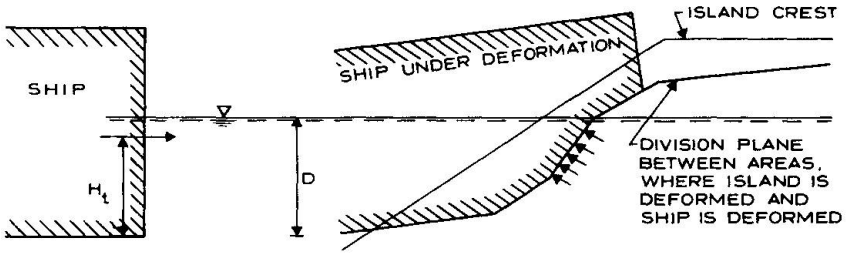

Fig. 3.2 Division Plane with equal Earth Pressure and Ship Strength

The generalized equations become rather complex and it is necessary to switch between equations concurrently when the deformation develops, but the solution technique is essentially the same as earlier described.

4. FORMULATION OF FORCE TRANSMISSION

The force transmission in front of the ships bow through the island material to the bridge pier has been formulated assuming a conical shaped force distribution, see Fig. 4.1.

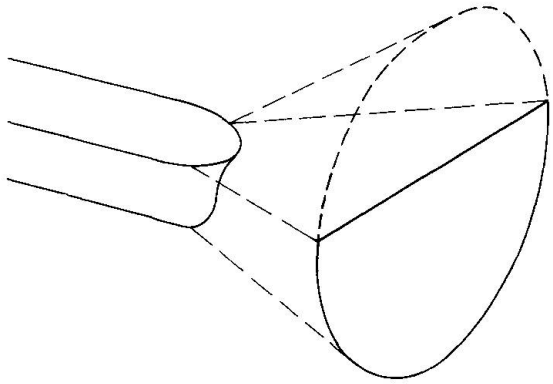

Fig. 4.1 Conical Force Distribution

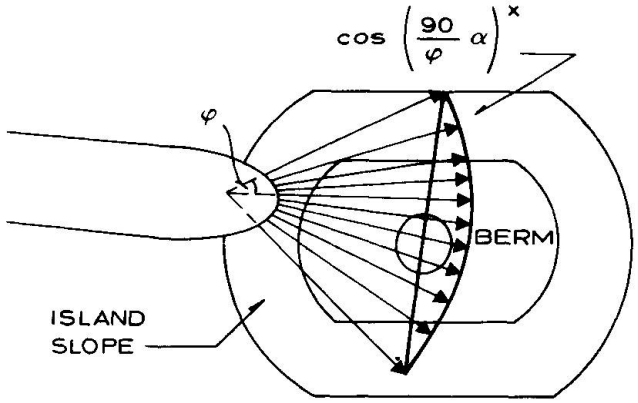

Fig 4.2 Horizontal Force Distribution

The active part of the cone will be the part which is situated inside the island, and the boundary values for the forces are known to be zero at the island crest and at the cone intersection.

The horizontal force distribution is approximated with a cosine function, the shape of which can be calibrated, see Fig. 4.2.

The vertical force distribution is assumed to grow linearly to its maximum at the bottom of the vessel, and to decrease thereafter with a function, which is subject to calibration, see Fig. 4.3.

The centerline of the cone is assumed to coincide with the resulting collision force, acting on the ship.

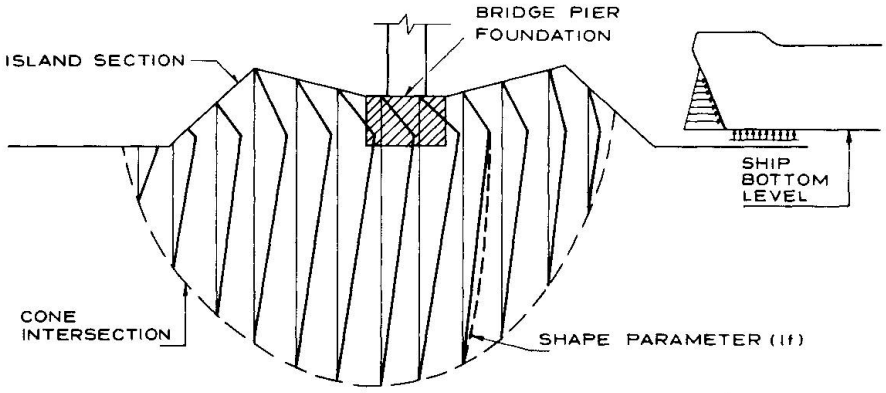

Fig. 4.3 Vertical Force Distribution

5. MODEL VERIFICATION/ISLAND DESIGN

5.1 Islands Stopping Ability

The mathematical model description of the protection islands with respect to stopping or deflecting approaching ships has been verified against two series of physical model tests:

a) The model tests for the Danish Great Belt bridge, which were carried out by DHI in early 1978.

b) The model tests for the Sunshine Skyway Pier Protection, which were carried out by Hydro Research Science Inc., in early 1984.

For both test-series, a good agreement for vessel intrusion in the islands was found between the mathematical and physical model, see Fig. 5.1.

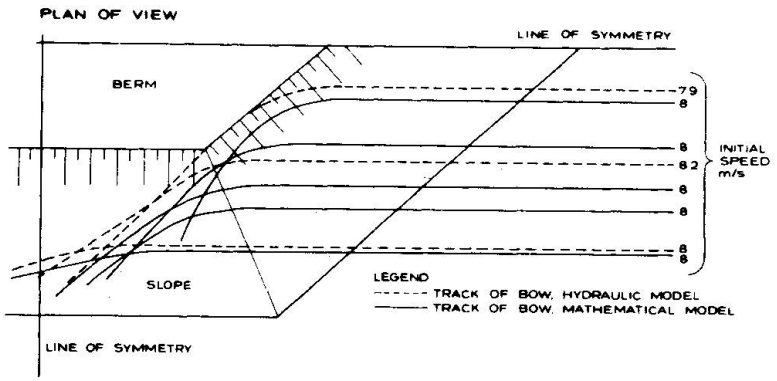

Fig. 5.1 Model Verification, Stopping and Deflection (Great Belt Bridge)

5.2 Force Transmission

Only little knowledge is available at present to support a complete formulation of the force transmission through the island material. The formulation used is based on static geotechnical considerations, and does not account for the dynamic effects.

However, with respect to the forces transmitted to the bridge pier, a fair agreement is found with the physical model tests for relatively high impact forces, which will be the design conditions.

Fig. 5.2 presents comparisons between the mathematical model formulation, the Great Belt Bridge tests and the Sunshine Skyway Pier protection tests with relatively high transmitted forces. The mathematical formulation has been presented as a straight line, defining the abcissa for each test on the horizontal axis. The corresponding measured ratios have been plotted along the ordinate.

5.3 Rigid Model Description

The rigid model assumption does not account for ships with large drafts, due to deformation of the ships bow. However, as the effective stopping length for these ships is relatively small, this deformation has only limited effect on the islands ability to stop the ship. Still, there can be a noteworthy decrease in the collision force, when the ships deformation is taken into account, and with respect to the force transmitted to the pier, a safety margin is thus built in the rigid assumption. Decreases in the transmitted impact force greater than 25% were estimated using a mathematical model with a deformable bow during this study.

5.4 Island Design

The final island design for the Sunshine Skyway Pier protection was derived in the following manner; first the mathematical model was used to define an approximate island layout, which was then tested in the physical model tests. Then the results from the physical model tests were used to calibrate the mathematical model before the final design simulations.

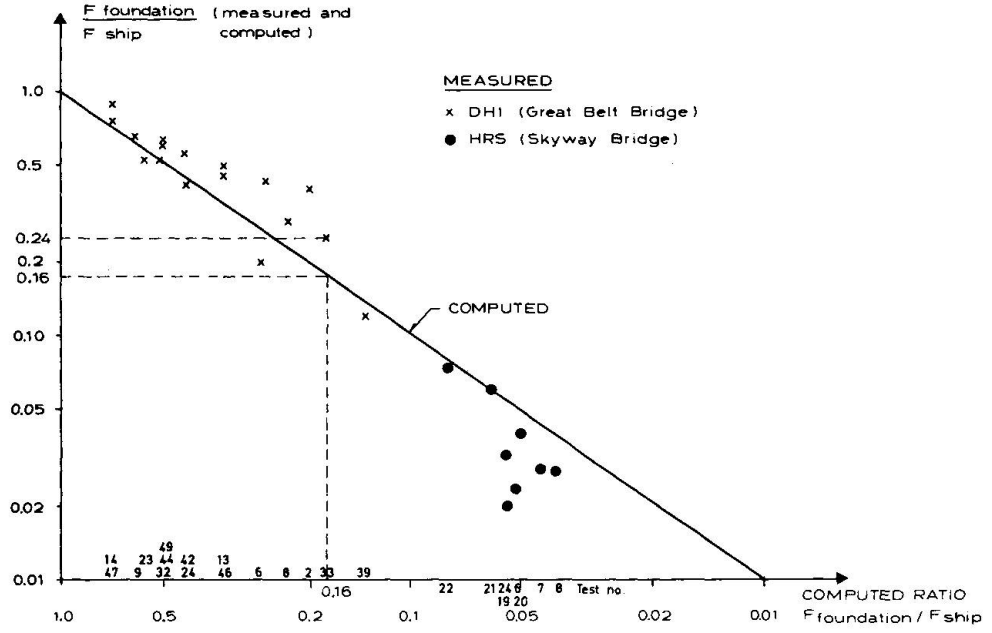

Fig. 5.2 Ratio between Pillar Force and Ship Force in Mathematical and Physical Models

The selected island section for the main pier protection island is shown on Fig. 5.3.

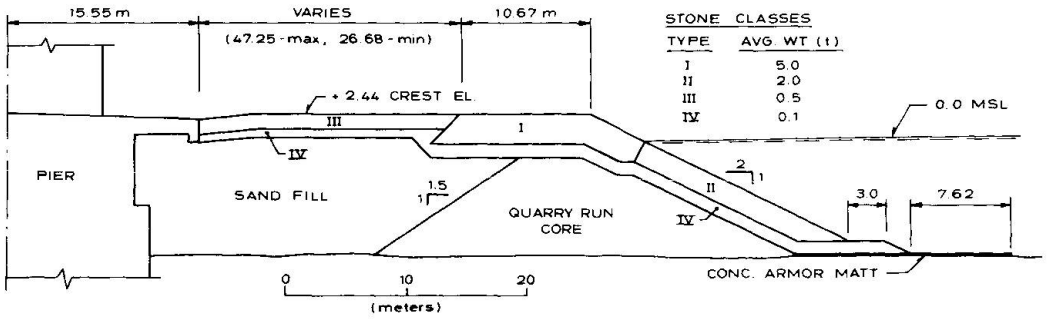

Fig. 5.3 Final Main Pier Island Design

For the design conditions, which involved various ship types, loading conditions, ship sizes up to 85,000 DWT, travelling speeds of 10 knots and extreme high water level conditions up to 0.73 m above mean sea level, the island was found to give sufficient protection to the piers.

The most dangerous situation was found to be the one, where an empty, trimmed vessel strikes the island under high water conditions. In this situation, the vessel tends to slide over the island, but is stopped about 6.1 m in front of the pier, see Fig. 5.4.

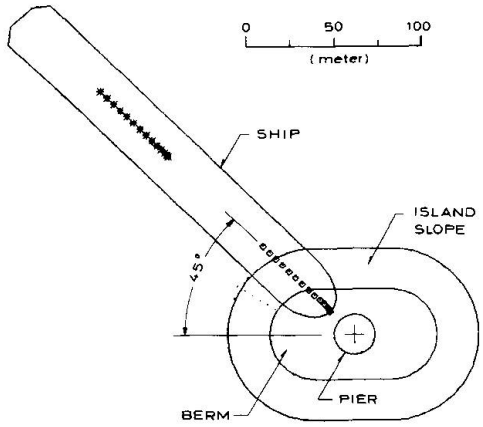

Fig. 5.5 Empty trimmed 85,000 DWT vessel hitting the Island with 10 Knots Speed in Extreme High Water

Due to the lifting of the ships bow, only little force is transmitted to the pier in this case.

5. CONCLUSION

For bridges and offshore structures located in waterways with merchant vessel activity, the potential for catastrophic ship collision must be evaluated in order to provide for a safe structure. The example of the Skyway bridge shows the incorporation of risk analysis and cost-effectiveness to establish the necessary pier protection system. An innovative island protection system which was evaluated with both physical and mathematical models was developed for the project.

6. REFERENCES

1. IABSE Colloquium "Ship Collision with Bridges and Offshore Structures", Copenhagen 1983, 3 vols.

2. GREINER EINGINEERING SCIENCES, Inc. "Ship Collision Risk analysis for Sunshine Skyway Bridge Replacement", Prepared for Florida Department of Transportation, December 1985.

3. DANISH HYDRAULIC INSTITUTE, "Sunshine Skyway Pier Protection - Mathematical Model Ship Collision Results", Final Report, April 1984.

Application of Decision Analysis to Design of Arctic Offshore Structures

Théorie de la décision et projet de structures en mer arctique

Entscheidungs-Theorie beim Entwurf von Offshore-Tragwerken in der Arktis

Peter BEIN
Consultant
Vancouver, BC, Canada

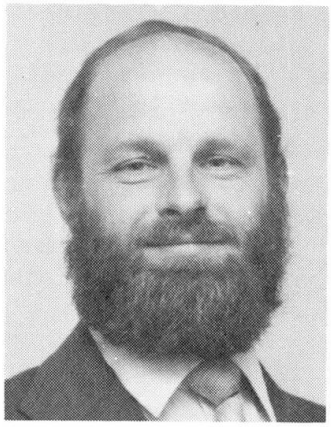

Peter Bein was involved in many aspects of civil engineering since graduation in 1970, and earned his doctorate in engineering systems analysis at the University of British Columbia. For the last six years he worked with two Canadian consulting firms prominent in the arctic offshore engineering, and now is a free-lance consultant.

SUMMARY

Application of decision analysis of the design of arctic offshore structures is discussed. The method proves useful in problems involving uncertain ice environment and multiple measures of merit of alternative solutions, and can help in selecting optimum design ice load criteria for structures.

RÉSUMÉ

La contribution présente une application de la théorie de la décision lors du projet de structures en mer arctique. La méthode est efficace et permet de résoudre des problèmes dans un environnement incertain de glace, en comparant diverses solutions selon leurs mérites. Elle permet également de déterminer les cas optimaux de charges de glace sur les structures.

ZUSAMMENFASSUNG

Die Anwendung von Entscheidungs-Theorien bei der Projektierung von Offshore-Tragwerken in der Arktis ist Thema dieses Beitrags. Die Methode hat sich als nützlich erwiesen in Fällen mit schwer abschätzbaren Eisverhältnissen und beim Vorliegen verschiedener brauchbarer Alternativen und gestattet die Festlegung optimaler Bemessungswerte für die Bemessung von Konstruktionen auf Eiswirkungen.

1. INTRODUCTION

Continued exploration, discovery and extraction of oil and gas from the arctic and sub-arctic frontiers is now becoming a reality. The development is taking place in an environment appreciably different from that encountered in offshore operations in more temperate climates. The presence of sea ice is the prominant factor that challenges the design, hampers the exploration, interfers with the installation and operation of drilling and production structures, and makes marine transportation of supplies, and later of the product to the markets, difficult and costly. Icebergs and sea ice intrude off the Canadian East Coast. Year-round ice up to 12 m thick covers waters between the islands of the Canadian Archipelago. Landfast ice develops along the coast in winter, and polar pack ice constantly moves in the Beaufort Sea. Every year drift ice proceeds southward in the Chukchi and Bering Seas. We cannot readily eliminate the problems created by nature in the arctic, and methods must be sought for dealing with them.

Since the beginning of arctic exploration a multitude of concepts have been proposed for structures capable of supporting all phases of development in each geographical area of the arctic offshore, but only the reasonably priced, reliable and safe technologies have been implemented. Among them are a number of exploration structures that have passed the tests of unusually severe ice conditions of the recent winters. These experiences add to the body of data being accummulated for use in designing more complex future production and transportation systems.

The new systems are necessarily costly because they have to meet the criteria of safe and uninterrupted operation. The designers are presently challenged to reduce the cost of structures, yet to assure safety and reliability at the same time. These are clearly conflicting objectives, and the uncertainties of the arctic further complicate decisions. This paper describes an application of decision analysis to the optimization of arctic offshore systems designed to operate in uncertain and random physical environment, and having conflicting decision criteria.

2. ARCTIC ICE AND STRUCTURES

The design of arctic offshore structures is dominated by lateral forces generated by sea ice. Wave conditions are less severe than in the more exposed sub-arctic waters because the fetch at most locations is limited by the presence of either ice or land. In the St. George Basin of the south Bering Sea, global wave and earthquake loads induced at the foundation level of a structure located in deep water may be comparable to loads produced by drifting ice in a severe winter, but further north, in the Navarin Basin ice loads will dominate design.

Along the coast of Labrador and Newfoundland particularly problematic are icebergs, which could still have a mass of some ten million tonnes on reaching the Hibernia oilfield on the Grand Banks. On the other end of the scale so-called "bergy bits" of the order of 50,000 tonnes and the even smaller "growlers" present great problems because of the difficulty of detecting them in the high seas and limited visibility common to the area. Accelerated by waves, they can produce impacts capable of damaging the mooring system or platform members at the water line [1]. Equally devastating can be the sea ice. Although it only appears at Hibernia every few years early in the year, sea ice is seasonal in the Beaufort and Labrador Seas. The bottom-founded mobile arctic caisson "Molikpaq", deployed in the Canadian Beaufort for exploratory drilling by Gulf Canada Resources in the summer of 1984, was designed for a 500 MN global lateral force from sea ice -- compared to 110 MN wave and 180 MN earthquake load [6].

Given their magnitude, ice loads likely to be encountered in the lifetime of a structure must be accurately estimated. The early designs were understandably conservative and provided structural redundancy so that damage or failure would

not lead to catastrophic consquences. As more is learned from the performance of already deployed structures, and from monitoring of the ice environment, the conservatism is gradually reduced. The continuing experience is central to efficient and economic design.

Exploration and production of hydrocarbons have different requirements for supporting structures. Exploration drilling is a temporary activity with the objective of obtaining definitive information about the geological structure, testing it for oil and gas producibility, and delineating the reservoir. The activity could last up to several months at one location. After the well is completed and tested, it is secured and abandoned. Because of the limited exposure, temporary or "disposable" structures are used for exploration in shallow water, such as sacrificial gravel islands, grounded ice islands, or floating artificial ice platforms. In deeper water, however, these systems are not feasible, and reusable mobile structures are used, such as ice-capable drillships and re-floatable caissons. The mobile structures can rapidly abandon the site in the event of extreme ice conditions.

Production, including storage and transportation of the product, is a longer-term activity, requiring more permanent and durable structures. Production systems can be artificial islands in shallow water, bottom-founded structures in intermediate water depths, or floating systems in deeper water. Both exploration and production structures dedicated to the development of a particular hydrocarbon field will function in the same physical environment, however the length of service expected from production structures is typically twenty years. The chance of experiencing extreme ice loading by the production structures is therefore larger. Also, the notion of extreme conditions is relative. The same ice load criteria that would be an extreme condition for a floating exploration platform, may well become an operating condition for a bottom- founded production structure.

The operating condition design ice loads are maximized using a number of design "tricks". Within the limits of practicality, structures are designed to have redundancy in the framing, so that ice loading exceeding the design values could be tolerated with local damage, but without catastrophic consequences. Some designs incorporate a sloping face with a low friction, low-adfreeze strength coating on the walls exposed to ice to promote flexural failure in the ice feature, and to obtain a vertically downward component from the load to assist in global stability. Foundations in clay seabeds are engineered to maximize tolerable base pressures and to mobilize shear strength of the seabed soil. This is accomplished by replacing the weak soils with sand or by placing a blanket layer of sand or gravel to increase the length of the failure surface, by using spud piles and by enlarging the structural base. Sand core structures, such as the caisson-retained islands and "Molikpaq", achieve stability against sliding largely through the resistance of the sand core. Other structures rely on their own mass plus ballast to develop sliding resistance through friction, and base keys (skirts) are used to ensure that the entire base area is mobilized even if the structure is set down directly on an unprepared, undulating bed. The CIDS (concrete island drilling system) and the new steel base mat for the SSDC (single steel drilling caisson) are examples of this application.

3. DEALING WITH EXTREME ICE LOADS

Although special gravity structures with massive fenders that would absorb the impact of a multi-million tonnes iceberg have been proposed, in most cases it would be uneconomic and impractical to design structures to withstand extreme ice loads likely to occur in the arctic waters. Instead, two general design philosophies have evolved to deal with the extreme conditions. The first one involves a careful monitoring of the ice conditions. The structure is moved out of the approaching extreme ice feature to avoid an impact, and returns to the site to

continue operations after the ice has receded.

Gulf Canada's drilling system consisting of a conical drillship 'Kulluk', and a sophisticated ice management apparatus is an example of a successful application of this philosophy. 'Kulluk' is kept on station in the Beaufort Sea by twelve mooring lines, and is designed to withstand moving ice up to 1.2 m thick. Ice conditions in the vicinity of the vessel are monitored by marine radar and aerial reconnaissance. More severe ice is either deflected away or broken up by four ice-breaking vessels into smaller fragments which the mooring system and the hull can withstand. Shortly after its arrival in the summer of 1983, 'Kulluk' had to be towed off station because of an incursion of heavy ice. After the ice receded the vessel was able to return. Floatable production platforms that can take evasive action if necessary, require special solutions to allow rapid yet reliable disconnection of production riser and subsequent reconnection with minimum downtime. Without doubt the experience gained with floating exploration systems such as 'Kulluk' will be incorporated into their design.

The second design philosophy concerns bottom-founded platforms which can be surrounded by a subsea berm. If properly sized, the berm can stop approaching deep-draft features before they have a chance of making contact with the structure. The berm induces breakage of the moving ice canopy, with the eventual accumulation of grounded ice rubble. When fully developed the rubble pile-ups can effectively absorb kinetic energy of giant ice flows and ice islands, and dissipate it to the berm. One disadvantage is that grounded ice pads impede supply vessel traffic and docking ability at the structure. The other limitation is determined by the economics of submerged berm construction in deeper waters, since the volume of fill required increases drastically with the water depth, becoming prohibitive in areas where fill borrow is at a premium.

To circumvent these problems Exxon protected the CIDS on its first drill site in the Alaskan Beaufort Sea by spraying water directly on the stationary ice. Using large-capacity water monitors for two months from the onset of freezeup in late October 1984, enough water was dumped on the ice to ground it in 15 m water depth, creating a 2 million tonnes ice monolith with an average freeboard of 18 m along the crest. The barrier was horseshoe shaped to allow supply vessel access from one side. After drilling two wells, CIDS lifted off in the next summer and was towed away from the protective berm through its open side. Although very appealing for floating drilling and permanent production platforms alike, the method is limited to Beaufort Sea waters less than 20 m deep, which have the stationary natural ice required during initial stages of the spraying operation until the barrier grounds.

4. DECISION ANALYSIS MODEL

Because the design of arctic offshore structures is dominated by forces generated by sea ice, relatively more attention must be given to the estimation of ice loads likely to be encountered in the lifetime of a structure than to the other loads. The fundamental characteristics of ice loads is the magnitude vs. return period curve. It is not a simple matter to obtain it. Simulations play an important role in the derivation of the curves, but the results depend on the assumptions about the physics of load generating processes, and on the assumed probability distributions of input variables [1]. The curve is often defined by combining available data, knowledge of physical processes and parallels with other arctic regions [11]. The uncertainty of ice loads is caused not just by nature's randomness, but also by our imperfect knowledge of the arctic, and fragmentary data, sometimes with a dramatic impact on design. For example, recent full-scale tests at the Hans Island indicate that conventional theories overpredict ice forces on production structures by a factor of ten [12].

The ice load return period that is eventually selected for design has important consequences for operations. Extreme conditions occur infrequently in a

structure's life, but the ice loads are high enough to displace and damage the structure, with the potential of oil spills from damaged storage and production facilities, well blow-out, and personnel casualties. Depending on the severity of damage, the structure could or could not be restored to an operable condition, but the repairs would be costly and time-consuming in the forbidding arctic environment. If the structure is lost, the capital investment is wasted and exploitation of the hydrocarbon reservoir delayed until the facility is replaced. Moreover, the current technology of oil spill countermeasures precludes an effective and environmentally acceptable clean-up of a major spill in ice-covered waters.

Shorter return periods imply smaller design loads and, consequently, smaller capital cost of the structure, but more frequent disruption of operations when the approaching ice features exceed the design limits. More extensive ice surveillance and more intensive control of ice feature size and movement by appropriate use of ice breakers and tugs are required to protect a structure designed to short return periods. If longer return periods are adopted the capital cost of the structure goes up, but the relative frequency of disruptions and the expected repair cost of damage decrease.

There is currently no accepted requirement for the level of environmental exposure used for arctic design -- largely due to the lack of experience in artic operations, and the poor data base. This paper proposes to use the decision analysis in defining ice load design criteria.

Many situations involving uncertain variables can be represented by a decision tree model [3]. The alternatives are a_i, and the system is described by a set of states s_j (Fig. 1). Uncertainty of states is quantified by probability distributions. When alternative a_i is selected and state s_j occurs, a consequence c_{ij} results. The consequence is measured by attributes derived at the problem definition step from the hierarchy of objectives of the decision maker and possibly other interest groups. The desirability of a consequence is expressed by a numerical measure u_{ij} termed utility. The theory prescribes the choice of an alternative with the highest expected utility to be the optimum criterion. The major data gathering task of decision analysis is to specify probability distributions and utility functions. Probability theory allows the analyst to make a maximum use of information available about uncertain states, while utility theory guarantees that the choice reflects the decision maker's true preferences.

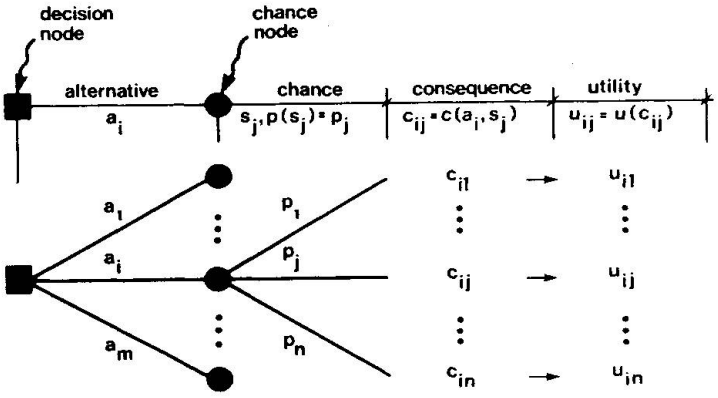

Fig. 1 Decision model

The model requires that a complex problem be divided into parts allocated to specialists. When re-assembled all parts fit into a clear structure facilitating meaningful sensitivity analyses and new insights into the problem, with a potential for reduction of costly experimentation in the arctic. Although past experience has shown that our knowledge cannot improve markedly until the structures are in actual service, supplementary analyses such as sensitivity or value of improved information can provide insights with a great potential for improving decisions prior to deployment of arctic structures.

The model is modified depending on a particular problem [8]. There are typically

vectors of attributes in multiple criteria arctic decision problems. Alternative a_i can denote a sequence of decisions over a period. State s_j becomes then a sequence of states that can occur with joint probability p_{ij}. The utility function can be a decision maker's or it can represent a compromise between conflicting preferences of multiple interest groups. If the decision maker is risk neutral and chooses to minimize expected cost, the utility function can be measured in monetary units.

In solving engineering problems for the arctic, the ability to quantify vagueness is at least as important as the facility of probability theory. This ability is now possible with the development of the theory of fuzzy sets. The theory has matured to the point of practical applications in decision analysis [9] and the first attempts have been made in arctic offshore engineering to apply it to imperfect knowledge of sea bottom scour by ice [13]. The marriage of the two approaches proves the decision model's flexibility and opens new avenues for a rigorous treatment of imperfect knowledge within the scheme of decision analysis.

The Committee on Reliability of Offshore Structures [4] have recognized the potential of decision analysis in selecting tolerable risk levels in the conventional offshore platform design. Maximization of expected utility has been identified among available methods to be the most flexible for dealing with multi-attribute consequences of structural failures, such as capital and operating costs, environmental contamination, life loss and injury.

The overwhelming uncertainty of the ice environment has led to an emphasis on the formulation of probability inputs into arctic technology evaluations, and only a few references apply the complete decision method. A decision tree approach has been employed to select the most preferred development plan, consisting of a chain of decisions on drilling, production, and transportation systems, on the basis of the highest net present worth and the lowest economic risk [5]. Jordaan [7] recommends decision analysis for risk assessment of systems, and for planning of operations in ice-infested waters. Bein [3] applies decision approach to screening of alternative production structures in the Beaufort Sea, and to optimization of arctic tanker terminal configurations.

5. APPLICATION

Since there is always a chance of disruption of operations and structure damage by ice loads higher than those adopted for design, the selection of their return periods shall be based on a calculated risk, which simultaneously optimzes:

- capital cost of the structure,
- operating cost of ice management required for the protection of the structure,
- downtime when operations are suspended as a precaution against ice hazards,
- costs of damage (time lost, repair, cleanup and well re-drilling),
- exposure to casualties of personnel engaged in evacuation, countermeasures, and restoration of operations, and
- impact of oil spills on the arctic habitat.

These are the consequences c_{ij} in the sense of Fig. 1.

Fig. 2 models a situation where a structure can be damaged with probability r in

$$r = 1 - (1 - 1/t)^n$$

t = return period of ice load
1/t = annual probability of damage
n = design life of structure
r = n-year probability of damage

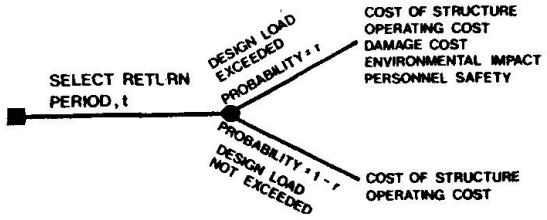

Fig. 2 Decision model for selecting design ice load return period

its lifespan. With probability (1-r) damage will not occur, and the consequences will be only the capital and operating costs. To find the optimum return period, the consequences are evaluated using a utility function. It can facilitate trade-offs between the conflicting consequences, and account for risks posed by consequences and by their probabilities and timing [8]. The decision maker's relative disliking of negative impacts associated with a return period is measured by a quantity termed disutility corresponding to u_{ij} in Fig. 1. The statistical expectation of disutility is the relative measure of merit of selecting return period t and having damage probability r in Fig. 2. For a range of return periods a graph (Fig. 3) can identify the optimum. If it happened to exceed the period required by codes, it would be the value for design, otherwise the code requirement would govern.

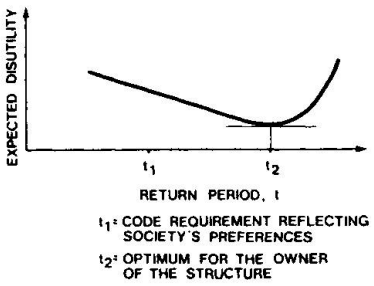

Fig. 3 Optimization of ice load return period

The acceptable return periods must be established by an engineer in consultation with the owner of the structure, but from the standpoint of public well-being it would be inappropriate for either of them to make value judgements concerning personnel and environmental safety. The usual way of encoding the public values necessary to consider in design is through the code stipulations. Lower bound return periods would be specified for arctic structures classified by design life, function, manning requirements, and environmental hazard. The owner would use return periods required by the code, unless longer periods would be more economical. No such guidelines are presently available for the arctic operators. One recommended practice states in too simple terms that the selection of design loads should be the prerogative of the owner [2], but a reported case demonstrates that the owner requires clear guidelines [6].

In the artic developments, where often no basis exists for comparing new designs with existing practice, the degree of conservatism in design may be unbalanced. It can be excessive and costly if the engineer derives design criteria with only rough guidelines [10]. If on the other hand the owner has the prerogative of selecting ice load criteria, the public concerns may tend to be overlooked, with possible adverse impacts following after project implementation.

CONCLUSIONS

Arctic ice is the major environmental load in the design of arctic offshore structures, yet its characterization is subject to considerable uncertainty caused by the natural randomness, poor data and insufficient knowledge. Although the uncertainty is being continuously reduced as more is learned both from the performance of structures placed in service and from improved observations of the ice environment, the choice of ice loads for design of structures must be based on a probabilistic basis because of the randomness. The costs and the reliability of structures strongly depend on the ice loads assumed for design. Success of the hydrocarbon development plans hinges on our ability to devise inexpensive technological solutions that are safe, reliable and bring us closer to energy self-sufficiency in spite of the extremities and variability of the arctic offshore environment.

Decision analysis can address those engineering, planning and design problems of arctic offshore systems that arise from conflicting decision criteria, and uncertain physical environment. From problem definition to decision maker's use of the results, the analysis provides a sound basis for improving current planning and design pratices. It can help define problems in code formulations,

feasibility studies, and preliminary design; it is a flexible analytical technique for systems design optimization; and finally, it is useful in relating engineering design to the overall development planning. This paper addresses selection of ice load design criteria as an example application.

Although the merit of decision analysis in prospecting for oil and gas, and in offshore engineering, has been established, more work is required to make it a credible tool for arctic offshore engineering. Data bases must be enlarged in order for probabilistic descriptions of ice characteristics to become more trustworthy. Ice-structures and ice-soil interaction mechanisms need better understanding to allow reliable simulations from fundamental data. The effects of structural damage on operations delay, habitat, personnel safety, and costs of repair under arctic conditions must be assessed for a range of structure types and materials, damage severity, mitigating measures, and contingency plans.

ACKNOWLEDGEMENTS

This paper is based in part on the author's work with Swan Wooster Engineering Co. Ltd. and DF Dickins Associates Ltd., both of Vancouver, Canada.

REFERENCES

1. ALLYN N., BEIN P., TSENG J., Probabilistic Approaches to Arctic Offshore Engineering. Proceedings Arctic'85, San Francisco, 1985.

2. AMERICAN PETROLEUM INSTITUTE, Recommended Practice for Planning, Designing and Constructing Fixed Offshore Platforms. API RP 2A, Dallas, 1981.

3. BEIN P., Decision Approach to Artic Offshore Developments. Proceedings International Conference on Modelling Under Uncertainty, London, 1986.

4. COMMITTEE ON RELIABILITY OF OFFSHORE STRUCTURES, Application of Reliability Methods in Design and Analysis of Offshore Platforms. Journal of Structural Engineering (ASCE), Vol. 109, No. 10, 1983.

5. FAECKE D., LESSO W., KNAPP R., An Offshore Development Planning Model Incorporating Risk Analysis. Offshore Technology Conference, Houston, 1981.

6. JEFFERIES M., STEWART H., THOMSON R., ROGERS B., Molikpaq Deployment at Tarsiut P-45. Proceedings Arctic'85, San Francisco, 1985.

7. JORDAAN I., Risk and Safety Assessment for Arctic Offshore Projects. Dyer I. and Chryssostomidis, C. (Editors), Arctic Technology and Policy. Hemisphere, Washington, 1984.

8. KEENEY R., RAIFFA H., Decisions with Multiple Objectives. Wiley, New York, 1976.

9. KICKERT W., Fuzzy Theories on Decision-Making: Leiden, Boston, 1978.

10. LEVITT R., LOGCHER R., QADDUMI N., Impact of Owner-Engineer Risk Sharing on Design Conservatism. Journal of Professional Issues in Engineering (American Society of Civil Engineers), Vol. 100, No. 4, 1984.

11. MYERS P., Selection of Environmental Design Criteria for Arctic Structures. Proceedings Arctic'85, San Francisco, 1985.

12. PALMER A., Ice Fracture - A Key to Cutting Down Force Estimates. Offshore Engineer, April 1985.

13. THIEL C., SINGH P., BOISSONNADE A., Risk Assessment of Sea Bottom Scouring Using Fuzzy Set Theory. Proceedings Arctic '85, San Francisco, 1985.

Quality Assurance for Buildings in Ground Movement Areas

Assurance de la qualité pour des bâtiments en zone de tassement

Qualitätssicherung von Gebäuden in Bergsenkungs-Gebieten

George NAWAR
Special Projects Engineer
Department of Housing
Bexley, NSW, Australia

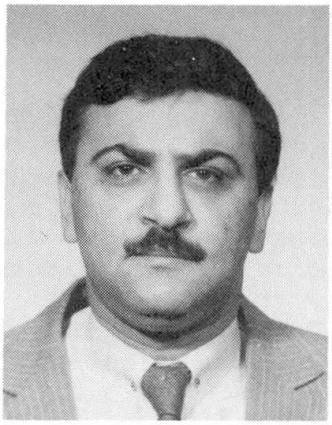

George Nawar, born 1949, graduated in 1977, and received his Masters in 1983. Since graduation, he has been responsible in the N.S.W. Department of Housing for investigating structural aspects in residential construction.

SUMMARY

This paper provides a practical example of planning quality assurance for Civil Engineering Structures at areas subject to the risk of mining subsidence. It highlights a procedure based on the identification and quantification of risk parameters, establishment of acceptable risks and methods of utilizing the hazard scenario to achieve an acceptable level of performance.

RÉSUMÉ

Cette contribution fournit un exemple pratique de l'assurance de la qualité de constructions de génie civil dans des régions sujettes au risque d'affaissement minier. Elle présente une procédure basée sur l'identification et la quantification des paramètres du risque, l'établissement de risques acceptables, et les méthodes de scénarios de dangers potentiels, afin d'atteindre un niveau de performance acceptable.

ZUSAMMENFASSUNG

Der Beitrag behandelt die Planung der Qualitätssicherung für Ingenieurbauten anhand eines Beispieles aus einem Bergsenkungs-Gebiet. Das angewendete Verfahren stützt sich auf die Identifikation und Quantifizierung von Risiko-Kenngrössen, die Festlegung akzeptierbarer Risiken und die Methode der Gefährdungsbilder. Seine Anwendung führt zu einem befriedigenden Verhalten von Bauwerken.

INTRODUCTION

The New South Wales Mine Subsidence Board was enacted in 1961 to provide payment of compensation and/or repair damages to surface structures caused by mine subsidence, following the extraction of coal and shale. The Board was also given powers to define areas subject to high risks of subsidence movement and control all surface improvement in these areas by approving its development through guidelines aimed at maintaining an equitable balance between maximum utilisation of mineral resources and minimum liability caused by related damage to surface development.

This paper is based on the results of a study carried out by the author to formulate such guidelines for the southern mine subsidence districts in N.S.W.

1. IDENTIFICATION OF THE RISK

The risk is defined as the damage to buildings caused by surface movement as a result of underground mining. Surface movement is described in terms of its components [1] as subsidence (s), tilt (g), strain (e) and curvature (ρ). Damage to buildings is caused by the combined effect of these parameters which vary considerably depending on the depth and extent of mining, type and layout of the structure as well as ground conditions [2]. The number of annually reported incidents of damage have increased by more than ten fold since 1962 with similar proportional increase in compensation and repair costs.
The characteristics of damage to other buildings caused by mining subsidence is very similar to that caused by other foundation conditions, [3] to the extent that each type of damage could not be isolated when both damages occur concurrently. For this purpose, positive identification of subsidence damage was limited to areas subject to mining activities with the inevitable short-coming of assuming that all damage is caused by subsidence in these areas. Depsite this broad identification, 58% of the reported damage was easily proven to have been caused by other than mining subsidence.

2. QUANTIFICATION OF THE RISK

Quantitative evaluation of the risk provides a useful tool for direct comparison under variable conditions as well as being a necessary parameter in all benefit cost analysis. In this example, the risk is analysed into two main components:

2.1 Probabalistic Component

This phase is concerned with the probability that subsidence will take place at a given location. It depends on the likelihood of the following events.

a) Mining taking place at that given location (P1). This phase is time dependent and is estimated over a period of 20 years by consultation with the lease holders in a given location.

b) Full extraction (P2). This phase depends on the proximity of development to major surface features requiring protection by reduction of extraction level.

c) Critical width of extraction (P3).
The probability of subsidence caused by single seam extraction (Pss) is then estimated by the product of probabilities such that (Pss) = (P1, P2, P3) and the probability of multi-seam extraction is taken as (Pms) = (Pss1, Pss2, Pss3). These values are plotted on a map of the given location to provide a quantitative scenario of the probabalistic risk component, (Figure 1).

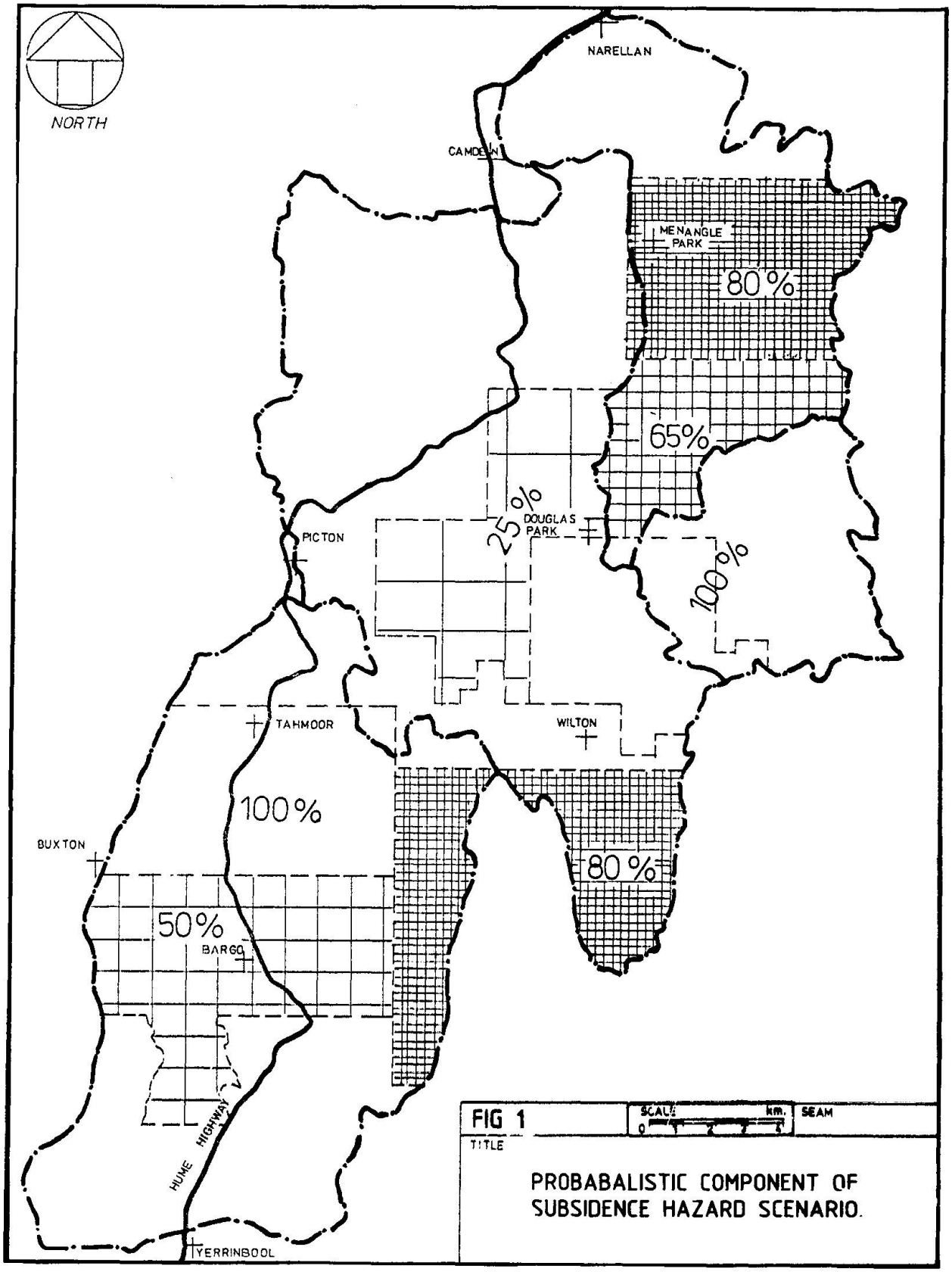
NORTH
NARELLAN
CAMDEN
MENANGLE PARK
80%
65%
25%
DOUGLAS PARK
PICTON
100%
TAHMOOR
WILTON
100%
80%
BUXTON
50%
BARGO
HUME HIGHWAY
YERRINBOOL
FIG 1
SCALE
km.
SEAM
TITLE
PROBABALISTIC COMPONENT OF SUBSIDENCE HAZARD SCENARIO.

2.2 Deterministic Component

This phase deals with the relationship between subsidence occurance and its consequent damage to structures.

In order to quantify this phase, the relationships between different components of ground movement were derived in terms of seam properties (i.e. depth h & thickness m) at critical width extraction as shown in figure (2).
Seam thickness (m) in this relationship is substituted by the maximum subsidence (S) which is linearly related by the equation (S) = 0.65(m), [4]. This relationship provided the basis for the two fundamental aspects of the analysis:

1. Quantifying the critical combinations of subsidence parameters along a subsidence wave into the following conditions as shown in Stages I to IV, (Figure 3).

a) Maximum tensile strain and convex curvature at which subsidence is 20% and tilt is 50% of their corresponding maximum values.

b) Maximum tilt at 50% of maximum subsidence and corresponding to no strain and no curvature.

c) Maximum compressive strain and concave curvature corresponding to approx 50% of maximum tilt and 85% of maximum subsidence.

d) Maximum subsidence at which no tilt strain or curvature occurs.

2. Converting subsidence induced conditions into damage parameters by assessing the separate effects of subsidence induced strains, tilts and curvature on the structures.

Strains represent the rate of lateral ground displacement, and affect the structure by its corresponding horizontal displacement in the building through the interaction between building footings and its immediate foundation material. Damage caused by strain is sensitive to the depth of footings, size of building and type of foundation material. This condition was found to be of minor significance [2] for small to medium size buildings on shallow footings.
Tilt represents the rate of change in vertical movement, and affects the structure by its corresponding differential vertival displacement which is directly related to the structure length and height. This condition was proven [2] to be the most significant cause of most subsidence damage in small buildings. Curvature represents the rate of change in tilt and causes damage by its corresponding tilt component. Finally, the combined effect of all subsidence induced movement as defined by the critical conditions in 1 above were analysed [2] and the design condition assessed as that of maximum tilt as described in condition II, (Figure 3).

At this stage damage to buildings has been directly related to the values of (S/h) and could then be plotted on maps of the given location to represent the deterministic risk component, (Figure 4).

3. ACCEPTABLE RISK

The issue of acceptable risk is a fairly emotional topic and tends in most applications to be governed by political constraints which are not necessarily based on equitable cost effectiveness. In this example considerable efforts were made to achieve acceptable risk by classifying subsidence induced damage into five categories and by relating each category to its corresponding subsidence induced tilt, for five types of construction as shown in table (1). This classification is based on maximum crack widths in walls and floors as related to differential vertical displacement.

FIG 2 TYPICAL SUBSIDENCE PARAMETERS FOR A CRITICAL WIDTH OF EXTRACTION.

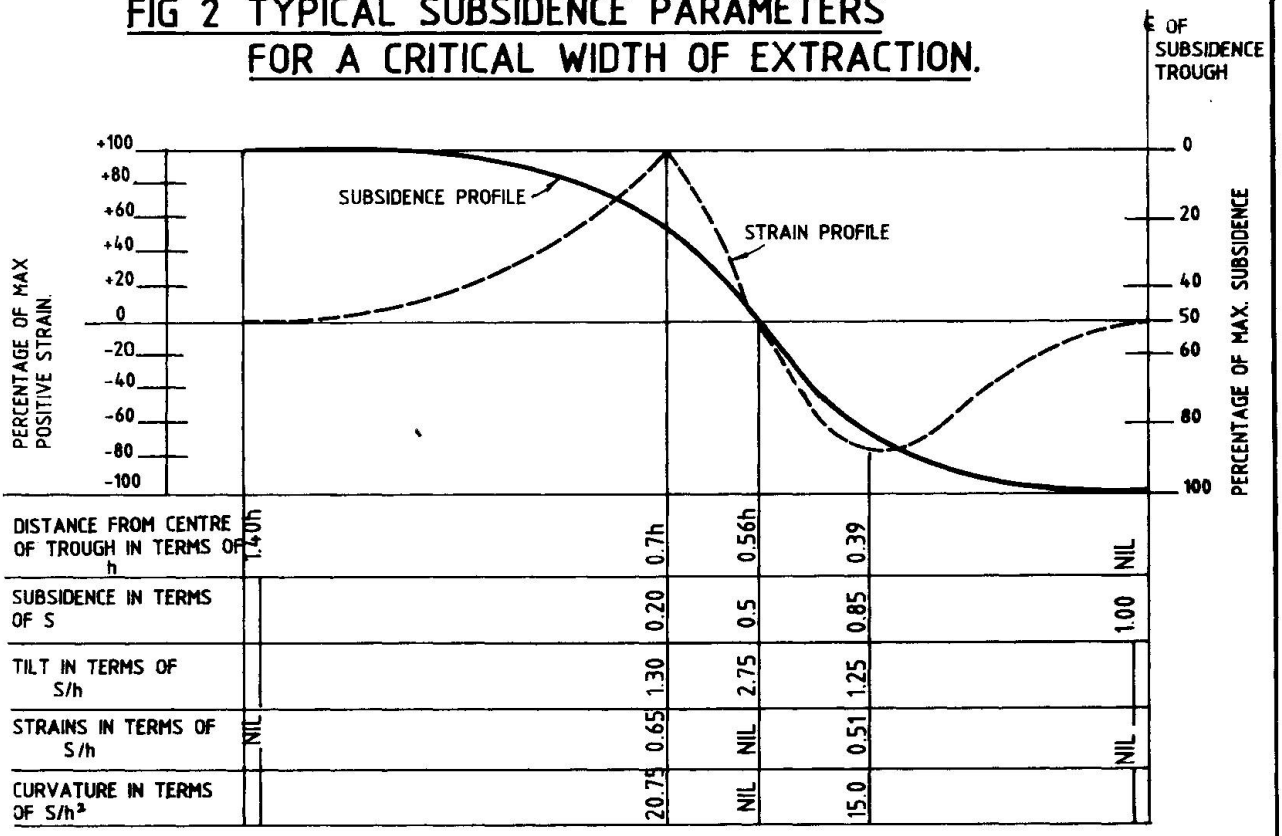

FIG 3 EFFECTS OF FACE PROGRESSION ON SURFACE STRUCTURES.

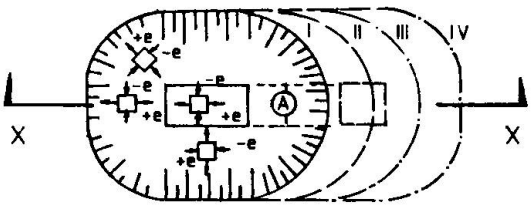

PLAN
-e Comp Strain.
+e Tensile Strain
Ⓐ Area of Consideration

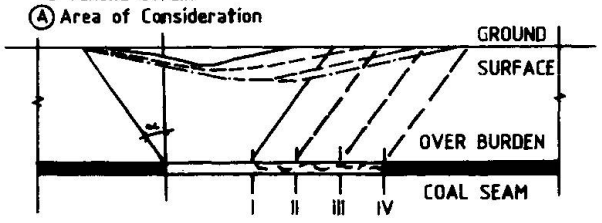

SECTIONAL ELEVATION

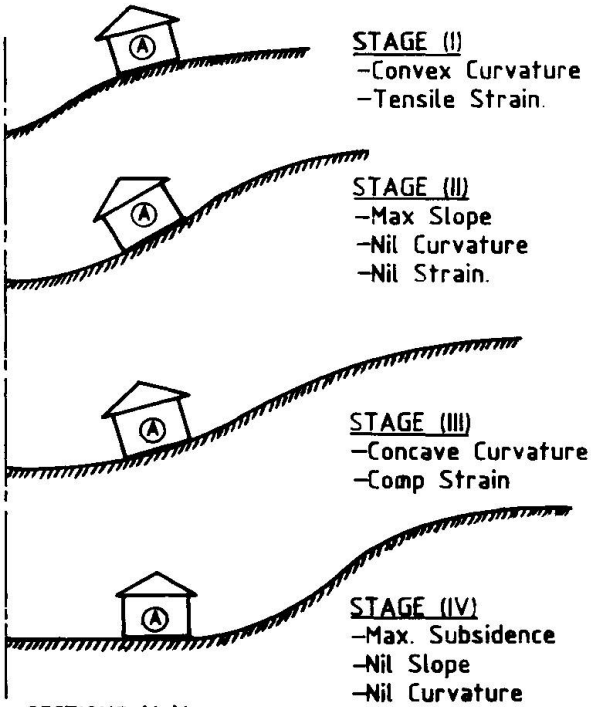

STAGE (I)
-Convex Curvature
-Tensile Strain.

STAGE (II)
-Max Slope
-Nil Curvature
-Nil Strain.

STAGE (III)
-Concave Curvature
-Comp Strain

STAGE (IV)
-Max. Subsidence
-Nil Slope
-Nil Curvature
-Nil Strain.

SECTIONS X-X
FACE PROGRESSION

Repair costs were estimated from the description of typical damage as percentage of replacement cost and acceptable damage is related to movement limits for houses, table (2), acceptable risk in terms of (S/h) could then be directly related to acceptable damage in terms of cost penalty.

TABLE 2, MOVEMENT LIMITS FOR HOUSES [6]

Type of Construction	Limit as a function of length.	Absolute Limit (mm)
Clad Frame	1/300	40
Masonry Veneer	1/500	25
Articulated Masonry Veneer	1/800	15
Articulated Masonry	1/800	15
Full Masonry	1/2000	7

4. MANAGEMENT OF THE RISK

Now that the risk is defined and quantified, and we know how much of that risk is tolerable, the next step is to manipulate these factors in planning to achieve safety and quality assurance. To this end planning aims at either reducing the risk, or improving the capacity of buildings to sustain this risk, or both. In this example both measures were adopted as follows.

4.1 Risk Reduction

By optimisation of the probabalistic hazard scenario (Figure 1) to minimise the effects of mining subsidence on surface structures. This is achieved by the establishment of a long term plan to govern the relationship between both mining and building activities in aspects such as geographical location, rate and extent of development, as well as the type and sequence of each development. This plan is implemented and controlled by the governing bodies such as the Department of Mineral Resources, Mine Subsidence Board and local Councils.

4.2 Improving Structures Capacity to Sustain the Risk

By optimisation of the deterministic hazards scenario (Figure 4) to minimise the effects of subsidence movement on surface structures. This is achieved by developing design methods aimed at improving the capacity of structures to withstand ground movement. Mehtods such as:

a) Isolating footings from surrounding ground movement by over excavation and back-filling with compactable material, avoiding deep footings and selecting flat rafts where possible in order to reduce friction forces on the underside of footings.

b) Designing footings to resist lateral and vertical differential movement by increased stiffness.

c) Making allowance to reduce the impact of damage caused by differential movement by articulation of the superstructure, maintaining uniform structural stiffness and making provisions for future relevelling including re-grading of sewer and storm water.

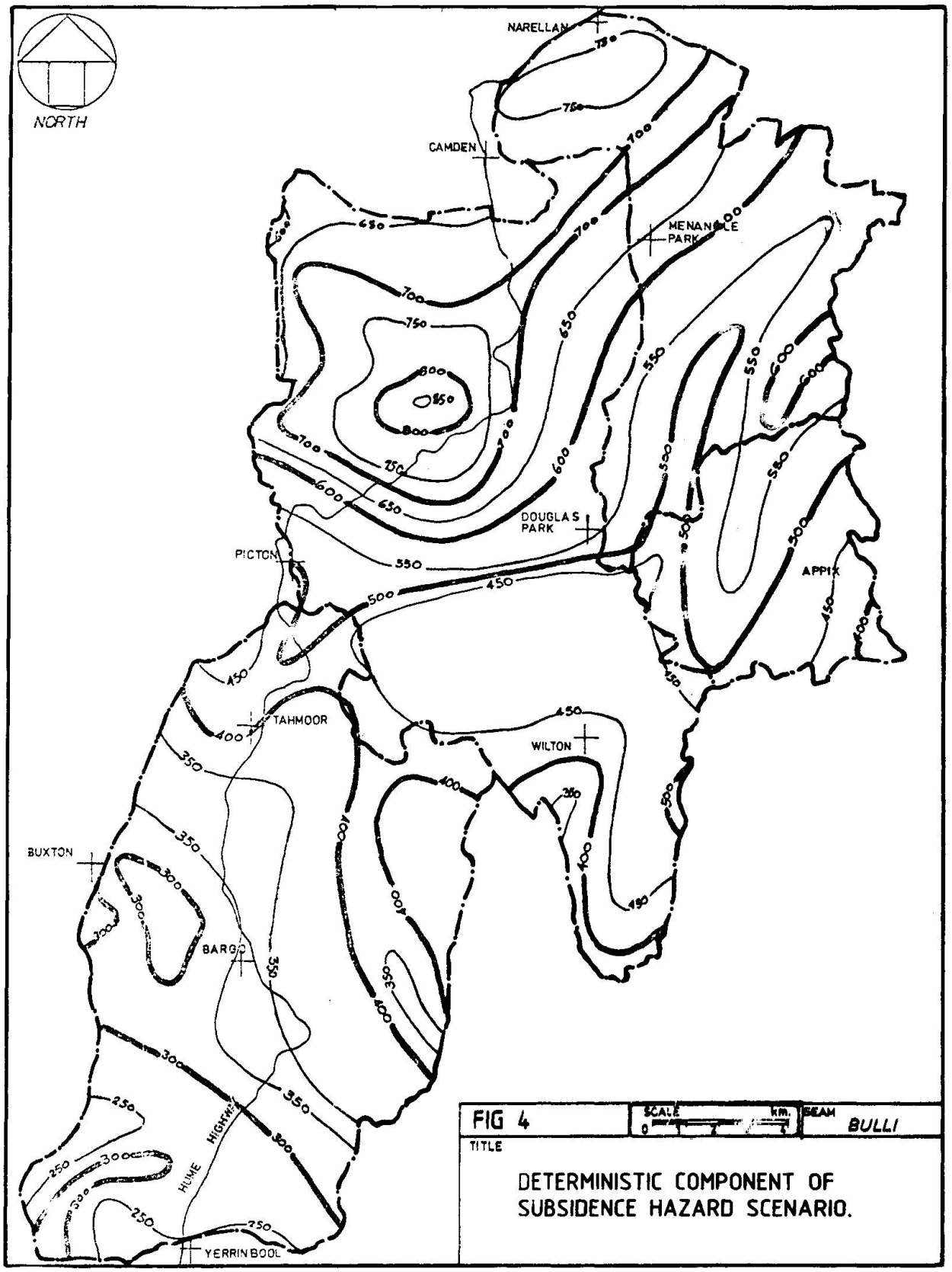
NORTH
NARELLAN
CAMDEN
MENANGLE PARK
DOUGLAS PARK
PICTON
TAHMOOR
WILTON
APPIN
BUXTON
BARGO
HUME HIGHWAY
YERRINBOOL
FIG 4
SCALE
km.
SEAM
BULLI
TITLE
DETERMINISTIC COMPONENT OF SUBSIDENCE HAZARD SCENARIO.

TABLE 1. CLASSIFICATION OF DAMAGE CAUSED BY TILT IN STRUCTURES UP TO 3.6m HIGH AS RELATED TO

i. SLOPE OF BUILDING g. GROUND TILT mm/m S/h. SEAM PROPERTIES mm/m

DEGREE & CLASS OF DAMAGE		CLAD FRAME	BV (ART).	BV	FB (ART).	FB	FLOOR CRACK WIDTH	WALLS CRACK WIDTH	DESCRIPTION OF TYPICAL DAMAGE	REPAIR COST
0 Negligible	i	1:300	1:500	1:800	1:800	1:2000	0.3 mm	0.1 mm	Hairline cracks not identifiable without magnifying glasses.	Nil
	g	5.2	3.2	2.0	2.0	0.8				
	S/h	2	1.2	0.8	0.8	0.3				
1 Very Slight	i	1:200	1:300	1:500	1:500	1:800	1.0	1.0	Isolated, rarely visible cracks at external wall. Easily treated during normal decoration.	Nil
	g	7.3	5.2	3.2	3.2	2.0				
	S/h	3	2	1.2	1.2	0.8				
2 Slight	i	1:150	1:200	1:300	1:300	1:500	2.0	5.0	Fine but noticeable cracks - easily repaired Doors & windows stick slightly.	1%
	g	10.5	7.3	5.2	5.2	3.2				
	S/h	4	3	2	2	1.2				
3 Moderate	i	1:100	1:150	1:200	1:200	1:300	4.0	15.0	Cracks impair weather tightness. Doors & windows stick - small sections may need replacement.	3-15%
	g	15.6	10.5	7.3	7.3	5.2				
	S/h	5.5	4	3	3	2				
4 Severe	i	1:75	1:100	1:150	1:150	1:200	7.5	25	Extensive repairs partial replacement. Repairs to frame.	10-20%
	g	20.8	15.6	10.5	10.5	7.3				
	S/h	7.5	5.5	4	4	3				
5 Very Severe	i	1:150	1:175	1:100	1:100	1:150	10	30	Structural integrity impaired. Building frame distorted. Major replacements	20%
	g	30	20.8	15.6	15.6	10.5				
	S/h	11	7.5	5.5	5.5	4				

This aspect has been covered by codification as design for mining subsidence is included in the Australian Standard on Residential Slabs and Footings [6].

ACKNOWLEDGEMENTS

The author wishes to express his appreciation to the NSW Department of Mineral Resources and Mines Subsidence Board for their assistance in carrying out the study and to Professor Owen Ingles for his constructive comments.

REFERENCES

[1] Subsidence Engineering Handbook, National Coal Board Mining Department, London, 1975.
[2] NAWAR G., Performance of Masonry Dwellings Under Ground Conditions Caused by Mining Subsidence. Proc., Inst. of Engineers Conference, Brisbane, 1985. (pp 26-31).
[3] INGLES O.G. & NAWAR G., Effects of Soil, Footings and Construction types on the Structural Performance of Domestic Dwellings. Proc., Quality Assurance, Codes, Safety and Risk in Structural Engineering and Geomechanics. Monash University, 1984. (pp 50-55)
[4] Frankham B.S. & MOULD G.R., Mining Subsidence in N.S.W. Proc., The Australian Istitute of Mining and Metallurgy, New Zealand, 1980.
[5] RYNCRAZ T., Ergebnisse von Modell Versuchen über den Einfluss von Oberflächenlasten auf den Absenkungstrog (poln), Arch górn 8 (1963), 111/28
[6] Dr. 85108, Draft Australian Standard on Residential Slabs and Footings. April, 1985.

KEYWORDS

Building Performance - Ground Movement.
Subsidence damage.

Leere Seite
Blank page
Page vide